

7

Excitation of Waveguides and Cavities

In this chapter we will examine the basic problems of radiation from a probe antenna and a small loop antenna in a rectangular waveguide. The impedance of an antenna in a waveguide is significantly different from that of an antenna located in free space. A very common type of waveguide antenna is a probe connected to a coaxial transmission line as shown in Fig. 7.1. By choosing the antenna length d and the short-circuit position ℓ correctly the input impedance can be made equal to the characteristic impedance Z_c of the input coaxial transmission line over a fairly broad range of impedances.

Two waveguides may be coupled by means of probe or loop antennas or a combination of the two. However, it is usually simpler to couple two waveguides by one or more apertures in the common wall. An approximate theory of coupling by small apertures was developed by Bethe [7.5]. We will give an improved version of this small-aperture theory that will provide for conservation of power and hence give more physically meaningful equivalent circuits.

In the latter part of the chapter we will develop the small-aperture theory for waveguide-to-cavity coupling. A cavity can also be excited by means of a small probe or loop antenna coupled to an input coaxial transmission line. The theory is similar to that for antennas in waveguides and for this reason will not be covered.

7.1. THE PROBE ANTENNA

The type of coaxial-line probe antenna to be analyzed is shown in Fig. 7.1. It consists of a small coaxial line, terminated in the center of the broad face of a rectangular waveguide, with its inner conductor extending a distance d into the waveguide. In order to have the antenna radiate in one direction only a short-circuiting plunger is placed a distance ℓ to the left of the probe. The probe has a radius r which we will assume to be small relative to the guide height b . However, for typical probes r is large enough that it is necessary to account for the probe thickness if accurate results for the antenna impedance are to be obtained. The field in the waveguide is excited by the unknown aperture fields in the coaxial-line opening. For an exact analysis we should express the field in the waveguide and coaxial line in terms of the unknown aperture electric field and impose the boundary conditions that require the tangential magnetic field to be continuous across the aperture opening. This procedure would lead to equations for determining the electric field in the aperture opening and the current on the probe.

In a typical arrangement the coaxial line is relatively small in diameter and the amplitudes of the higher order coaxial-line modes that are excited are small. A reasonable approximation is to assume that only an incident and a reflected TEM mode exist in the coaxial line. Thus

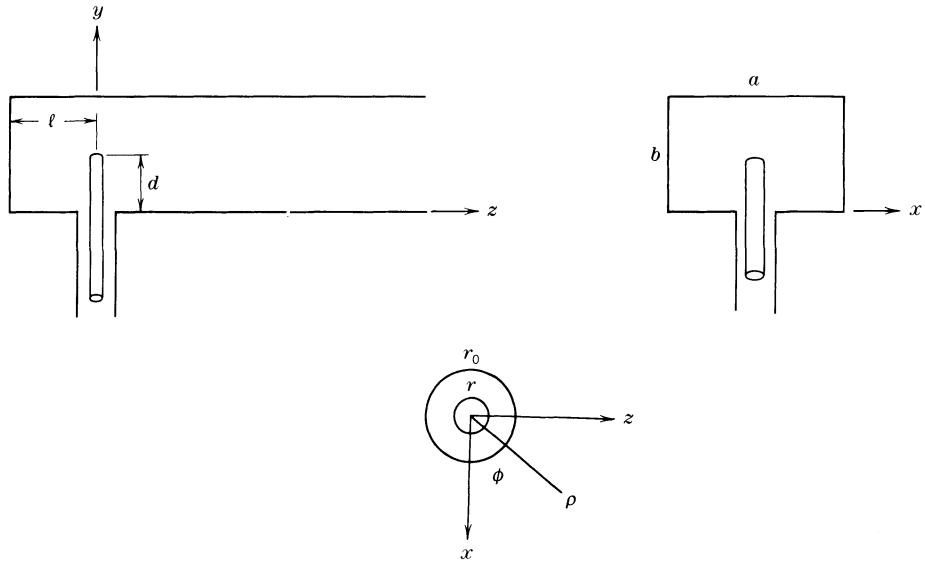


Fig. 7.1. Waveguide probe antenna.

we will assume that in the coaxial line, at the aperture opening,

$$E_r = (V^+ + V^-) \frac{1}{\rho \ln r_0/r} \quad (1a)$$

$$H_\phi = \frac{V^+ - V^-}{Z_c} \frac{1}{2\pi\rho} \quad (1b)$$

where r_0 is the outer-conductor radius, ρ is the radial coordinate, Z_c is the characteristic impedance, and V^+ and V^- are the amplitudes of the incident and reflected TEM waves. The total input current at the probe input equals $2\pi r H_\phi(r) = I_0$ and the antenna input impedance equals

$$Z_{in} = (V^+ + V^-)/I_0 = V/I_0.$$

If we introduce a dyadic Green's function $\bar{\mathbf{G}}_e$ that satisfies the boundary condition $\mathbf{n} \times \bar{\mathbf{G}}_e = 0$ on the waveguide walls and the radiation condition as z approaches infinity, we can express the electric field in the form

$$\mathbf{E}(\mathbf{r}') = \iint_{S_a} \mathbf{n} \times \mathbf{E}(\mathbf{r}) \cdot \nabla \times \bar{\mathbf{G}}_e(\mathbf{r}, \mathbf{r}') dS - j\omega\mu_0 \iint_{S_0} \mathbf{J}(\mathbf{r}) \cdot \bar{\mathbf{G}}_e(\mathbf{r}, \mathbf{r}') dS \quad (2)$$

where S_a is the coaxial-line aperture and S_0 is the surface of the probe. This result follows from applying Green's theorem to the surface shown in Fig. 7.2 and making use of the boundary conditions satisfied by \mathbf{E} and $\bar{\mathbf{G}}_e$ on the waveguide walls, the probe surface, and at infinity. The first integral over the surface S_a gives the applied field acting on the probe which will be called \mathbf{E}_a . The boundary condition on the probe is $\mathbf{n} \times \mathbf{E} = 0$ and leads to the

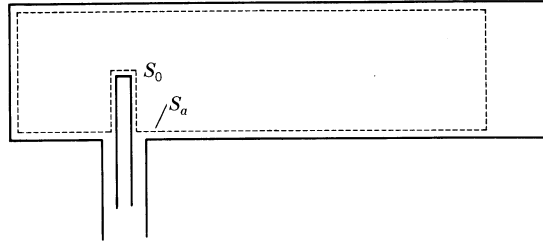


Fig. 7.2. Surface of integration for Green's theorem.

following integral equation for the probe current \mathbf{J} :

$$\iint_{S_0} \mathbf{J}(\mathbf{r}) \cdot \bar{\mathbf{G}}(\mathbf{r}, \mathbf{r}') dS \times \mathbf{n} = -\mathbf{E}_a \times \mathbf{n}, \quad \mathbf{r}' \text{ on } S_0 \quad (3)$$

where $\bar{\mathbf{G}} = -j\omega\mu_0\bar{\mathbf{G}}_e$.

We will develop a variational expression for an impedance functional Z from which we can find the antenna input impedance Z_{in} . We will then show that this variational method gives the same solution as that obtained by solving the integral equation (3) using the method of moments and Galerkin's procedure. The variational method for antenna impedance was developed by Storer¹ and was formulated for the case when the applied electric field acted over a vanishingly small length of the antenna, essentially a delta function source. We will generalize the method so as to take account of an applied electric field that acts along the full length of the antenna.

The integral equation (3) involves the tangential components along the probe. Instead of taking a cross product with the unit normal \mathbf{n} we will take a scalar product with $\mathbf{J}(\mathbf{r}')$ and integrate over the probe surface, which gives

$$\iint_{S_0} \iint_{S_0} \mathbf{J}(\mathbf{r}) \cdot \bar{\mathbf{G}}(\mathbf{r}, \mathbf{r}') \cdot \mathbf{J}(\mathbf{r}') dS dS' = - \iint_{S_0} \mathbf{E}_a(\mathbf{r}') \cdot \mathbf{J}(\mathbf{r}') dS'.$$

We now define the impedance functional

$$Z = \frac{V^2}{\iint_{S_0} \mathbf{J} \cdot \mathbf{E}_a dS} \quad (4)$$

and consider its variation δZ using

$$\iint_{S_0} \iint_{S_0} \mathbf{J}(\mathbf{r}) \cdot \bar{\mathbf{G}}(\mathbf{r}, \mathbf{r}') \cdot \mathbf{J}(\mathbf{r}') dS dS' + \frac{Z}{V^2} \left[\iint_{S_0} \mathbf{J}(\mathbf{r}') \cdot \mathbf{E}_a(\mathbf{r}') dS' \right]^2 = 0. \quad (5)$$

¹An account of Storer's method may be found in [7.1].

The variation δZ in Z due to a variation $\delta \mathbf{J}$ in the current distribution is given by

$$\frac{\delta Z}{V^2} \left[\iint_{S_0} \mathbf{J} \cdot \mathbf{E}_a dS' \right]^2 = - \iint_{S_0} \iint_{S_0} \left[\delta \mathbf{J} \cdot \bar{\mathbf{G}} \cdot \mathbf{J} + \mathbf{J} \cdot \bar{\mathbf{G}} \cdot \delta \mathbf{J} + \frac{Z}{V^2} 2 \delta \mathbf{J} \cdot \mathbf{E}_a \mathbf{J} \cdot \mathbf{E}_a \right] dS dS'. \quad (6)$$

By using the symmetry property of $\bar{\mathbf{G}}$, namely that $\mathbf{J}(\mathbf{r}) \cdot \bar{\mathbf{G}}(\mathbf{r}, \mathbf{r}') \cdot \delta \mathbf{J}(\mathbf{r}') = \delta \mathbf{J}(\mathbf{r}') \cdot \bar{\mathbf{G}}(\mathbf{r}', \mathbf{r}) \cdot \mathbf{J}(\mathbf{r})$, and relabeling the variables \mathbf{r} and \mathbf{r}' as appropriate we obtain

$$\frac{\delta Z}{V^2} \left[\iint_{S_0} \mathbf{J} \cdot \mathbf{E}_a dS' \right]^2 = -2 \iint_{S_0} \left[\iint_{S_0} \mathbf{J}(\mathbf{r}) \cdot \bar{\mathbf{G}}(\mathbf{r}, \mathbf{r}') dS + \mathbf{E}_a(\mathbf{r}') \right] \cdot \delta \mathbf{J}(\mathbf{r}') dS' \quad (7)$$

where we have also made use of (4). Since the current \mathbf{J} is a solution of the integral equation (3) we see that $\delta Z = 0$. Hence (5) is a variational expression for the impedance functional Z .

At this point we need to establish the relationship between Z and the antenna input impedance Z_{in} . If the applied field was a delta function source $V\delta(y)$ then (4) gives

$$Z = \frac{V^2}{\iint_{S_0} V\delta(y) J_y(y) dy r d\phi} = \frac{V}{\int_0^{2\pi} J_y(0) r d\phi} = \frac{V}{I_0} = Z_{\text{in}} \quad (8)$$

so Z equals Z_{in} in this special situation. The electric field $\mathbf{E}_a(y) \cdot \mathbf{a}_y$ acting along the probe will be linearly proportional to V , the voltage associated with the aperture field in the coaxial-line opening. Hence we can write

$$\mathbf{E}_a(y) \cdot \mathbf{a}_y = V e_a(y)$$

where $e_a(y)$ is a normalized electric field along the probe. From the definitions of Z and Z_{in} we have

$$Z_{\text{in}} = \frac{V}{I_0} = \frac{V^2}{\iint_{S_0} \mathbf{E}_a \cdot \mathbf{J} dS} \frac{\iint_{S_0} e_a J_y dS}{I_0} = \frac{Z}{I_0} \int_0^d e_a(y) I_y(y) dy \quad (9)$$

where $I_y(y) = \int_0^{2\pi} J_y(y) r d\phi = 2\pi r J_y(y)$ is the total current on the probe. We have assumed that the current $J_y(y)$ is uniform around the circumference of the probe.

We can expand the current I_y in terms of a suitable set of basis functions $\psi_n(y)$ so that

$$I_y(y) = \sum_{n=1}^N I_n \psi_n(y). \quad (10)$$

We can always choose the $\psi_n(y)$ so that $\psi_n(0) = 1$. Hence we will have

$$I_0 = \sum_{n=1}^N I_n. \quad (11)$$

When we use this expansion in (5) and also make use of (9) we obtain the following expression for Z_{in} :

$$Z_{\text{in}} = \frac{\sum_{n=1}^N \sum_{m=1}^N G_{nm} I_n I_m}{\left(\sum_{n=1}^N f_n I_n \right)^2} = \frac{\sum_{n=1}^N f_n I_n}{\sum_{n=1}^N I_n} = \frac{\sum_{n=1}^N \sum_{m=1}^N G_{nm} I_n I_m}{\sum_{n=1}^N I_n \sum_{n=1}^N f_n I_n} \quad (12)$$

where

$$G_{nm} = \frac{-1}{(2\pi r)^2} \iint_{S_0} \iint_{S_0} \psi_n(y) G_{yy}(r, r') \psi_m(y') dS dS'$$

$$f_n = \int_0^d \psi_n(y) e_a(y) dy.$$

The equations for determining the I_n are obtained by using the current expansion in (5) and setting $\delta Z = 0$; thus,

$$\sum_{n=1}^N G_{mn} I_n = Z f_m \sum_{n=1}^N f_n I_n = C f_m, \quad m = 1, 2, \dots, N \quad (13)$$

where $C = Z \sum_{n=1}^N f_n I_n$ is a constant for each equation. We will show next that Galerkin's method leads to the same solution for Z_{in} .

Galerkin's Method of Solution

In the method-of-moments solution we substitute the expansion for $J_y(y) = I_y(y)/2\pi r$ into the integral equation and then test the resultant equation with each of the basis functions $\psi_m(y)$ in turn. This procedure results in the following system of equations:

$$\sum_{n=1}^N G_{mn} I_n = \frac{1}{2\pi r} \iint_{S_0} V e_a(y) \psi_m(y) dy r d\phi = f_m V, \quad m = 1, 2, \dots, N. \quad (14)$$

This system of equations is the same as that given by (13) with the possible exception of the normalization of the I_n . We can multiply (14) by I_m , sum over m , and solve for V . We then find that

$$Z_{\text{in}} = \frac{V}{I_0} = \frac{\sum_{n=1}^N \sum_{m=1}^N G_{mn} I_m I_n}{\sum_{n=1}^N I_n \sum_{m=1}^N f_m I_m} = \frac{V}{\sum_{n=1}^N I_n} \quad (15)$$

which is the same solution as given by (12). This solution for Z_{in} is not dependent on how the I_n are normalized. The solution for Z_{in} is, in general, not a stationary value. The impedance functional Z given by (4) is stationary for the correct current distribution, but since Z_{in} is given by the product of Z and a functional of $J_y(y)$ that is not stationary, Z_{in} is not stationary. Variational expressions for complex quantities such as Z do not have any unusual properties as regards the stationary values. These are not absolute maxima or minima. In actuality, if the current distribution contains several variational parameters we could adjust these so that the variational expression for Z would give the exact value for Z , if we knew that value a priori. This current distribution will generally not be the same as the one obtained by setting the first variation equal to zero. What one can infer from the variational expression for Z is that if the trial function chosen for $J(y)$ is a good approximation to the true current distribution then the error in Z is of second order. If the trial function is a poor approximation very little can be said about the accuracy of the stationary value of Z relative to the true value. On the other hand, it has been found in practice that in the case of a delta function source term the variational solution for Z_{in} agrees closely with that obtained by other methods of analysis. Consequently, we can anticipate that Galerkin's method will also give good estimates for Z_{in} using relatively low order expansions for $I_y(y)$.

Solution for Z_{in}

We only need the G_{yy} component of the Green's dyadic function when we assume that \mathbf{J} has only a y component. This is tantamount to neglecting the radial current on the end of the probe, which is justifiable for a thin probe. We can readily construct the required Green's function from the vector potential A_y due to a y -directed current element. The required Green's function that will give the electric field E_y from a y -directed current element is

$$G = \frac{2jZ_0}{abk_0} \sum_{n=1}^{\infty} \sum_{m=0}^{\infty} \frac{\epsilon_{0m} k_m^2}{\Gamma_{nm}} \sin \frac{n\pi x}{a} \sin \frac{n\pi x'}{a} \cos \frac{m\pi y}{b} \cdot \cos \frac{m\pi y'}{b} e^{-\Gamma_{nm}(z_< + \ell)} \sinh \Gamma_{nm}(z_< + \ell) \quad (16)$$

where $k_m^2 = (m\pi/b)^2 - k_0^2$ and $\Gamma_{nm}^2 = (n\pi/a)^2 + k_m^2$. For a centered probe we only need the terms for $n = 1, 3, 5, \dots$ in (16). Also, with the exception of the $n = 1, m = 0$, and possibly the $n = 2, m = 0$, and $n = 1, m = 1$ modes, we can replace the hyperbolic sine function by $\frac{1}{2}e^{\Gamma_{nm}(z_< + \ell)}$. In order to obtain a more rapidly converging series than the one over n in (16) and to also facilitate the integration around the circumference of the probe, we introduce the image series given by (91) in Chapter 2. For the $m > 0$ modes where $k_m^2 > 0$ we have

$$\begin{aligned} & \sum_{n=1}^{\infty} \frac{\sin \frac{n\pi x}{a} \sin \frac{n\pi x'}{a}}{\Gamma_{nm} a} e^{-\Gamma_{nm}|z-z'|} \\ &= -\frac{j}{4} H_0^2(-jk_m \sqrt{(x-x')^2 + (z-z')^2}) \\ &+ \frac{j}{4} H_0^2(-jk_m \sqrt{(x+x')^2 + (z-z')^2}) \\ &- \frac{j}{4} \sum_{n=-\infty}^{\infty}' [H_0^2(-jk_m \sqrt{(x-x'-2na)^2 + (z-z')^2}) \\ &- H_0^2(-jk_m \sqrt{(x+x'+2na)^2 + (z-z')^2})] \end{aligned} \quad (17)$$

where the prime means that the $n = 0$ term is excluded from the sum. In all terms but the first we can put $x = x' = a/2$ and $z = z' = 0$ with little error. In the first term we use $x = (a/2) + r \cos \phi$, $z = r \sin \phi$ and similar expressions for x' and z' . We then find that

$$\sum_{n=1,3,\dots}^{\infty} \frac{\sin \frac{n\pi x}{a} \sin \frac{n\pi x'}{a}}{\Gamma_{nm} a} e^{-\Gamma_{nm}|z-z'|} = \frac{1}{2\pi} \left\{ K_0 \left(2k_m r \left| \sin \frac{\phi - \phi'}{2} \right| \right) + \sum_{n=1}^{\infty} [4K_0(2k_m n a) - 2K_0(k_m n a)] \right\} \quad (18)$$

where K_0 is the modified Bessel function of the second kind. The average value of the integral of the first term over the angles ϕ and ϕ' is given by

$$\frac{1}{(2\pi)^2} \iint_0^{2\pi} K_0 \left(2k_m r \left| \sin \frac{\phi - \phi'}{2} \right| \right) d\phi' d\phi = I_0(k_m r) K_0(k_m r) \quad (19)$$

as obtained by using $x = \sin(\phi - \phi')/2$ and

$$\int_0^1 \frac{K_0(2k_m r x)}{\sqrt{1-x^2}} dx = \frac{\pi}{2} I_0(k_m r) K_0(k_m r).$$

The Bessel function series converges rapidly because of the exponential decay of the K_0 functions. For the $m = 0$ terms $-jk_m$ becomes equal to k_0 and the image series involves a slowly converging series of Hankel functions. We can use the same approximations for x and x' in all terms but the first. We also use $z = r \sin \phi$, $z' = r \sin \phi'$ in the first term but use $z - z' = r$ in all the higher order terms so as to generate the following series, after averaging over ϕ and ϕ' :

$$\begin{aligned} & -\frac{j}{4}[J_0(k_0 r) - 1]H_0^2(k_0 r) - \frac{j}{4}H_0^2(k_0 r) + \frac{j}{4}H_0^2(k_0 \sqrt{a^2 + r^2}) \\ & - \frac{j}{4} \sum_{n=-\infty}' [H_0^2(k_0 \sqrt{(2na)^2 + r^2}) - H_0^2(k_0 \sqrt{(2n+1)^2 a^2 + r^2})] \\ & = -\frac{j}{4}[J_0(k_0 r) - 1]H_0^2(k_0 r) + \sum_{n=1,3,\dots}^{\infty} \frac{e^{-\Gamma_{n0} r}}{\Gamma_{n0} a}. \end{aligned} \quad (20)$$

We next use $J_0(k_0 r) - 1 \approx -(k_0 r/2)^2$, $H_0^2(k_0 r) \approx 1 - j(2/\pi)(\gamma + \ln k_0 r/2)$ where $\gamma = 0.5772$, and express the series in the form

$$\begin{aligned} & \sum_{n=1,3,\dots}^{\infty} \left[\frac{e^{-n\pi r/a}}{n\pi} + \left(\frac{e^{-\Gamma_{n0} r}}{\Gamma_{n0} a} - \frac{e^{-n\pi r/a}}{n\pi} \right) \right] \\ & = -\frac{1}{2\pi} \ln \tanh \frac{\pi r}{2a} + \sum_{n=1,3,\dots}^{\infty} \left(\frac{e^{-\Gamma_{n0} r}}{\Gamma_{n0} a} - \frac{e^{-n\pi r/a}}{n\pi} \right). \end{aligned} \quad (21)$$

We can also approximate $\tanh \pi r/2a$ by its argument. By this means the $m = 0$ terms, averaged

over the angles ϕ, ϕ' , become

$$\frac{jk_0^2 r^2}{16} + \frac{k_0^2 r^2}{8\pi} \left(\gamma + \ln \frac{k_0 r}{2} \right) - \frac{1}{2\pi} \ln \frac{\pi r}{2a} + \sum_{n=1,3,\dots}^{\infty} \left(\frac{e^{-\Gamma_{n0}r}}{\Gamma_{n0}a} - \frac{e^{-n\pi r/a}}{n\pi} \right).$$

The terms corresponding to the modes reflected from the short circuit have the factor

$$\sin \frac{n\pi x}{a} \sin \frac{n\pi x'}{a} e^{-2\Gamma_{nm}\ell - \Gamma_{nm}(z+z')}.$$

For these terms we use $x = (a/2) + r \cos \phi, z = r \sin \phi$ and similarly for x' and z' . By means of a Taylor series expansion about $x = x' = a/2$ and $z = z' = 0$ we get

$$e^{-2\Gamma_{nm}\ell} \left[1 - \left(\frac{n\pi}{a} \right)^2 \frac{r^2}{2} (\cos^2 \phi + \cos^2 \phi') + \Gamma_{nm}^2 \frac{r^2}{2} (\sin \phi + \sin \phi')^2 - \Gamma_{nm} r (\sin \phi + \sin \phi') \right]$$

to order r^2 . The average over ϕ and ϕ' gives

$$e^{-2\Gamma_{nm}\ell} \left[1 + \left(\Gamma_{nm}^2 - \frac{n^2\pi^2}{a^2} \right) \frac{r^2}{2} \right] = e^{-2\Gamma_{nm}\ell} \left(1 + k_m^2 \frac{r^2}{2} \right).$$

Since these terms are significant only for the lowest values of n and m , the approximation is adequate for the terms we need.

We now collect all of these results so as to rewrite the fundamental integral equation for the probe current $I(y)$ in the form

$$\begin{aligned} & \frac{jZ_0 k_0}{b} \left[\frac{jk_0^2 r^2}{16} + \frac{k_0^2 r^2}{8\pi} \left(\gamma + \ln \frac{k_0 r}{2} \right) - \frac{1}{2\pi} \ln \frac{\pi r}{2a} + \sum_{n=1,3,\dots}^{\infty} \left(\frac{e^{-\Gamma_{n0}r}}{\Gamma_{n0}a} - \frac{e^{-n\pi r/a}}{n\pi} \right) \right. \\ & \quad \left. + \left(1 - \frac{k_0^2 r^2}{2} \right) \sum_{n=1,3,\dots}^{\infty} \frac{e^{-2\Gamma_{n0}\ell}}{\Gamma_{n0}a} \right] \int_0^d I(y) dy - \frac{2jZ_0}{k_0 b} \\ & \quad \cdot \sum_{m=1}^{\infty} \left[\frac{1}{2\pi} I_0(k_m r) K_0(k_m r) + \sum_{n=1}^{\infty} \frac{4K_0(k_m 2na) - 2K_0(k_m na)}{2\pi} \right. \\ & \quad \left. - \left(1 + \frac{k_m^2 r^2}{2} \right) \sum_{n=1,3,\dots}^{\infty} \frac{e^{-2\Gamma_{nm}\ell}}{\Gamma_{nm}a} \right] k_m^2 \cos \frac{m\pi y'}{b} \int_0^d I(y) \cos \frac{m\pi y}{b} dy = Ve_a(y'). \end{aligned} \tag{22}$$

All the series in this expression converge very rapidly so only a few terms need to be retained.

The basis functions that will be used to represent $I(y)$ are

$$\psi_1(y) = \frac{\sin k_0(d-y)}{\sin k_0 d} \tag{23a}$$

$$\psi_2(y) = \frac{1 - \cos k_0(d-y)}{1 - \cos k_0 d}. \tag{23b}$$

For these functions

$$\int_0^d \psi_1(y) \cos \frac{m\pi y}{b} dy = P_m = \frac{k_0 \left(\cos k_0 d - \cos \frac{m\pi d}{b} \right)}{k_m^2 \sin k_0 d} \quad (24a)$$

$$\int_0^d \psi_2(y) \cos \frac{m\pi y}{b} dy = Q_m = \frac{k_0 \sin k_0 d - (k_0^2 b / m\pi) \sin m\pi d / b}{k_m^2 (1 - \cos k_0 d)}. \quad (24b)$$

By using these expressions the matrix elements G_{nm} are readily evaluated. In order to simplify the expressions we will express (22) in the form

$$g_0 \int_0^d I(y) dy + \sum_{m=1}^{\infty} g_m \cos \frac{m\pi y'}{b} \int_0^d I(y) \cos \frac{m\pi y}{b} dy = V e_a(y')$$

and then

$$G_{11} = g_0 P_0^2 + \sum_{m=1}^{\infty} g_m P_m^2 \quad (25a)$$

$$G_{12} = G_{21} = g_0 P_0 Q_0 + \sum_{m=1}^{\infty} g_m P_m Q_m \quad (25b)$$

$$G_{22} = g_0 Q_0^2 + \sum_{m=1}^{\infty} g_m Q_m^2. \quad (25c)$$

The solution for Z_{in} is given by (15). Upon solving (14) for I_1 and I_2 we obtain

$$Z_{in} = \frac{G_{11}G_{22} - G_{12}^2}{f_1 G_{22} + f_2 G_{11} - (f_1 + f_2) G_{12}}. \quad (26)$$

In order to evaluate this expression we need to find the coefficients f_1 and f_2 . The field $e_a(y')$ is given by

$$\int_0^{2\pi} \int_r^{r_0} \mathbf{a}_y \times \mathbf{a}_{\rho} \frac{1}{\ln r_0 / r} \cdot \nabla \times \bar{\mathbf{G}}_e \cdot \mathbf{a}_y d\rho d\phi.$$

The field $e_a(y)$ is localized near the probe input at $y = 0$ so we can approximate it by using a quasi-static solution. The curl of the free-space dyadic Green's function and its image in the $y = 0$ plane in the quasi-static approximation is simply

$$\nabla \times \frac{\bar{\mathbf{I}}}{2\pi R} = \frac{1}{2\pi} \nabla \frac{1}{R} \times \bar{\mathbf{I}}.$$

Hence

$$\begin{aligned} e_a(y) &\approx \frac{-1}{2\pi \ln r_0/r} \int_r^{r_0} \int_0^{2\pi} \frac{\partial}{\partial \rho} \frac{1}{R} d\phi d\rho \\ &= \frac{-2}{\pi \ln r_0/r} \int_0^{\pi/2} \left[\frac{1}{\sqrt{y^2 + (r_0 + r)^2 - 4r_0 r \cos^2 u}} - \frac{1}{\sqrt{y^2 + 4r^2 - 4r^2 \cos^2 u}} \right] du \end{aligned}$$

where we have put $\phi - \phi' = 2u$ and used $R = |\mathbf{a}_y y + \mathbf{a}_x(\rho \cos \phi - r \cos \phi') + \mathbf{a}_z(\rho \sin \phi - r \sin \phi')|$.

The parameters f_1 and f_2 are given by

$$f_1 = \int_0^d \psi_1(y) e_a(y) dy \quad (27a)$$

$$f_2 = \int_0^d \psi_2(y) e_a(y) dy \quad (27b)$$

and are evaluated numerically using the approximate solution for $e_a(y)$. The solution for $e_a(y)$ can be expressed in terms of elliptic integrals if desired; thus

$$e_a(y) = \frac{-2}{\pi \ln r_0/r} \left[\frac{k_1 K(k_1)}{2\sqrt{rr_0}} - \frac{k_2 K(k_2)}{2r} \right]$$

where $k_1^2 = 4rr_0/[y^2 + (r + r_0)^2]$, $k_2^2 = 4r^2/[y^2 + 4r^2]$ and K is the complete elliptic integral of the first kind. When y approaches zero k_2 approaches one and the field $e_a(y)$ takes on the limiting value

$$e_a(y) \sim \frac{-1}{r\pi \ln r_0/r} \ln \frac{y}{8r}.$$

In view of this logarithmic singularity the numerical evaluation of (27) must be done carefully. A convenient procedure is to use

$$\int_0^d \psi_i(y) e_a(y) dy = \int_0^d [\psi_i(y) - 1] e_a(y) dy + \int_0^d e_a(y) dy$$

where we have used $\psi_i(0) = 1$, $i = 1, 2$. The last integral is given by

$$\begin{aligned} &\frac{2}{\pi \ln r_0/r} \left[\int_0^{\pi/2} \ln \frac{d + \sqrt{d^2 + (r_0 + r)^2 - 4rr_0 \cos^2 u}}{d + \sqrt{d^2 + 4r^2 - 4r^2 \cos^2 u}} du \right. \\ &\quad \left. + \int_0^{\pi/2} \ln 2r \sin u du - \frac{1}{2} \int_0^{\pi/2} \ln[(r_0 + r)^2 - 4rr_0 \cos^2 u] du \right] \\ &= -1 + \frac{2}{\pi \ln r_0/r} \int_0^{\pi/2} \ln \frac{d + \sqrt{d^2 + (r_0 + r)^2 - 4rr_0 \cos^2 u}}{d + \sqrt{d^2 + 4r^2 - 4r^2 \cos^2 u}} du. \end{aligned}$$

This procedure eliminates the troublesome singularity that occurs at $y = 0$. The integral

involving $\psi_i(y) - 1$ has a vanishing integrand at $y = 0$ and can be evaluated numerically in a straightforward manner.

A worthwhile improvement in the accuracy of the solution for the input impedance is obtained by including a frequency-dependent contribution to the applied electric field. The following approximation can be used:

$$\frac{e^{-jk_0R}}{2\pi R} = \frac{1}{2\pi R} - \frac{jk_0}{2\pi} - \frac{k_0^2 R}{4\pi} + \frac{jk_0^3 R^2}{12\pi}.$$

Since $e_a(y)$ is generated by taking a derivative with respect to ρ followed by an integral over ρ the corrections to the constants f_1 and f_2 are readily evaluated and are

$$\begin{aligned} \Delta f_i = & -\frac{k_0^2}{\pi \ln(r_0/r)} \int_0^d \int_0^{\pi/2} \psi_i(y) [\sqrt{y^2 + (r_0 + r)^2 - 4rr_0 \cos^2 u} \\ & - \sqrt{y^2 + 4r^2 - 4r^2 \cos^2 u}] du dy \\ & + \frac{jk_0^3(r_0^2 - r^2)}{6 \ln(r_0/r)} \begin{cases} P(0), & i = 1 \\ Q(0), & i = 2. \end{cases} \end{aligned}$$

These corrections produce a 5 to 10% change in the computed values of Z_{in} and thus demonstrate that Z_{in} is quite sensitive to the values of the applied electric field that acts on the probe.

In Fig. 7.3 we show some computed values for the probe resistance R and reactance X as a function of frequency. The results shown are based on the formulas given above and include the corrections Δf_i . The data apply for a standard X -band waveguide with $a = 2.286$ cm, $b = 1.016$ cm, and a probe length $d = 0.62$ cm. For the two probe radii of 1 and 1.5 mm the short-circuit position $\ell = 0.495$ cm. For the thin probe having $r = 0.5$ mm the short-circuit position is at $\ell = 0.505$ cm. In Fig. 7.4 the return loss, given by

$$\text{Loss} = 20 \log |\Gamma|$$

where Γ is the reflection coefficient, is shown. For both figures the coaxial line has a characteristic impedance of 50 ohms. From Fig. 7.4 it is quite clear that the thick probe provides a broader bandwidth of operation. At the -30 dB return loss level the thick probe has a bandwidth of 9%, while the corresponding bandwidth of the thin probe is about 4.5%.

In Fig. 7.5 we show the probe impedance for various probe lengths. The probe radius is 1 mm and the short-circuit position ℓ is chosen so that $2\beta\ell = \pi/2$ at 10 GHz, i.e., $\ell = 0.609$ cm. This choice of ℓ maximizes the inductive loading from the H_{10} standing wave at 10 GHz. Of particular interest are the decreasing values of probe reactance with increasing frequency when the probe length is greater than about 0.65 cm. This feature can be used to design a broadband waveguide to waveguide probe-probe coupling system of the type shown in Fig. 7.6. At the center of the frequency band of interest the transmission-line length is chosen so as to transform the impedance of one probe into the complex conjugate of the impedance of the second probe. When the frequency changes, the changing electrical length of the transmission line is compensated for by the manner in which the reactance of the probes changes with frequency. This compensation results in a relatively well matched system over a broad band of frequencies.

The input impedance was also computed using three basis functions to expand the current.

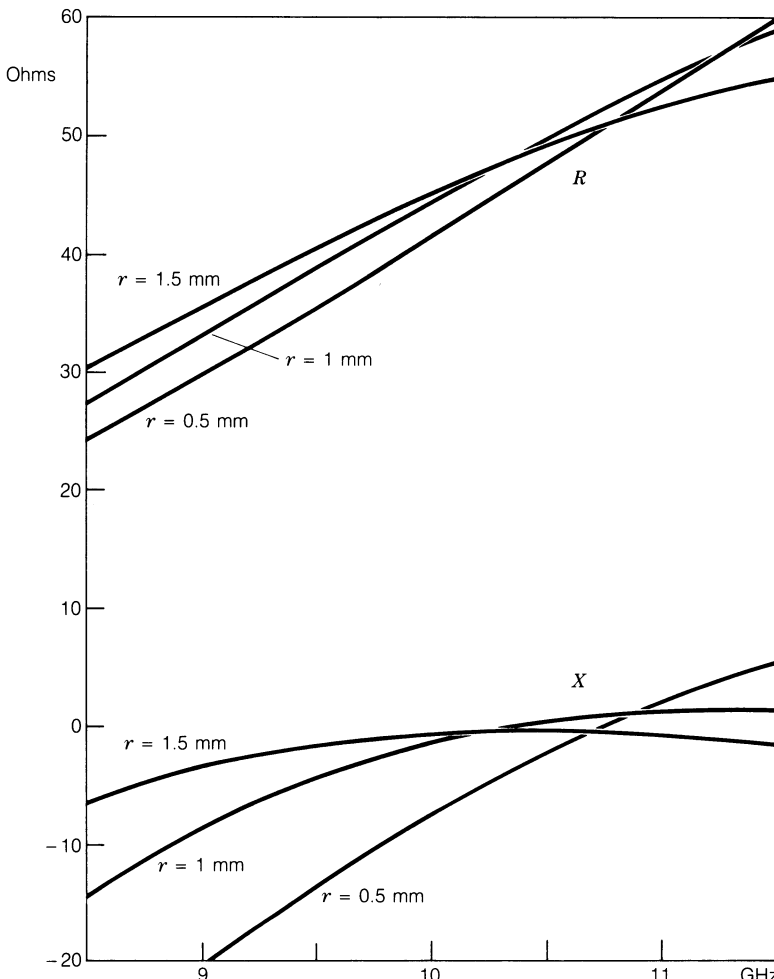


Fig. 7.3. Probe input resistance and reactance as a function of frequency for $d = 0.62$ cm, $\ell = 0.495$ cm, $a = 2.286$ cm, $b = 1.016$ cm. For the thin probe $r = 0.5$ mm, $\ell = 0.505$ cm.

The first was $\psi_1(y)$ as already specified and the other two were

$$\psi_2 = \cos 3\pi y/2d$$

$$\psi_3 = \cos 5\pi y/2d.$$

Some representative results are shown in Fig. 7.5 as broken curves for $d = 0.5$ cm and 0.8 cm. For short probes the use of two basis functions appears to be adequate, but for the longer probes the use of three basis functions makes a significant difference in the computed values of the probe impedance.

There is very little experimental data on waveguide probe antenna impedance that can be used to check the accuracy of the approximate theory given above. Jarem has made calculations similar to the above using the same basis functions for the expansion of the current and found the agreement with experimental results to be quite good for a moderately thick probe [7.17].

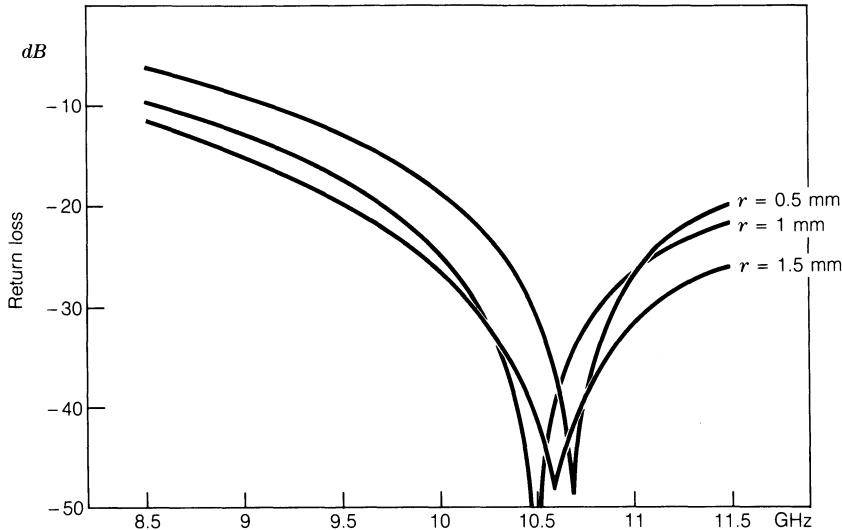


Fig. 7.4. Return loss for the probe antennas of Fig. 7.3.

Ragan has described a probe antenna in [7.20] for which $a = 7.2136 \text{ cm}$, $b = 3.4036 \text{ cm}$, $r_0 = 1.9393 \text{ cm}$, $r = 0.7937 \text{ cm}$, $\ell = 2.55 \text{ cm}$, $d = 1.91 \text{ cm}$ and that is impedance matched at 2.747 GHz. For this case our theory gives $Z_{\text{in}} = 57.3 - j18$. The line impedance is 53.4 ohms so the return loss is only -15.72 dB . By increasing the probe length to 2.12 cm and reducing ℓ to 1.95 cm our theory predicts an impedance match (return loss of -51 dB). If we use $\cos(3\pi y/2d)$ for the second basis function $\psi_2(y)$ we find that $d = 1.994 \text{ cm}$ and $\ell = 2.17 \text{ cm}$ for an impedance match. These values are in closer agreement with those given by Ragan and thus indicate that the second choice is a better one for the basis function ψ_2 .

In another example involving an *X*-band waveguide the optimum values of d and ℓ are given as $d = 0.635 \text{ cm}$ and $\ell = 0.787 \text{ cm}$ at 9.09 GHz. Our theory requires $d = 0.67 \text{ cm}$ and $\ell = 0.55 \text{ cm}$. If we use the alternative basis function ψ_2 given above we find that we require $d = 0.632 \text{ cm}$ and $\ell = 0.62 \text{ cm}$. These values are in better agreement with the experimental ones. When we use three basis functions we find that the optimum value of ℓ is 0.601 cm for $d = 0.635 \text{ cm}$. The evidence suggests that the theory predicts an optimum value of ℓ that is too small. Furthermore, the limitation does not appear to be the number of basis functions used to expand the current. The probes for which the theory is being compared against experimental data are thick probes. It can be expected that for these cases it will be necessary to include the effects of higher order modes in the coaxial transmission line and to use a better approximation for the applied field $e_a(y)$.

The theory as given does not appear to be of high accuracy for probes that are as thick as those used in typical coaxial-line-waveguide transitions. The results given by Jarem, for which good agreement with experimental data was obtained, involved a probe of radius approximately equal to $0.03a$. For the examples discussed above the probe radii are $0.11a$ and $0.07a$, respectively, which are significantly larger.

7.2. THE LOOP ANTENNA

As an example of a loop antenna, we consider a coaxial line terminated in the narrow wall of an infinitely long rectangular guide and with its center conductor bent into a semicircular

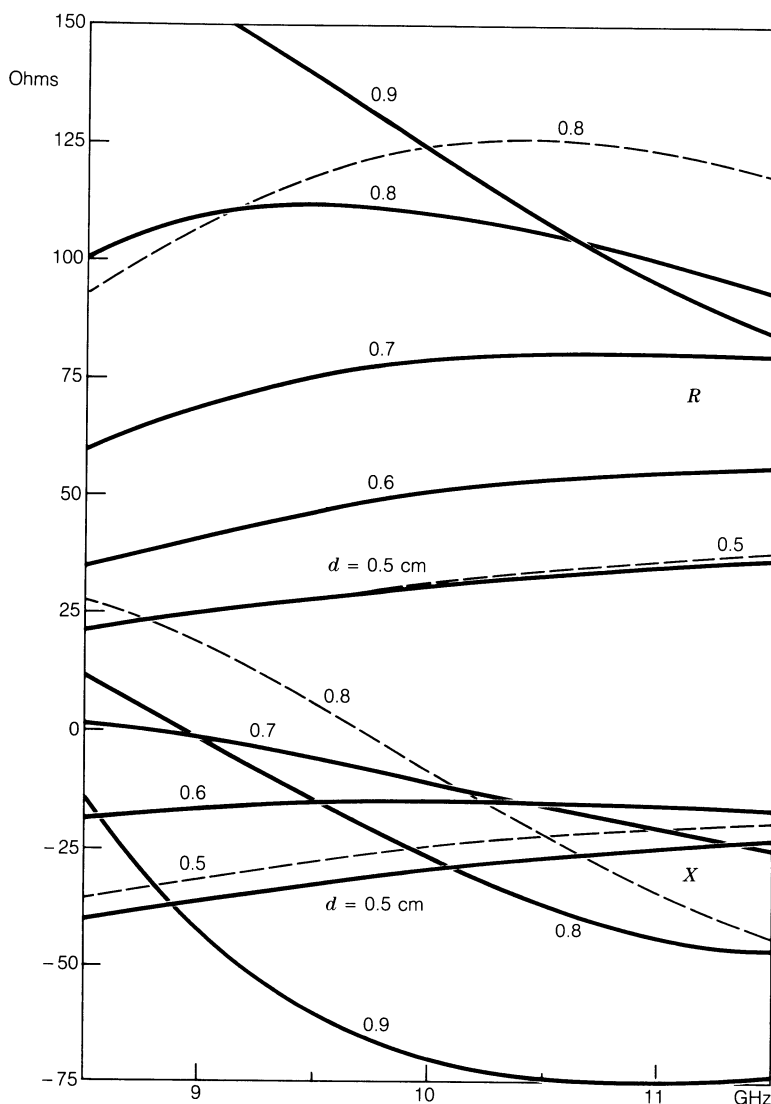


Fig. 7.5. Probe impedance data for various probe lengths. a and b as in Fig. 7.3, $\ell = 0.609$ cm, $r = 1$ mm. The broken curves are based on the use of three basis functions.

loop of radius d , as in Fig. 7.7. The center of the loop is located midway between the top and bottom walls of the guide and coincides with the origin of the coordinate system to be used. The plane of the loop is parallel to the xy plane, and hence only those modes (H_{nm} modes) with an axial magnetic field component are excited. Provided the size of the loop is small compared with a wavelength, say d less than $0.1\lambda_0$, the current in the loop may be assumed constant.

For the purpose of computing the power radiated into the guide, the current may be considered concentrated in a thin filament along the center of the conductor. The evaluation of the

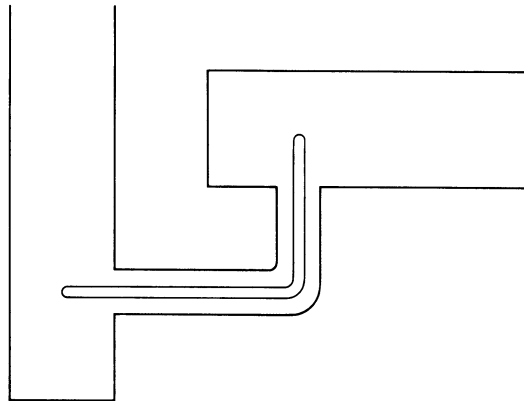


Fig. 7.6. Probe-probe coupling of two waveguides.

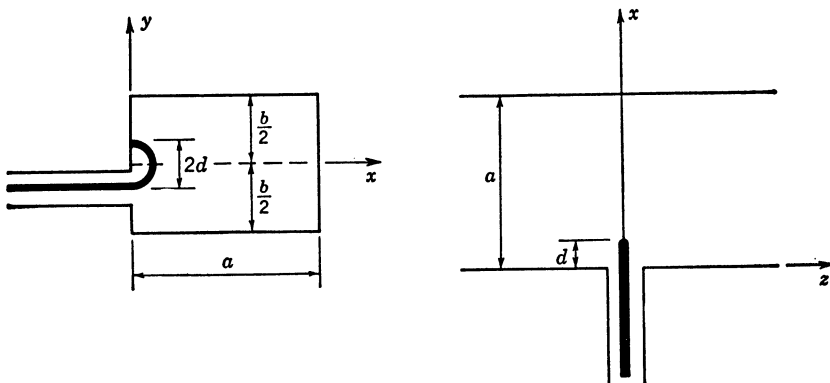


Fig. 7.7. Coaxial-line loop antenna.

radiated power leads directly to an expression for the input resistance (radiation resistance) of the antenna. The radiated power is readily evaluated by finding the coupling coefficient between the propagating H_{10} mode (all other modes are assumed to be evanescent) and the loop antenna, according to the methods given in Section 5.6. To evaluate the input reactance to the antenna, the finite radius r of the conductor must be taken into account, or else we run into the embarrassing situation of an infinite reactance. To evaluate the reactance term, the antenna and guide will be replaced by a double infinite array of image antennas. Our calculation then reduces to finding the self-inductance of a single loop in free space and the mutual inductance between the loop at the origin and all the image loops. In this formulation it is quite clear what approximations can be made with negligible error. An analysis based entirely on an expansion in terms of the normal waveguide modes could also be carried out, but the approximations that can be made are not so apparent in this case.

The normalized H_{nm} modes may be derived from the scalar function

$$\psi_{nm}(x, y) = \left(\frac{\epsilon_0 n \epsilon_m}{ab j k_0 Z_0 \Gamma_{nm} k_{c,nm}^2} \right)^{1/2} \cos \frac{n\pi x}{a} \cos m\pi \frac{2y - b}{b} \quad (28)$$

by means of the following equations:

$$\mathbf{h}_{znm} = \mathbf{a}_z k_{c,nm}^2 \psi_{nm} \quad (29a)$$

$$\mathbf{h}_{nm} = -\Gamma_{nm} \nabla_t \psi_{nm} \quad (29b)$$

$$\mathbf{e}_{nm} = \frac{jk_0 Z_0}{\Gamma_{nm}} (\mathbf{a}_x \mathbf{a}_y - \mathbf{a}_y \mathbf{a}_x) \cdot \mathbf{h}_{nm} \quad (29c)$$

$$\mathbf{E}_{nm}^{\pm} = \mathbf{e}_{nm} e^{\mp \Gamma_{nm} z} \quad (29d)$$

$$\mathbf{H}_{nm}^{\pm} = (\pm \mathbf{h}_{nm} + \mathbf{h}_{znm}) e^{\mp \Gamma_{nm} z} \quad (29e)$$

where $k_{c,nm}^2 = (m\pi/b)^2 + (n\pi/a)^2$, \mathbf{h}_{nm} and \mathbf{e}_{nm} are the transverse magnetic and electric normal mode fields, and $\Gamma_{nm}^2 = k_{c,nm}^2 - k_0^2$. The normalization in (28) has been chosen so that

$$\int_0^a \int_0^b \mathbf{e}_{nm} \times \mathbf{h}_{nm} \cdot \mathbf{a}_z dx dy = 1. \quad (30)$$

The axial magnetic field in the two regions $z < 0$ and $z > 0$ may be represented as an expansion in terms of the above normal mode functions as follows:

$$\mathbf{H}_z = \begin{cases} \sum_{n=0}^{\infty} \sum_{m=0}^{\infty} C_{nm} \mathbf{h}_{znm} e^{-\Gamma_{nm} z}, & z > 0 \\ \sum_{n=0}^{\infty} \sum_{m=0}^{\infty} D_{nm} \mathbf{h}_{znm} e^{\Gamma_{nm} z}, & z < 0. \end{cases} \quad (31)$$

From Chapter 5, Eqs. (82) and (83), the coefficients are given by

$$C_{nm} = D_{nm} = \frac{j\omega\mu_0 I_0}{2} \iint_{S_0} \mathbf{h}_{znm} \cdot \mathbf{a}_z dx dy \quad (32)$$

where S_0 is the surface spanned by the loop, and I_0 is the total loop current assumed concentrated in a thin filament. For the H_{10} mode, the coupling coefficient C_{10} is given by

$$C_{10} = \frac{j\omega\mu_0 I_0}{2} \left(\frac{\pi}{a} \right)^2 \left(\frac{2a}{jk_0 Z_0 \Gamma_{10} \pi^2 b} \right)^{1/2} \iint_{S_0} \cos \frac{\pi x}{a} dx. \quad (33)$$

Introducing a local cylindrical coordinate system $t\theta$ as in Fig. 7.8 and expanding $\cos(\pi x/a)$ since $\pi d/a$ is small, the integral in (33) becomes

$$\int_0^d \int_0^\pi \left(1 - \frac{1}{2} \frac{\pi^2}{a^2} t^2 \cos^2 \theta \right) t dt d\theta = \frac{\pi d^2}{2} \left(1 - \frac{\pi^2 d^2}{8a^2} \right) \approx \frac{\pi d^2}{2}.$$

The power radiated into the guide is twice that radiated in one direction and, hence, is given

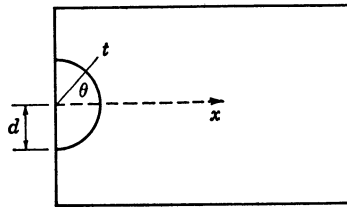


Fig. 7.8.

by

$$P = \int_0^a \int_0^b C_{10} C_{10}^* \mathbf{e}_{10} \times \mathbf{h}_{10}^* \cdot \mathbf{a}_z dx dy = C_{10} C_{10}^*$$

since, from the definition of the normal mode functions and the normalization condition (30), we have

$$\int_0^a \int_0^b \mathbf{e}_{nm} \times \mathbf{h}_{nm}^* \cdot \mathbf{a}_z dx dy = \begin{cases} 1 & \Gamma_{nm} \text{ imaginary} \\ j & \Gamma_{nm} \text{ real.} \end{cases}$$

Substituting for C_{10} , we get

$$P = \frac{k_0 Z_0}{2\beta_{10} ab} \left(\frac{\pi}{a}\right)^2 \left(\frac{\pi d^2}{2}\right)^2 I_0^2 \quad (34)$$

where $\beta_{10}^2 = k_0^2 - (\pi/a)^2$. If the higher order modes in the coaxial line are neglected, the integral of the complex Poynting vector over the coaxial-line opening gives $\frac{1}{2}Z_{in}I_0^2$, since I_0 may be assumed real. The input impedance is given by

$$Z_{in} = \frac{P + 2j\omega(W_m - W_e)}{\frac{1}{2}I_0^2}$$

and, hence, the input resistance, i.e., radiation resistance, is

$$R = \frac{k_0 Z_0}{ab\beta_{10}} \left(\frac{\pi}{a}\right)^2 \left(\frac{\pi d^2}{2}\right)^2. \quad (35)$$

The radiation resistance is seen to be proportional to the square of the loop area and for a small loop is quite small; typical values range from 10 to 30 ohms.

To evaluate the input reactance, we replace the semicircular loop and the guide by a lattice of loop antennas as illustrated in Fig. 7.9. After we have found the field radiated by a single circular loop, it will be seen that the system of loop antennas in Fig. 7.9 radiates a total field which has a zero tangential electric field on the guide boundary. The semicircular loop and its image in the $x = 0$ guide wall are illustrated in Fig. 7.10 and are equivalent to a circular loop driven by a voltage generator having twice the voltage required to maintain the current in the semicircular loop.

To evaluate the input reactance to the antenna, we must compute the total flux linking the loop at the origin due to all of the image antennas, plus the self-flux linkage arising from the magnetic field set up by its own current. The time rate of change of the flux linking the antenna

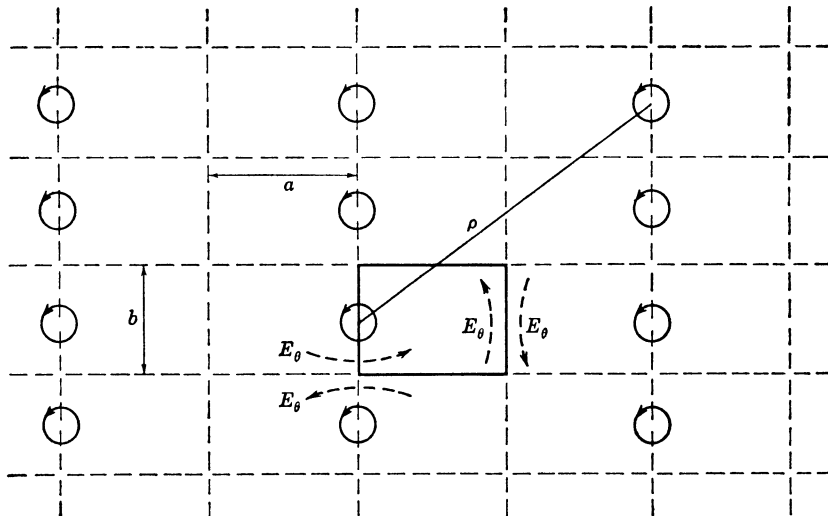


Fig. 7.9. The loop antenna and its images.

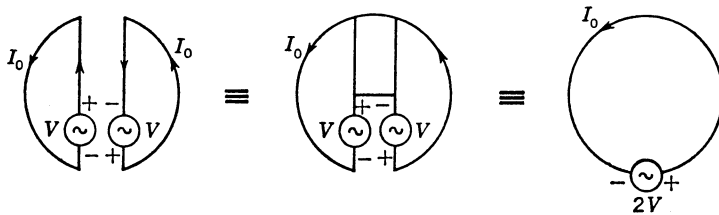


Fig. 7.10. Semicircular loop, its image, and their equivalent loop configuration.

results in a back emf being induced. The applied voltage must be equal and opposite to this induced emf, in order to maintain the current I_0 in the loop. The flux linking the antenna and in phase with the current I_0 leads to an induced emf in phase quadrature with the current. It is this flux which gives rise to the inductive reactance term. The flux linking the antenna and in phase quadrature with the current gives rise to an emf in phase with the current, and hence contributes to the radiation resistance. Since we have already obtained an expression for the radiation resistance, we are interested only in that part of the flux linkage which is in phase with the current I_0 .

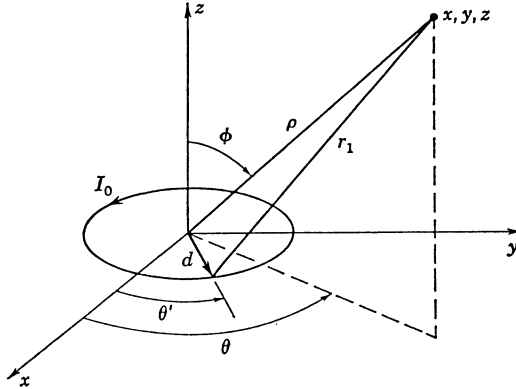
The field from the image antennas at the position of the loop located at the origin may be found with negligible error by assuming the current I_0 to be concentrated in a thin filament. Each image loop may be replaced by a z -directed magnetic dipole of moment $M = I_0\pi d^2$. To find the field radiated by this array of magnetic dipoles it is convenient to first find a magnetic-type Hertzian potential Π_z having only a z component. The relevant equations are

$$\nabla^2 \Pi_z + k_0^2 \Pi_z = -M$$

$$H_z = k_0^2 \Pi_z + \frac{\partial^2 \Pi_z}{\partial z^2}.$$

For a single loop antenna located at the origin as in Fig. 7.11 the solution is

$$\Pi = \frac{M}{4\pi\rho} e^{-jk_0\rho}$$

Fig. 7.11. Loop antenna in the xy plane.

where $\rho = (x^2 + y^2 + z^2)^{1/2}$. For a row of dipoles located at $y = mb$, $m = 0, \pm 1, \pm 2, \dots$, the potential is given by

$$\Pi_1 = \frac{M}{4\pi} \sum_{m=-\infty}^{\infty} \frac{\exp\{-jk_0[x^2 + z^2 + (y - mb)^2]^{1/2}\}}{[x^2 + z^2 + (y - mb)^2]^{1/2}}. \quad (36)$$

This series is readily converted to a more rapidly converging one by using the Poisson summation formula. The required Fourier transform is

$$\int_{-\infty}^{\infty} e^{jwu} \frac{\exp\{-jk_0[x^2 + z^2 + (y - u)^2]^{1/2}\}}{[x^2 + z^2 + (y - u)^2]^{1/2}} du = 2e^{jwy} K_0[(x^2 + z^2)(w^2 - k_0^2)]^{1/2} \quad (37)$$

where K_0 is the modified Bessel function of the second kind. Using the Poisson summation formula now converts (36) into the following:

$$\begin{aligned} & \frac{M}{4\pi} \sum_{m=-\infty}^{\infty} \frac{\exp\{-jk_0[x^2 + z^2 + (y - mb)^2]^{1/2}\}}{[x^2 + z^2 + (y - mb)^2]^{1/2}} \\ &= \frac{M}{2\pi b} \sum_{m=-\infty}^{\infty} e^{j2m\pi y/b} K_0[\Gamma_{0m}(x^2 + z^2)^{1/2}] \\ &= \frac{M}{\pi b} \left\{ \frac{1}{2} K_0[jk_0(x^2 + z^2)^{1/2}] + \sum_{m=1}^{\infty} \cos \frac{2m\pi y}{b} K_0[\Gamma_{0m}(x^2 + z^2)^{1/2}] \right\} \end{aligned} \quad (38)$$

where $\Gamma_{0m} = [(2m\pi/b)^2 - k_0^2]^{1/2}$.

The potential arising from all the image dipoles is obtained by replacing x by $x - 2na$ in (38) and summing over all n but excluding the contribution from the dipole at the origin (the driven loop). The flux linkage will be computed by evaluating the magnetic field at the center of the loop and multiplying by the loop area. The evaluation of H_z involves derivatives with respect to z only, and so we may place x and y equal to zero at this point. For the rows of dipoles located at $x = 2na$, $n = \pm 1, \pm 2, \dots$, we get, from (38),

$$\Pi_2 = \frac{M}{2\pi b} \sum_{n=-\infty}^{\infty}' K_0[jk_0(z^2 + 4n^2a^2)^{1/2}] + \frac{2M}{\pi b} \sum_{n=1}^{\infty} \sum_{m=1}^{\infty} K_0[\Gamma_{0m}(z^2 + 4n^2a^2)^{1/2}]. \quad (39a)$$

To the above we must add the contribution from dipoles located at $x = z = 0$, $y = mb$, $m = \pm 1, \pm 2, \dots$. This latter contribution is, from (36),

$$\frac{M}{2\pi} \sum_{m=1}^{\infty} \frac{\exp[-jk_0(z^2 + m^2 b^2)^{1/2}]}{(z^2 + m^2 b^2)^{1/2}}. \quad (39b)$$

In (39a) the double series may be neglected, since, for the range of parameters involved here, $K_0[\Gamma_{0m}(z^2 + 4n^2 a^2)^{1/2}]$ is extremely small. The first series, however, converges very slowly because the argument is imaginary. By using the Poisson summation formula again, this series may be transformed as follows [the required transform may be obtained by inverting (37)]:

$$\frac{M}{2\pi b} \sum_{n=-\infty}^{\infty} K_0[jk_0(z^2 + 4n^2 a^2)^{1/2}] - \frac{M}{2\pi b} K_0(jk_0 z) = \frac{M}{4ab} \sum_{n=-\infty}^{\infty} \frac{e^{-\Gamma_{n0} z}}{\Gamma_{n0}} - \frac{M}{2\pi b} K_0(jk_0 z)$$

where $\Gamma_{n0} = [(n\pi/a)^2 - k_0^2]^{1/2}$. Our final expression for the total Hertzian potential is

$$\Pi_z = \frac{M}{4ab} \sum_{n=-\infty}^{\infty} \frac{e^{-\Gamma_{n0} z}}{\Gamma_{n0}} - \frac{M}{2\pi b} K_0(jk_0 z) + \frac{M}{2\pi} \sum_{m=1}^{\infty} \frac{\exp[-jk_0(z^2 + m^2 b^2)^{1/2}]}{(z^2 + m^2 b^2)^{1/2}}. \quad (40)$$

The field H_z , at the origin, is given by $k_0^2 \Pi_z + \partial^2 \Pi_z / \partial z^2$ evaluated for $z = 0$. The first term gives a contribution

$$\frac{k_0^2 M}{4ab} \sum_{n=-\infty}^{\infty} \frac{e^{-\Gamma_{n0} z}}{\Gamma_{n0}} - \frac{k_0^2 M}{2\pi b} K_0(jk_0 z) + \frac{k_0^2 M}{2\pi} \sum_{m=1}^{\infty} \frac{e^{-jk_0 m b}}{mb}$$

where the limit as z tends to zero is to be taken. We have $\Gamma_{n0}^{-1} \approx a/n\pi$, and hence the first series is a dominant series

$$\frac{k_0^2 M}{2ab} \sum_{m=1}^{\infty} \frac{ae^{-n\pi z/a}}{n\pi}$$

together with the correction series

$$\frac{k_0^2 M}{2ab} \left[\sum_{n=1}^{\infty} \left(\frac{1}{\Gamma_{n0}} - \frac{a}{n\pi} \right) - \frac{j}{2k_0} \right].$$

The dominant series is readily summed by the methods given in the Mathematical Appendix to give

$$-\frac{k_0^2 a M}{2\pi ab} \left(\ln 2 \sinh \frac{\pi z}{2a} - \frac{\pi z}{2a} \right).$$

The logarithmic singularity occurring here is canceled by that arising from the term $K_0(jk_0 z)$ since for z small we have $K_0(jk_0 z) \rightarrow -[\gamma + \ln(jk_0 z/2)]$, where $\gamma = 0.577$ and is Euler's constant. If the series in m is also summed and the real part of all terms taken, we finally

obtain for the part of $k_0^2 \Pi_z$ which is in phase with the current I_0 the result

$$\operatorname{Re}(k_0^2 \Pi_z) = \frac{k_0^2 M}{2\pi b} \left[\gamma + \ln \frac{k_0 a}{2\pi} - \ln 2 \sin \frac{k_0 b}{2} + \frac{\pi}{a} \sum_{n=2}^{\infty} \left(\frac{1}{\Gamma_{n0}} - \frac{a}{n\pi} \right) - 1 \right]. \quad (41)$$

To find the second part of H_z , we first evaluate $\partial^2 \Pi_z / \partial z^2$ to get

$$\begin{aligned} \frac{\partial^2 \Pi_z}{\partial z^2} &= \frac{M}{4ab} \sum_{n=-\infty}^{\infty} \Gamma_{n0} e^{-\Gamma_{n0} z} + \frac{M k_0^2}{2\pi b} \left[K_0(jk_0 z) + \frac{K_1(jk_0 z)}{jk_0 z} \right] \\ &\quad + \frac{M}{2\pi} \sum_{m=1}^{\infty} \frac{e^{-jk_0 r_m}}{r_m} \left[\frac{jk_0 z}{r_m^2} + \frac{2z}{r_m^3} - \frac{k_0^2 z}{r_m} + \frac{jk_0 z}{r_m^2} - \left(jk_0 + \frac{1}{r_m} \right) \left(\frac{1}{r_m} - \frac{z^2}{r_m^3} \right) \right] \end{aligned}$$

where $r_m = (z^2 + m^2 b^2)^{1/2}$.

The first series consists of a dominant part

$$\frac{M}{2ab} \left[\sum_{n=1}^{\infty} e^{-n\pi z/a} \left(\frac{n\pi}{a} - \frac{k_0^2 a}{2\pi n} \right) \right]$$

plus a correction series

$$\frac{M}{2ab} \left[\sum_{n=1}^{\infty} \left(\Gamma_{n0} - \frac{n\pi}{a} + \frac{k_0^2 a}{2\pi n} \right) + \frac{jk_0}{2} \right]$$

since $\Gamma_{n0} \approx n\pi/a - k_0^2 a / 2\pi n$. The dominant part of the series sums to

$$\frac{M}{2ab} \left[\frac{\pi}{4a \sinh^2(\pi z/2a)} + \frac{k_0^2 a}{2\pi} \left(\ln 2 \sinh \frac{\pi z}{2a} - \frac{\pi z}{2a} \right) \right].$$

As z approaches zero, the singularities occurring in the above expression are canceled by those arising from the Bessel functions K_0 and K_1 . As x approaches zero, we have $K_0(x) \rightarrow -[\gamma + \ln(x/2)]$, and $K_1(x) \rightarrow x^{-1} + [\ln(x/2) + \gamma - \frac{1}{2}]x/2$, and these expansions may be used to evaluate the contribution from the terms $K_0(jk_0 z)$ and $K_1(jk_0 z)$.

In the series over m , we may place z equal to zero, and the resultant series are then readily summed. The required summation formulas are tabulated in the Mathematical Appendix, so we will write down only the final results that we require. After performing the indicated steps, we obtain for the real part of $\partial^2 \Pi_z / \partial z^2$ the following result:

$$\begin{aligned} \operatorname{Re} \frac{\partial^2 \Pi_z}{\partial z^2} &= \frac{M}{2ab} \left[\sum_{n=2}^{\infty} \left(\Gamma_{n0} - \frac{n\pi}{a} + \frac{k_0^2 a}{2\pi n} \right) - \frac{13\pi}{12a} + \frac{k_0^2 a}{4\pi} - \frac{\gamma k_0^2 a}{2\pi} \right. \\ &\quad \left. + \frac{k_0^2 a}{2\pi} \ln \frac{2\pi}{k_0 a} \right] - \frac{M}{2\pi b^3} \left(1.2 + \frac{k_0^2 b^2}{4} + \frac{3k_0^4 b^4}{288} - \frac{k_0^2 b^2}{2} \ln k_0 b \right). \quad (42) \end{aligned}$$

The total in phase flux linking the loop antenna at the origin is obtained by multiplying the real part of the field H_z from the image antennas by $\mu_0 \pi d^2$, that is, multiplying the sum of (41) and (42) by $\mu_0 \pi d^2$. Thus, the in phase flux linkage arising from the mutual coupling with

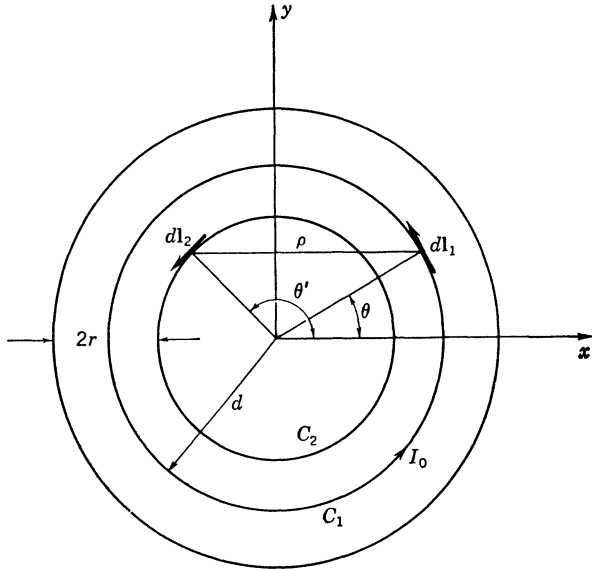


Fig. 7.12. Coordinate system for a single loop antenna.

the image antennas is given by

$$\sum'_{n,m} F_{nm} = \mu_0 \pi d^2 I_0 \pi d^2 \left[\frac{k_0^2}{4\pi b} \ln \frac{k_0^2 ab}{4\pi(1 - \cos k_0 b)} - \frac{k_0^2}{4\pi b} (2 - \gamma) - \frac{13\pi}{24a^2 b} \right. \\ \left. - \frac{0.6}{\pi b^3} - \frac{3k_0^4 b}{576\pi} + \frac{1}{2ab} \sum_{n=2}^{\infty} \left(\frac{k_0^2}{\Gamma_{n0}} + \Gamma_{n0} - \frac{n\pi}{a} - \frac{k_0^2 a}{2n\pi} \right) \right] \quad (43)$$

where M has been replaced by $I_0 \pi d^2$.

The only flux linkage left to be evaluated is that due to the current in the loop at the origin, i.e., the flux giving rise to the self-inductance of the loop. The vector potential is given by

$$\mathbf{A} = \frac{\mu_0}{4\pi} \iint_{S_0} \mathbf{J}_0 \frac{e^{-jk_0\rho}}{\rho} dS$$

where \mathbf{J}_0 is the uniform circumferential current density on the loop antenna surface S_0 , and ρ is the radial distance from a current element to the point in space where \mathbf{A} is computed. For a small loop with $\rho \leq 2d$, the exponential term does not vary significantly across the domain of the loop. To be consistent with our assumption of a uniform loop current, we place $e^{-jk_0\rho}$ equal to unity, and we are then left with the static field problem of evaluating the self-inductance of a small circular loop of radius d with a conductor radius r . The real part of the flux linkage will be correct to order $(k_0 d)^2$, since the second term in the expansion of $e^{-jk_0\rho}$ is $-jk_0\rho$, and contributes to the radiation resistance only. With reference to Fig. 7.12, the field at the surface of the conductor is $H = J_0 = I_0/2\pi r$, and is the same as that produced by a current filament I_0 at the center, i.e., located along the contour C_1 . The magnetic field does not penetrate into the conductor, and, hence, we only require the flux linking the contour

C_2 which coincides with the inner surface of the conductor. This flux linkage is given by

$$F_{00} = \iint \mathbf{B} \cdot d\mathbf{S} = \iint \nabla \times \mathbf{A} \cdot d\mathbf{S} = \oint_{C_2} \mathbf{A} \cdot d\mathbf{l}_2.$$

Substituting for \mathbf{A} gives

$$F_{00} = \frac{\mu_0 I_0}{4\pi} \oint_{C_2} \oint_{C_1} \frac{d\mathbf{l}_1 \cdot d\mathbf{l}_2}{\rho}. \quad (44)$$

From the figure it is seen that

$$\rho = [d^2 + (d - r)^2 - 2d(d - r) \cos(\theta' - \theta)]^{1/2}$$

and $d\mathbf{l}_1 \cdot d\mathbf{l}_2 = d(d - r) \cos(\theta' - \theta) d\theta d\theta'$. If we integrate over θ first, we must get a result independent of θ' in view of the symmetry involved. We may, therefore, place θ' equal to zero, and replace the integration over θ' by a factor 2π . Hence we get

$$\begin{aligned} F_{00} &= \frac{\mu_0 I_0}{2} \int_0^{2\pi} \frac{d(d - r) \cos \theta d\theta}{[d^2 + (d - r)^2 - 2d(d - r) \cos \theta]^{1/2}} \\ &= -\mu_0 I_0 d(d - r) \int_0^\pi \frac{\cos \theta d\theta}{[d^2 + (d - r)^2 + 2d(d - r) \cos \theta]^{1/2}}. \end{aligned}$$

This integral may be reduced to the standard form for elliptic integrals with the following substitutions: $\theta = 2\phi$, $\cos \theta = 1 - 2 \sin^2 \phi$, and

$$k^2 = \frac{4d(d - r)}{(2d - r)^2}.$$

We now get

$$\begin{aligned} &-\frac{2d - r}{2} \mu_0 I_0 k^2 \int_0^{\pi/2} \frac{1 - 2 \sin^2 \phi}{(1 - k^2 \sin^2 \phi)^{1/2}} d\phi \\ &= (2d - r) \mu_0 I_0 \left[\left(1 - \frac{k^2}{2}\right) \int_0^{\pi/2} \frac{d\phi}{(1 - k^2 \sin^2 \phi)^{1/2}} - \int_0^{\pi/2} \frac{1 - k^2 \sin^2 \phi}{(1 - k^2 \sin^2 \phi)^{1/2}} d\phi \right] \\ &= (2d - r) \mu_0 I_0 \left[\left(1 - \frac{k^2}{2}\right) K(k) - E(k) \right] \end{aligned} \quad (45)$$

where K and E are complete elliptic integrals of modulus k [7.2]. Referring back to the definition of k , it is seen that $k \approx 1$ and, hence, $K(k) \approx \ln[4/(1 - k^2)^{1/2}]$, $E(k) \approx 1$. Replacing $(1 - k^2)^{1/2}$ by $r/2d$, we get

$$F_{00} = \mu_0 I_0 d \left(\ln \frac{8d}{r} - 2 \right). \quad (46)$$

If F is the total flux linkage, the total induced back emf will be $j\omega F$ and must equal the

applied voltage $2V$. Hence we have

$$2V = j\omega F$$

$$2VI_0 = 2I_0^2 Z_{\text{in}} = j\omega F I_0$$

$$Z_{\text{in}} = R + jX = \frac{j\omega F}{2I_0}$$

and

$$X = \text{Re} \frac{\omega F}{2I_0}.$$

Adding together all the contributions to F gives the following expression for the input reactance to the small-loop antenna:

$$X = \frac{Z_0 k_0 d}{2} \left(\ln \frac{8d}{r} - 2 \right) - \frac{\pi^2 d^4 k_0 Z_0}{2} \left[\frac{k_0^2}{4\pi b} (2 - \gamma) + \frac{13\pi}{24a^2 b} + \frac{0.6}{\pi b^3} + \frac{3k_0^4 b}{576\pi} \right. \\ \left. - \frac{k_0^2}{4\pi b} \ln \frac{k_0^2 ab}{4\pi(1 - \cos k_0 b)} - \frac{1}{2ab} \sum_{n=2}^{\infty} \left(\frac{k_0^2}{\Gamma_{n0}} + \Gamma_{n0} - \frac{n\pi}{a} - \frac{k_0^2 a}{2n\pi} \right) \right]. \quad (47)$$

For a small loop and a thin conductor (r small), the self-inductance term predominates.

For the purpose of obtaining an antenna radiating in one direction only, a short-circuiting plunger may be placed a distance l away from the loop. This has negligible effect on the evanescent modes excited by the antenna, since these will have decayed to a negligible value at the short-circuit position for $l > \lambda_0/4$. The effect on the dominant mode is the same as superimposing the H_{10} mode radiated by an image antenna carrying a current $-I_0$ and located at $z = -2l$. The total H_{10} -mode axial magnetic field in the guide for $z > 0$ becomes

$$C_{10} \mathbf{h}_{z10} (e^{-\Gamma_{10} z} - e^{-\Gamma_{10} z - 2\Gamma_{10} l}) = 2j C_{10} \mathbf{h}_{z10} e^{-\Gamma_{10}(z+l)} \sin \beta_{10} l$$

where $\beta_{10} = |\Gamma_{10}|$. The amplitude of the wave propagating in the positive z direction is increased by a factor $2 \sin \beta_{10} l$, and the power flow is increased by a factor $4 \sin^2 \beta_{10} l$ in the positive z direction and reduced to zero in the negative z direction. The total radiated power, and hence the radiation resistance, becomes

$$R_0 = \frac{k_0 Z_0}{ab \beta_{10}} \left(\frac{\pi}{a} \right)^2 \frac{(\pi d^2)^2}{2} \sin^2 \beta_{10} l. \quad (48)$$

The reactive energy associated with the H_{10} -mode standing wave between the antenna and short-circuiting plunger is given by

$$2j\omega(W_m - W_e)_{10} = \frac{1}{2} \int_0^a \int_0^b E_y H_x^* dx dy$$

where, for $z = 0$, we have

$$\mathbf{a}_y E_y = C_{10} (1 - e^{-j2\beta_{10}l}) \mathbf{e}_{10}$$

$$\mathbf{a}_x H_x = -C_{10} (1 + e^{-j2\beta_{10}l}) \mathbf{h}_{10}.$$

Since

$$\int_0^a \int_0^b \mathbf{e}_{10} \times \mathbf{h}_{10}^* \cdot \mathbf{a}_z dx dy = 1$$

we get, after substituting for C_{10} ,

$$2j\omega(W_m - W_e)_{10} = jC_{10}C_{10}^* \sin 2\beta_{10}l = jP \sin 2\beta_{10}l$$

where P is given by (34). The additional contribution to the input reactance is obtained by dividing by $\frac{1}{2}I_0^2$, and the total antenna reactance now becomes

$$X_0 = \frac{k_0 Z_0}{ab\beta_{10}} \left(\frac{\pi}{a}\right)^2 \left(\frac{\pi d^2}{2}\right)^2 \sin 2\beta_{10}l + X \quad (49)$$

where X is given by (47). To partially cancel the inductive term X , the value of l should be between $\lambda_g/4$ and $\lambda_g/2$, where λ_g is the guide wavelength.

In Fig. 7.13 the input reactance X and radiation resistance R of a small loop in an infinite guide are plotted as a function of loop radius d for the following parameters: $k_0 = 2$, $a = 0.9$ inch, $b = 0.4$ inch, $r = 0.5$ mm. The self-inductance part is very large (for $d = 0.4$ cm, it is equal to 324 ohms), and, consequently, placing a short-circuiting plunger in the guide will

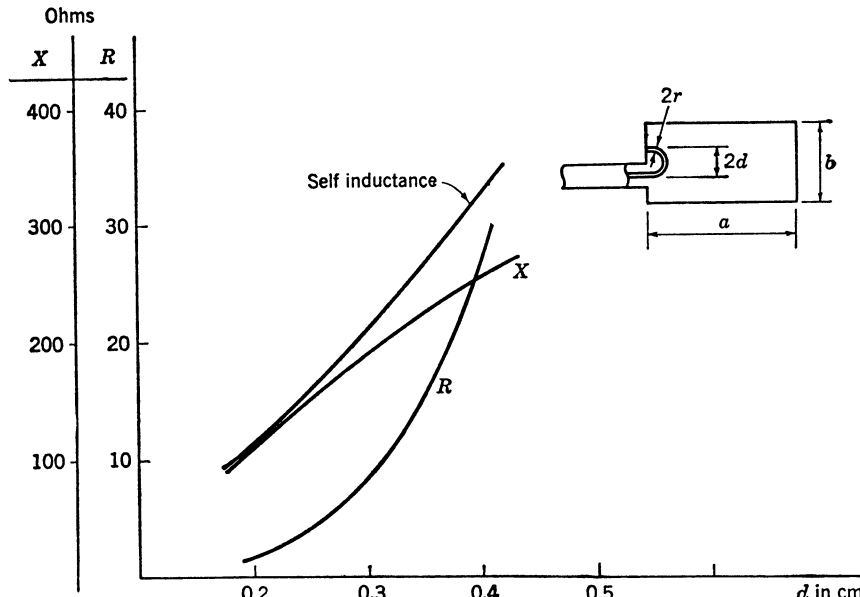


Fig. 7.13. Radiation resistance and input reactance of a small-loop antenna in an infinite waveguide plotted as a function of loop radius d for $a = 0.9$ inch, $b = 0.4$ inch, $r = 0.5$ mm, $\lambda_0 = 3.14$ cm.

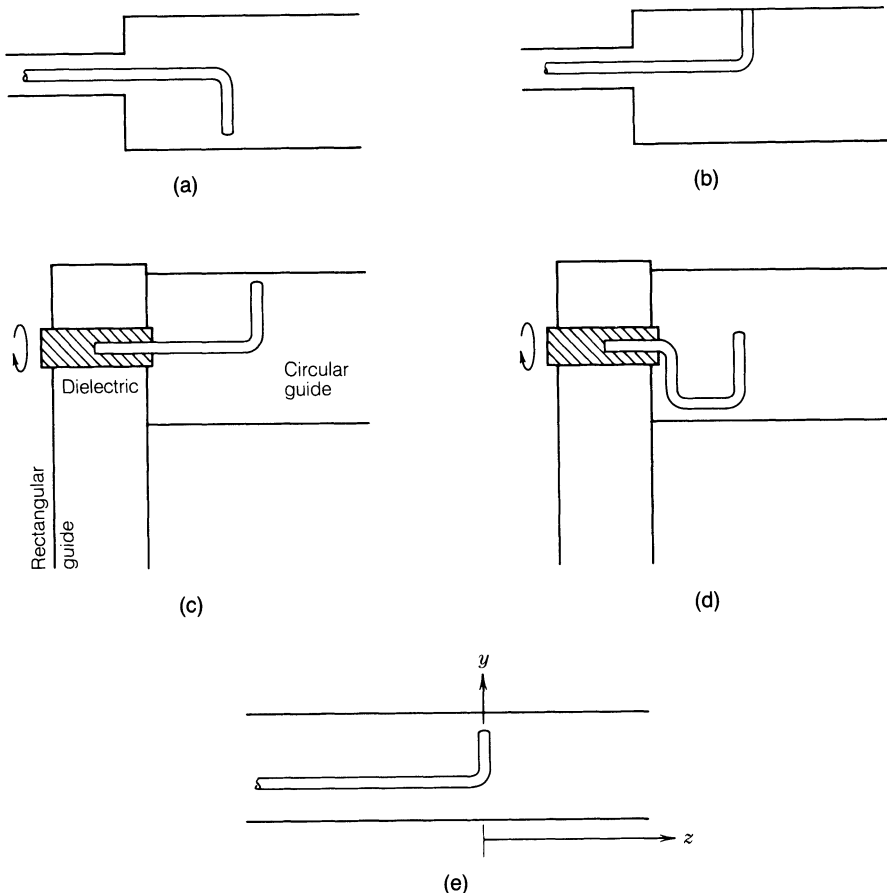


Fig. 7.14. (a) End-fed probe antenna. (b) End-fed loop antenna. (c) Rectangular to circular waveguide guide coupling with a rotatable probe system. (d) Broadband rectangular to circular waveguide probe coupling system. (e) Transmission-line-fed waveguide probe antenna.

not produce enough capacitive loading on the loop to tune out the inductive reactance. The maximum capacitive reactance which can be obtained is equal to the radiation resistance R as plotted, although, with one end of the guide short-circuited, the radiation resistance R must be multiplied by $2 \sin^2 \beta_{10} l$ to obtain the radiation resistance R_0 which is applicable now.

Other Waveguide Probe and Loop Antennas

There is an almost endless variety of probe and loop antenna configurations that can be used in a waveguide. In Figs. 7.14(a) and (b) we show basic end-fed probe and loop antennas. This particular loop antenna configuration in a circular waveguide has been analyzed in an approximate way by Deshpande and Das [7.19]. These authors have assumed that the current on the loop is that associated with the dominant transmission-line standing-wave current distribution and have neglected mutual coupling between the two sections of the loop antenna. In Figs. 7.14(c) and (d) we show probe antenna systems that are used to couple circular and rectangular waveguides. The probes can be rotated by means of a small motor. These systems are used as part of the prime focus feed in satellite receive-only earth stations and make it easy to orient

the probe for the reception of a signal having a particular polarization. The probe system shown in Fig. 7.14(c) is a narrow-band system unless additional matching elements are added [7.3]. The system shown in Fig. 7.14(d), on the other hand, has an unusually broad band response due to the particular transmission-line arrangement that is employed [7.4]. The basic antenna configuration that is representative of the above systems is shown in Fig. 7.14(e). We will outline the formulation of the theory for this latter antenna system in order to illustrate the main features involved in the analytical solution.

If we consider a rectangular waveguide then the vector potentials from y - and z -directed current elements are given by

$$A_y = \frac{\mu_0}{ab} \sum_{n=1}^{\infty} \sum_{m=0}^{\infty} \epsilon_{0m} \sin \frac{n\pi x}{a} \sin \frac{n\pi x'}{a} \cos \frac{m\pi y}{b} \cos \frac{m\pi y'}{b} \frac{e^{-\Gamma_{nm}|z-z'|}}{\Gamma_{nm}} \quad (50a)$$

$$A_z = \frac{2\mu_0}{ab} \sum_{n=1}^{\infty} \sum_{m=1}^{\infty} \sin \frac{n\pi x}{a} \sin \frac{n\pi x'}{a} \sin \frac{m\pi y}{b} \sin \frac{m\pi y'}{b} \frac{e^{-\Gamma_{nm}|z-z'|}}{\Gamma_{nm}}. \quad (50b)$$

The components of the Green's dyadic function that will give the y and z components of the electric field are given by

$$G_{yy} = \frac{1}{j\omega\mu_0\epsilon_0} \left(k_0^2 + \frac{\partial^2}{\partial y^2} \right) A_y \quad (51a)$$

$$G_{yz} = \frac{1}{j\omega\mu_0\epsilon_0} \frac{\partial^2}{\partial y \partial z} A_z \quad (51b)$$

$$G_{zy} = \frac{1}{j\omega\mu_0\epsilon_0} \frac{\partial^2}{\partial z \partial y} A_y \quad (51c)$$

$$G_{zz} = \frac{1}{j\omega\mu_0\epsilon_0} \left(k_0^2 + \frac{\partial^2}{\partial z^2} \right) A_z. \quad (51d)$$

The electric field radiated by the current on the transmission line and probe sections is given by

$$\mathbf{E}(\mathbf{r}) = \iint_S \bar{\mathbf{G}}(\mathbf{r}, \mathbf{r}') \cdot \mathbf{J}(\mathbf{r}') dS'.$$

The tangential component of the electric field must vanish along the transmission-line conductor and on the probe. This boundary condition gives the integral equation

$$\mathbf{n} \times \iint_S \bar{\mathbf{G}} \cdot \mathbf{J} dS' = 0, \quad \mathbf{r} \text{ on } S$$

where S is the conductor surface.

The current on the transmission line consists of the TEM-mode current plus some additional

current that is localized near the probe:

$$\frac{I^+ e^{-jk_0 z}}{2\pi r} - \frac{I^- e^{jk_0 z}}{2\pi r} + J_z$$

where we have assumed that the current is uniform around the conductor and I^+ , I^- are the incident and reflected TEM-mode current amplitudes.

We now consider the electric field acting along the probe due to the TEM-mode currents. The latter is given by

$$\frac{1}{2\pi} \int_{-\infty}^0 \int_0^{2\pi} G_{yz}(I^+ e^{-jk_0 z'} - I^- e^{jk_0 z'}) d\phi' dz'$$

where the integration over ϕ' is around the periphery of the transmission-line conductor. A typical term to be evaluated is

$$\int_{-\infty}^0 e^{-\Gamma_{nm}|z-z'| \mp jk_0 z'} dz'.$$

After performing the z' integration we find the following contribution to A_z :

$$\begin{aligned} \frac{\mu_0}{\pi ab} \sum_{n=1}^{\infty} \sum_{m=1}^{\infty} \sin \frac{n\pi x}{a} \sin \frac{m\pi y}{b} \int_0^{2\pi} \sin \frac{n\pi x'}{a} \sin \frac{m\pi y'}{b} d\phi' \frac{1}{\Gamma_{nm}^2 + k_0^2} \\ \cdot \left[2I^+ e^{-jk_0 z} - 2I^- e^{jk_0 z} + \frac{jk_0}{\Gamma_{nm}} (I^+ + I^-) e^{\Gamma_{nm} z} - (I^+ - I^-) e^{\Gamma_{nm} z} \right]. \end{aligned}$$

At $z = 0$ the electric field E_y is given by

$$\begin{aligned} E_y = \frac{jZ_0}{2\pi k_0 ab} \sum_{n=1}^{\infty} \sum_{m=1}^{\infty} \frac{m\pi}{b} \sin \frac{n\pi x}{a} \cos \frac{m\pi y}{b} \\ \cdot \int_0^{2\pi} \sin \frac{n\pi x'}{a} \sin \frac{m\pi y'}{b} d\phi' \frac{jk_0 (I^+ + I^-) + \Gamma_{nm} (I^+ - I^-)}{\Gamma_{nm}^2 + k_0^2}. \quad (52) \end{aligned}$$

The term proportional to $I^+ + I^- = V/Z_c$ is the TEM-mode electric field acting on the probe. We can view this as the applied electric field and consider V to be a given voltage. By using this as the forcing function the integral equation for \mathbf{J} can be formulated as a pair of coupled integral equations by setting $E_y = 0$ on the probe and $E_z = 0$ on the transmission-line conductor. The solution for the current can be obtained using Galerkin's method. The probe impedance is given by

$$Z_{\text{in}} = \frac{V}{I^+ - I^-} = \frac{V}{I}.$$

At $z = 0$ the total z -directed current must be made equal to the total y -directed current. This junction boundary condition requires that

$$2\pi r J_z(0) + I^+ - I^- = 2\pi r J_y(0).$$

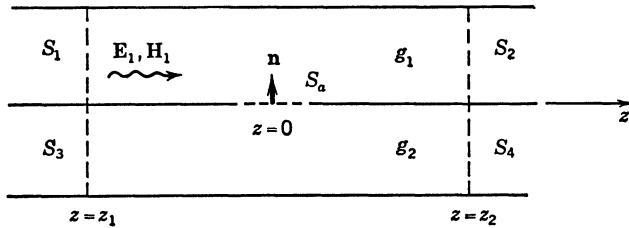


Fig. 7.15. Two guides coupled by a small aperture.

7.3. COUPLING BY SMALL APERTURES

Electromagnetic energy may be coupled from one waveguide into another guide or into a cavity resonator by a small aperture located at a suitable position in the common wall. For apertures whose linear dimensions are small compared with the wavelength, an approximate theory is available which states that the aperture is equivalent to a combination of radiating electric and magnetic dipoles, whose dipole moments are respectively proportional to the normal electric field and the tangential magnetic field of the incident wave. This theory, originally developed by Bethe [7.5], will be presented here. The approach to be used here differs from that of Bethe, and has been chosen because it leads to the final result in a somewhat more direct manner. We will also modify the Bethe theory so that power conservation will hold.

Consider the problem of coupling between two waveguides by means of a small aperture in a common sidewall as shown in Fig. 7.15. The solution procedure to be followed, which is based on one of Schelkunoff's field equivalence principles, consists of the following sequence of steps. We first close the aperture by a perfect magnetic wall. The incident field, which is chosen as the field in the absence of the aperture, will induce a magnetic current \mathbf{J}_m and a magnetic charge ρ_m on the magnetic wall surface S_a . These sources produce a scattered field that can be expressed as a field radiated by the dipole moments of the source distribution. After the field scattered into guide g_1 has been found the aperture is opened and a magnetic current $-\mathbf{J}_m$ is placed in the aperture. The field radiated by this source into the two guides, together with the specified incident field and the scattered field in g_1 found earlier, represents the total unique solution to the coupling problem. The total field as given is readily shown to have tangential electric and magnetic field components that are continuous across the aperture opening. Since all of the required boundary conditions are satisfied the solution is the correct and unique one.

With the aperture closed by a magnetic wall, let a normal mode $\mathbf{E}_1, \mathbf{H}_1$ be incident from the left. Because of the magnetic wall discontinuity, a scattered field $\mathbf{E}_s, \mathbf{H}_s$ will be excited such that the total field satisfies the following boundary conditions on the magnetic wall in the aperture S_a :

$$\mathbf{n} \times \mathbf{H}_s = -\mathbf{n} \times \mathbf{H}_1 \quad \text{or} \quad \mathbf{n} \times (\mathbf{H}_s + \mathbf{H}_1) = 0 \quad (53a)$$

$$\mathbf{n} \cdot \mathbf{E}_s = -\mathbf{n} \cdot \mathbf{E}_1 \quad \text{or} \quad \mathbf{n} \cdot (\mathbf{E}_s + \mathbf{E}_1) = 0. \quad (53b)$$

The normal magnetic field and the tangential electric field are not equal to zero on S_a , and, hence, a magnetic charge and a magnetic current distribution given by

$$\rho_m = \mu_0 \mathbf{n} \cdot \mathbf{H}_s \quad (54a)$$

$$\mathbf{J}_m = -\mathbf{n} \times \mathbf{E}_s \quad (54b)$$

will exist on S_a . For the incident mode, we have $\mathbf{n} \cdot \mathbf{H}_1 = \mathbf{n} \times \mathbf{E}_1 = 0$ on S_a . The scattered field may be expanded in terms of the normal waveguide modes as follows (see Section 5.6):

$$\mathbf{E}_s = \sum a_n \mathbf{E}_n^+, \quad z > 0 \quad (55a)$$

$$\mathbf{H}_s = \sum a_n \mathbf{H}_n^+, \quad z > 0 \quad (55b)$$

$$\mathbf{E}_s = \sum b_n \mathbf{E}_n^-, \quad z < 0 \quad (55c)$$

$$\mathbf{H}_s = \sum b_n \mathbf{H}_n^-, \quad z < 0. \quad (55d)$$

The scattered field is a solution of the equations

$$\nabla \times \mathbf{E}_s = -j\omega\mu_0 \mathbf{H}_s - \mathbf{J}_m$$

$$\nabla \times \mathbf{H}_s = j\omega\epsilon_0 \mathbf{E}_s$$

while each normal mode function \mathbf{E}_n , \mathbf{H}_n is a solution of the source-free equations. If we apply the Lorentz reciprocity theorem along the same lines as was done in Section 5.6, we find that the expansion coefficients a_n , b_n are given by

$$2b_n = \iint_{S_a} \mathbf{H}_n^+ \cdot \mathbf{J}_m dS \quad (56a)$$

$$2a_n = \iint_{S_a} \mathbf{H}_n^- \cdot \mathbf{J}_m dS. \quad (56b)$$

For a small aperture we will show that Eqs. (56) represent coupling to an electric and magnetic dipole plus a magnetic quadrupole.

With reference to Fig. 7.16 the following parameters are introduced:

1. τ a unit vector tangent to the aperture contour C ,
2. \mathbf{n}_1 a unit vector normal to τ and in the plane of the aperture,
3. \mathbf{n} a unit vector perpendicular to S_a and directed into guide g_1 ,
4. u, v, w a localized rectangular coordinate system with the origin at the center of the aperture and w directed along \mathbf{n} , and
5. \mathbf{n}_0 a unit vector normal to S_a and directed from guide g_1 into guide g_2 .

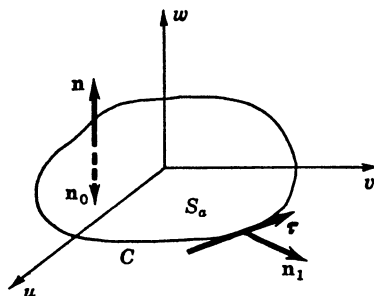


Fig. 7.16. Aperture coordinates.

The scattered field satisfies the boundary condition $\tau \cdot \mathbf{E}_s = 0$, and, hence, $\mathbf{n}_1 \cdot \mathbf{J}_m$ equals zero on C ; that is, there is no normal component of magnetic current at the boundary of the aperture. Since $\rho_m = \mu_0 \mathbf{n} \cdot \mathbf{H}_s$, we have

$$\mu_0^{-1} \iint_{S_a} \rho_m dS = \iint_{S_a} \mathbf{H}_s \cdot \mathbf{n} dS = \iint_{S_a} \frac{\nabla \times \mathbf{E}_s \cdot \mathbf{n}}{-j\omega\mu_0} dS = -\frac{1}{j\omega\mu_0} \oint_C \mathbf{E}_s \cdot \tau dl = 0$$

which shows that there is no net magnetic charge on S_a . For a small aperture we may expand \mathbf{H}_n in a Taylor series about the origin to get

$$\mathbf{H}_n(u, v) = \mathbf{H}_n(0) + \left. \frac{u \partial \mathbf{H}_n}{\partial u} \right|_0 + \left. \frac{v \partial \mathbf{H}_n}{\partial v} \right|_0 + \dots \approx \mathbf{H}_n(0) + \mathbf{r} \cdot \nabla \mathbf{H}_n$$

where $\mathbf{r} = \mathbf{a}_u u + \mathbf{a}_v v$, and $\nabla \mathbf{H}_n$ is to be evaluated at the origin. The coupling coefficient b_n is given by

$$2b_n = \iint_{S_a} \mathbf{H}_n^+ \cdot \mathbf{J}_m dS = \mathbf{H}_n^+(0) \cdot \iint_{S_a} \mathbf{J}_m dS + \iint_{S_a} (\mathbf{r} \cdot \nabla \mathbf{H}_n^+) \cdot \mathbf{J}_m dS. \quad (57)$$

Consider the following integral:

$$\iint_{S_a} \nabla \cdot \phi \mathbf{J}_m dS = \iint_{S_a} (\phi \nabla \cdot \mathbf{J}_m + \mathbf{J}_m \cdot \nabla \phi) dS = \oint_C \phi \mathbf{J}_m \cdot \mathbf{n}_1 dl = 0$$

since $\mathbf{J}_m \cdot \mathbf{n}_1 = 0$, and ϕ is an arbitrary scalar function. Let $\phi = u$, and the above result gives

$$\mathbf{a}_u \iint_{S_a} \mathbf{J}_m \cdot \nabla u dS = \mathbf{a}_u \iint_{S_a} \mathbf{J}_m \cdot \mathbf{a}_u dS = -\mathbf{a}_u \iint_{S_a} u \nabla \cdot \mathbf{J}_m dS. \quad (58)$$

A similar result is obtained if we let $\phi = v$. Combining the two results for $\phi = u$ and v gives

$$\iint_{S_a} \mathbf{J}_m dS = -\iint_{S_a} \mathbf{r} \nabla \cdot \mathbf{J}_m dS = j\omega \iint_{S_a} \mathbf{r} \rho_m dS = j\omega \mu_0 \mathbf{M} \quad (59)$$

since $\nabla \cdot \mathbf{J}_m = -j\omega \rho_m$ from the continuity equation relating current and charge, and the integral $(1/\mu_0) \iint_{S_a} \mathbf{r} \rho_m dS$ defines an equivalent magnetic dipole moment \mathbf{M} in direct analogy with the electric dipole moment arising from electric charge ρ . The first term on the right-hand side in (57) is thus seen to represent coupling with a magnetic dipole \mathbf{M} .

The second integral on the right-hand side in (57) is readily evaluated by writing the integrand in component form. We have

$$\begin{aligned} \mathbf{r} \cdot \nabla \mathbf{H}_n^+ \cdot \mathbf{J}_m &= (\mathbf{a}_u u + \mathbf{a}_v v) \cdot \left(\mathbf{a}_u \mathbf{a}_u \frac{\partial H_{nu}^+}{\partial u} + \mathbf{a}_u \mathbf{a}_v \frac{\partial H_{nv}^+}{\partial u} + \mathbf{a}_v \mathbf{a}_u \frac{\partial H_{nu}^+}{\partial v} \right. \\ &\quad \left. + \mathbf{a}_v \mathbf{a}_v \frac{\partial H_{nv}^+}{\partial v} \right) \cdot (\mathbf{a}_u J_{mu} + \mathbf{a}_v J_{mv}) \\ &= u \frac{\partial H_{nu}^+}{\partial u} J_{mu} + u \frac{\partial H_{nv}^+}{\partial u} J_{mv} + v \frac{\partial H_{nu}^+}{\partial v} J_{mu} + v \frac{\partial H_{nv}^+}{\partial v} J_{mv}. \end{aligned}$$

Subtracting and adding similar terms, this may be rewritten as

$$\begin{aligned} \frac{u}{2} J_{mv} \left(\frac{\partial H_{nv}^+}{\partial u} - \frac{\partial H_{nu}^+}{\partial v} \right) - \frac{v J_{mu}}{2} \left(\frac{\partial H_{nv}^+}{\partial u} - \frac{\partial H_{nu}^+}{\partial v} \right) + \frac{u J_{mv}}{2} \frac{\partial H_{nu}^+}{\partial v} \\ + \frac{v J_{mu}}{2} \frac{\partial H_{nv}^+}{\partial u} + u J_{mu} \frac{\partial H_{nu}^+}{\partial u} + v J_{mv} \frac{\partial H_{nv}^+}{\partial v} + \frac{u J_{mv}}{2} \frac{\partial H_{nv}^+}{\partial u} + \frac{v J_{mu}}{2} \frac{\partial H_{nu}^+}{\partial v}. \quad (60) \end{aligned}$$

The first two terms are readily recognized as being equal to $j\omega\epsilon_0\mathbf{E}_n^+(0)\cdot(\mathbf{r} \times \mathbf{J}_m)/2$. The magnetic dipole moment of an electric current distribution is defined by the integral

$$\iiint \frac{\mathbf{r} \times \mathbf{J}}{2} dV.$$

By analogy, we now see that

$$-j\omega\epsilon_0\mathbf{E}_n^+(0)\cdot \iint_{S_a} \frac{-\mathbf{r} \times \mathbf{J}_m}{2} dS = -j\omega\mathbf{E}_n^+(0)\cdot\mathbf{P}$$

where \mathbf{P} is the equivalent electric dipole moment of the circulating magnetic current. This dipole is directed normal to the aperture.

If we let $\phi = u^2/2$, $v^2/2$, and uv in turn, then in (58) we get the results

$$\begin{aligned} \iint_{S_a} u J_{mu} dS &= - \iint_{S_a} \frac{u^2}{2} \nabla \cdot \mathbf{J}_m dS = \frac{j\omega}{2} \iint_{S_a} u^2 \rho_m dS \\ \iint_{S_a} v J_{mv} dS &= \frac{j\omega}{2} \iint_{S_a} v^2 \rho_m dS \\ \iint_{S_a} (v J_{mu} + u J_{mv}) dS &= j\omega \iint_{S_a} uv \rho_m dS. \end{aligned}$$

The components of a dyadic magnetic quadrupole $\bar{\mathbf{Q}}$ are given by

$$\begin{aligned} Q_{uu} &= \frac{1}{\mu_0} \iint_{S_a} u^2 \rho_m dS \\ Q_{vu} = Q_{uv} &= \frac{1}{\mu_0} \iint_{S_a} uv \rho_m dS \quad \text{etc.} \end{aligned}$$

and, hence, the last six terms in (60) may be combined by using the above relations to give finally

$$\frac{j\omega\mu_0}{2} \nabla \mathbf{H}_n^+ : \bar{\mathbf{Q}}$$

where the double-dot product is taken between the two dyadics $\nabla \mathbf{H}_n^+$ and $\bar{\mathbf{Q}}$.

The expansion coefficients a_n and b_n are thus seen to be given by

$$2a_n = j\omega \left(\mu_0 \mathbf{H}_n^- \cdot \mathbf{M} - \mathbf{E}_n^- \cdot \mathbf{P} + \frac{\mu_0}{2} \nabla \mathbf{H}_n^- : \bar{\mathbf{Q}} \right) \quad (61a)$$

$$2b_n = j\omega \left(\mu_0 \mathbf{H}_n^+ \cdot \mathbf{M} - \mathbf{E}_n^+ \cdot \mathbf{P} + \frac{\mu_0}{2} \nabla \mathbf{H}_n^+ : \bar{\mathbf{Q}} \right). \quad (61b)$$

In the definition of the dipole moments, the origin for the radius vector \mathbf{r} is arbitrary, since there is no net charge in the aperture. The magnetic dipole moments have been defined to be dimensionally the same as \mathbf{H} times length cubed. In most applications the quadrupole term can be neglected, since it represents a small quantity depending on the fourth power of the aperture dimension.

Although we have written the expansion coefficients in terms of equivalent dipole moments, we do not know these before we find a solution for the current \mathbf{J}_m and the charge ρ_m in the aperture. This solution is difficult to obtain in general. However, we may find a static field solution for the dipole moments of small elliptic- and circular-shaped apertures quite readily. In the practical application of the theory, it is found that the static field solution gives results of acceptable accuracy for small apertures. To further enhance the applicability of the theory, Cohn has described an electrolytic-tank method for measuring polarizabilities of arbitrarily shaped apertures [7.6].

Before presenting the static field solution for the dipole moments, the rest of the theory required to obtain the field coupled through the aperture into guide g_2 will be given. When the aperture is open, the field in g_2 is that radiated by an equivalent current $-\mathbf{J}_m$ on S_a . The field in g_1 is the sum of the field radiated by $-\mathbf{J}_m$ in the aperture and the field $\mathbf{E}_1 + \mathbf{E}_s$, $\mathbf{H}_1 + \mathbf{H}_s$ existing in g_1 with the aperture closed by a magnetic wall. Let the current $-\mathbf{J}_m$ radiate a field \mathbf{E}_{s1} , \mathbf{H}_{s1} into g_1 , and \mathbf{E}_{s2} , \mathbf{H}_{s2} into g_2 . At the aperture, the total tangential magnetic field must be continuous, and, hence, $\mathbf{n}_0 \times \mathbf{H}_{s2} = \mathbf{n}_0 \times (\mathbf{H}_{s1} + \mathbf{H}_s + \mathbf{H}_1) = \mathbf{n}_0 \times \mathbf{H}_{s1}$ from (53a). The total tangential electric field must also be continuous, and so we have $\mathbf{n}_0 \times \mathbf{E}_{s2} = \mathbf{n}_0 \times (\mathbf{E}_{s1} + \mathbf{E}_s + \mathbf{E}_1)$, or, by using (54b), $\mathbf{n}_0 \times (\mathbf{E}_{s1} - \mathbf{E}_{s2}) = -\mathbf{J}_m$. The field in g_2 may be expanded in terms of the normal mode functions for this guide as follows:

$$\mathbf{E}_{s2} = \sum c_n \mathbf{E}_{n2}^+, \quad z > 0 \quad (62a)$$

$$\mathbf{H}_{s2} = \sum c_n \mathbf{H}_{n2}^+, \quad z > 0 \quad (62b)$$

$$\mathbf{E}_{s2} = \sum d_n \mathbf{E}_{n2}^-, \quad z < 0 \quad (62c)$$

$$\mathbf{H}_{s2} = \sum d_n \mathbf{H}_{n2}^-, \quad z < 0 \quad (62d)$$

where the additional subscript 2 is used to distinguish between the normal modes for the two guides. If the two guides are identical, then the current $-\mathbf{J}_m$ will radiate identical fields into the two guides. The expansion coefficients may be found in the same way as for the field \mathbf{E}_s , \mathbf{H}_s , but it must be borne in mind that the tangential electric field and normal magnetic field in one guide will undergo only one-half the discontinuous change across the source region that the field \mathbf{E}_s , \mathbf{H}_s did. The effective dipole moments associated with the aperture current $-\mathbf{J}_m$ and charge $-\rho_m$ for radiation into guide g_2 will be $-\mathbf{M}/2$ and $-\mathbf{P}/2$. One-half the

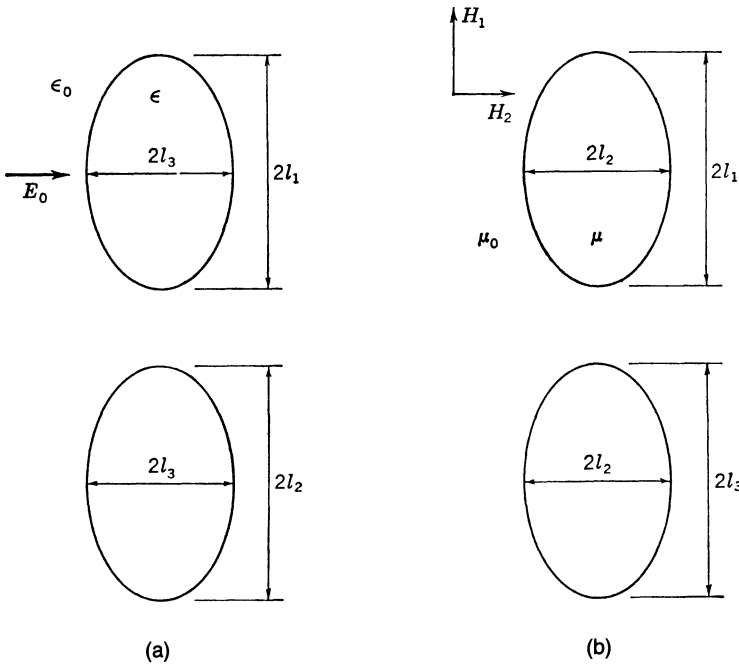


Fig. 7.17. (a) Dielectric ellipsoid. (b) Permeable magnetic ellipsoid.

required discontinuity across the source is provided by \mathbf{E}_{s2} , \mathbf{H}_{s2} ; the other half by \mathbf{E}_{s1} , \mathbf{H}_{s1} . The total field in g_1 is now seen to be equivalent to the sum of the incident fields \mathbf{E}_1 , \mathbf{H}_1 and the field radiated by dipoles of strength $\mathbf{M}/2$ and $\mathbf{P}/2$ since the field radiated by $-\mathbf{M}/2$, $-\mathbf{P}/2$ cancels one-half of the field \mathbf{E}_s , \mathbf{H}_s radiated by \mathbf{M} and \mathbf{P} .

In the more general case, when the two guides are not identical, this symmetry argument no longer applies. We will present a method later on that will enable the problem of coupling between dissimilar regions to also be solved as two uncoupled excitation problems. Before we proceed with that task we will derive expressions for the polarizabilities of small elliptical-shaped apertures.

Dipole Moments of Elliptic Apertures

The dipole moments of an elliptic aperture may be obtained from the static dipole moments of general ellipsoidal dielectric and permeable magnetic bodies, placed in uniform static electric and magnetic fields, by suitable limiting processes. Consider a dielectric ellipsoid with semiaxes l_1, l_2, l_3 placed in a uniform electric field E_0 directed along the l_3 axis as in Fig. 7.17(a).

The problem of the ellipsoid in a uniform field is readily solved in ellipsoidal coordinates [7.7]. We find that the total field in the interior is uniform and parallel to the applied field if the latter is directed along one of the axes of the ellipsoid. The dipole polarization per unit volume, therefore, has zero divergence, and the equivalent polarization volume charge in the interior is zero. On the surface, an equivalent surface-polarization charge density equal to the discontinuity in the normal component of the polarization vector exists. The total dipole moment of the ellipsoid may be calculated by a volume integral either in terms of the polarization density or in terms of the equivalent polarization surface charge. The field outside the ellipsoid is the sum of the applied field plus a dipole field arising from an elementary dipole

at the origin and having a moment equal to the dipole moment of the ellipsoid. According to Stratton, the dipole moment P_3 , when a uniform field E_0 is applied along the l_3 axis, is

$$P_3 = \frac{\epsilon_0 E_0 V}{L_3 + \epsilon_0 / (\epsilon - \epsilon_0)} \quad (63)$$

where

$$L_3 = \frac{l_1 l_2 l_3}{2} \int_0^\infty \frac{ds}{(s + l_3^2)[(s + l_1^2)(s + l_2^2)(s + l_3^2)]^{1/2}}$$

and $V = \frac{4}{3}\pi l_1 l_2 l_3$ is the volume of the ellipsoid. If we let ϵ be equal to zero, we obtain the dual of a perfect diamagnetic material. For $\epsilon = 0$, the internal polarization sets up a field equal and opposite to the applied field, so that the net internal displacement flux D is zero. The surface polarization charge now gives rise to an external field, which cancels the normal component of the applied field E_0 at the surface of the ellipsoid. This is precisely the boundary condition that the electric field must satisfy at a magnetic wall. Hence, a dielectric body with $\epsilon = 0$ is equivalent to a body with a magnetic wall surface. If we now let l_3 approach zero, (63) gives the dipole moment of an elliptic disk which is made from a perfect "magnetic conductor." The dipole moment of the aperture is only one-half that of a disk, since only one side of the aperture is under consideration while the disk has two sides with polarization charge on both. Finally, the effective radiating dipole moment in the aperture is one-half of the moment of an aperture closed by a magnetic wall, and hence equals one-quarter of the moment of a complete disk. Before evaluating the integral for L_3 , we will give the expressions for the magnetic dipole moments of an ellipsoid.

Figure 7.17(b) illustrates a permeable ellipsoid placed in a uniform magnetic field. There are two dipole moments to consider: M_1 due to a field H_1 along the l_1 axis, and M_2 due to a field H_2 along the l_2 axis. Each case may be treated separately, and each solution is essentially the same as for the dielectric case. We find that

$$M_1 = \frac{VH_1}{L_1 + \mu_0 / (\mu - \mu_0)} \quad (64a)$$

where

$$L_1 = \frac{l_1 l_2 l_3}{2} \int_0^\infty \frac{ds}{(s + l_1^2)[(s + l_1^2)(s + l_2^2)(s + l_3^2)]^{1/2}}$$

and

$$M_2 = \frac{VH_2}{L_2 + \mu_0 / (\mu - \mu_0)} \quad (64b)$$

where

$$L_2 = \frac{l_1 l_2 l_3}{2} \int_0^\infty \frac{ds}{(s + l_2^2)[(s + l_1^2)(s + l_2^2)(s + l_3^2)(s + l_1^2)^2]^{1/2}}.$$

If we let μ approach infinity, the internal magnetic field vanishes, since $\mathbf{n} \cdot \mu_0 \mathbf{H}_e$ equals $\mathbf{n} \cdot \mu \mathbf{H}_i$, where \mathbf{H}_e is the external field and \mathbf{H}_i is the internal field, and, hence, the product $\mu \mathbf{H}_i$ is finite and \mathbf{H}_i tends to zero as μ tends to infinity. For an external field applied along a principal axis, the internal field is uniform and parallel with the applied field, and, since it vanishes at

the surface, it follows that the induced external field just cancels the tangential component of the applied field at the surface. Again we have boundary conditions corresponding to those at a magnetic wall, so that, by letting l_3 approach zero and μ tend to infinity, we obtain the magnetic dipole moments of an elliptical disk having perfect magnetic conductivity.

The integrals for L_1 , L_2 , and L_3 may be evaluated in terms of elliptic integrals. First we show that $L_1 + L_2 + L_3 = 1$, and so we need evaluate only two of the integrals. If a new variable

$$u^2 = (s + l_1^2)(s + l_2^2)(s + l_3^2)$$

is introduced, we get

$$L_1 + L_2 + L_3 = \frac{l_1 l_2 l_3}{2} \int_0^\infty \frac{(s + l_2^2)(s + l_3^2) + (s + l_3^2)(s + l_1^2) + (s + l_1^2)(s + l_2^2)}{u^3} ds.$$

Using the familiar rule for the differential of a product, it is seen at once that the numerator is equal to $2u du$. Putting in the proper limits of integration for the variable u , the integral becomes

$$\frac{l_1 l_2 l_3}{2} \int_{l_1 l_2 l_3}^\infty \frac{2 du}{u^2} = 1.$$

The integrals for L_1 and L_2 are somewhat easier to evaluate than that for L_3 . The procedure used will be given only for the case of L_2 , the evaluation of L_1 being similar. We may take $l_1 > l_2 > l_3$ without any loss in generality. In the integral for L_2 , we introduce a new variable t according to the relation $s + l_2^2 = t^2$ and get

$$L_2 = l_1 l_2 l_3 \int_{l_2}^\infty \frac{dt}{t^2(t^2 + l_1^2 - l_2^2)^{1/2}(t^2 - l_2^2 + l_3^2)^{1/2}}.$$

Multiplying the numerator by $[(t^2 + l_1^2 - l_2^2) - t^2]/(l_1^2 - l_2^2)$ the integral may be split into two parts as follows:

$$\frac{l_1 l_2 l_3}{l_1^2 - l_2^2} \left[\int_{l_2}^\infty \frac{(t^2 + l_1^2 - l_2^2)^{1/2}}{t^2(t^2 - l_2^2 + l_3^2)^{1/2}} dt - \int_{l_2}^\infty \frac{dt}{(t^2 + l_1^2 - l_2^2)^{1/2}(t^2 - l_2^2 + l_3^2)^{1/2}} \right].$$

Apart from the limits of integration, the integrals occurring here are of the form that Jahnke and Emde tabulated the solutions for.² In order to use the solutions presented, the integrals here are rewritten as the sum of two integrals with limits chosen as indicated below:

$$\int_{l_2}^x = \int_{(l_2^2 - l_3^2)^{1/2}}^x - \int_{(l_2^2 - l_3^2)^{1/2}}^{l_2}.$$

For our application we will set l_3 equal to zero eventually, and so the second integral will vanish and, therefore, will not be evaluated. The value of the required integral is

$$\frac{l_1 l_2 l_3}{l_1^2 - l_2^2} \left[\frac{(l_1^2 - l_3^2)^{1/2}}{l_2^2 - l_3^2} \mathcal{E}(k, \phi) - \frac{1}{(l_1^2 - l_3^2)^{1/2}} F(k, \phi) \right]$$

²See [7.2, p. 58]. Fifth formula pair for evaluation of L_2 , and last pair for evaluation of L_1 .

where

$$k = \left(\frac{l_1^2 - l_2^2}{l_1^2 - l_3^2} \right)^{1/2} \quad \cos \phi = \frac{(l_2^2 - l_3^2)^{1/2}}{x}$$

and F and E are the incomplete elliptic integrals of the first and second kind. As x tends to infinity, ϕ becomes equal to $\pi/2$, and, when l_3 is placed equal to zero, we get

$$\frac{L_2}{V} = \frac{3}{4\pi l_1^3 e^2} [(1 - e^2)^{-1} E(e) - K(e)] \quad (65)$$

where K and E are complete elliptic integrals of the first and second kind with modulus e equal to the eccentricity $(1 - l_2^2/l_1^2)^{1/2}$ of the ellipse.

In a similar fashion we find that

$$\frac{L_1}{V} = \frac{3}{4\pi l_1^3 e^2} [K(e) - E(e)] \quad (66)$$

$$\frac{L_3 - 1}{V} = -\frac{L_1 + L_2}{V} = \frac{-3E(e)}{4\pi l_1^3 (1 - e^2)}. \quad (67)$$

Substituting into (63) and (64), the dipole moments are obtained:

$$P_3 = -\frac{4\pi l_1^3 (1 - e^2)}{3E(e)} \epsilon_0 E_0 \quad (68a)$$

$$M_1 = \frac{4\pi l_1^3 e^2}{3[K(e) - E(e)]} H_1 \quad (68b)$$

$$M_2 = \frac{4\pi l_1^3 e^2 (1 - e^2)}{3[E(e) - (1 - e^2)K(e)]} H_2. \quad (68c)$$

Returning to our waveguide-coupling problem, let \mathbf{E}_1 , \mathbf{H}_1 be the incident mode in guide g_1 . The scattered field in this guide is that radiated by an electric dipole $\mathbf{P}_0 = \frac{1}{2}\mathbf{P}$ and a magnetic dipole $\mathbf{M}_0 = \frac{1}{2}\mathbf{M}$. In the Bethe theory these dipole strengths are chosen equal to the static values induced by the incident fields; thus

$$\mathbf{P}_0 = \epsilon_0 \alpha_e \mathbf{n} \cdot \mathbf{E}_1 \quad (69a)$$

$$\mathbf{M}_0 = \bar{\alpha}_m \mathbf{n} \cdot \mathbf{H}_1 \quad (69b)$$

where from (68) we have, after dividing by 4,

$$\alpha_e = -\frac{\pi l_1^3 (1 - e^2)}{3E(e)} \quad (70a)$$

$$\bar{\alpha}_m = \mathbf{a}_u \mathbf{a}_u \frac{\pi l_1^3 e^2}{3[K(e) - E(e)]} + \mathbf{a}_v \mathbf{a}_v \frac{\pi l_1^3 e^2 (1 - e^2)}{3[E(e) - (1 - e^2)K(e)]}. \quad (70b)$$

In (70a), α_e is the electric polarizability of the aperture, while, in (70b), $\bar{\alpha}_m$ is the dyadic magnetic polarizability of the aperture. The aperture coordinates u and v are to be oriented with u along the major axis of the ellipse. For small values of e , the following formulas may be used to evaluate the elliptic integrals:

$$E = \frac{\pi}{2} \left(1 - \frac{e^2}{4} \right)$$

$$K = \frac{\pi}{2} \left(1 + \frac{e^2}{4} \right)$$

while, for values of e approaching unity,

$$E = 1$$

$$K = \ln 4 \frac{l_1}{l_2}.$$

For e equal to zero, we obtain a circular aperture with polarizabilities

$$\alpha_e = -\frac{2}{3}l^3 \quad (71)$$

$$\bar{\alpha}_m = \frac{4}{3}l^3(\mathbf{a}_u \mathbf{a}_u + \mathbf{a}_v \mathbf{a}_v) \quad (72)$$

where l is the radius of the aperture. The field radiated into guide g_2 is that due to radiating dipoles $-\mathbf{P}_0$ and $-\mathbf{M}_0$ in the aperture.

Radiation Reaction Fields

When we try to determine an equivalent network to represent the small aperture using the static polarizability tensors to determine the dipole strengths we find that we do not obtain a physically meaningful circuit and power is not conserved. One procedure to overcome these difficulties is to derive expressions for dynamic polarizability tensors. This can be done using a power series expansion in k_0 of the incident and scattered fields. Such a procedure requires an expansion up to terms including k_0^3 and the resultant expressions for $\bar{\alpha}_e$ and $\bar{\alpha}_m$ will depend on the geometrical shapes of the input and output waveguides. Thus the polarizabilities of a given aperture are no longer characteristic parameters of the aperture alone. Fortunately, there is an alternative procedure that can be followed which still allows one to use the static polarizabilities but corrects for the lack of power conservation by introducing the radiation reaction fields as part of the polarizing field. The basic concept will be described by considering the problem of the scattering of a plane wave by a small conducting sphere of radius a [7.8].

Consider a plane wave

$$\mathbf{E} = E_0 e^{j k_0 x} \mathbf{a}_z$$

$$\mathbf{H} = H_0 e^{j k_0 x} \mathbf{a}_y$$

incident on a conducting sphere located at the origin. When $k_0 a \ll 1$ we can assume that a

constant electric field $E_0 \mathbf{a}_z$ acts on the sphere. This static field problem can be readily solved and we find that a charge distribution is induced on the sphere such that the dipole moment has a value $\mathbf{P} = 4\pi\epsilon_0 a^3 E_0 \mathbf{a}_z$.

Under dynamic conditions the normal component of the total magnetic field must vanish at the conducting surface. The equivalent static field problem is that of a perfect diamagnetic sphere immersed in a field $H_0 \mathbf{a}_y$. The induced magnetic dipole moment is $\mathbf{M} = -2\pi a^3 H_0 \mathbf{a}_y$ as will be shown in Chapter 12. If we determine static fields in the region $r > a$ from these dipoles located at the origin then the boundary conditions $\mathbf{n} \times (\mathbf{E}_0 + \mathbf{E}_i) = 0$ and $\mathbf{n} \cdot (\mathbf{H}_0 + \mathbf{H}_i) = 0$ at $r = a$ will be satisfied where \mathbf{E}_i and \mathbf{H}_i are the induced or scattered fields. However, if we determine dynamic fields from these dipoles we will find that the boundary conditions are violated.

The dynamic electric field produced by a time-harmonic electric dipole P is given by [Eq. (79), Chapter 1]

$$\mathbf{E}_s = \left(k_0^2 \mathbf{a}_z + \nabla \frac{\partial}{\partial z} \right) \frac{Pe^{-jk_0 r}}{4\pi\epsilon_0 r}.$$

When we expand this field in a power series in k_0 we obtain

$$\mathbf{E}_s = \frac{P}{4\pi\epsilon_0} \left[\left(\frac{2\mathbf{a}_r \cos \theta + \mathbf{a}_\theta \sin \theta}{r^3} \right) + \frac{k_0^2}{2r} (2\mathbf{a}_r \cos \theta - \mathbf{a}_\theta \sin \theta) - jk_0^3 \frac{2}{3} \mathbf{a}_z + \dots \right].$$

The first term is the static-like field whose tangential component cancels that of the applied field. The second term is a small correction of order $k_0^2 r^2$. The third term is also a small correction but it is the leading imaginary term. This term represents a uniform field that is not canceled by the applied field at the surface of the sphere. In order to cancel this term we can include it as part of the applied field in a self-consistent manner. Thus we determine the dipole moment using the expression

$$\mathbf{P} = \epsilon_0 \bar{\alpha}_e \cdot \left[E_0 \mathbf{a}_z - jk_0^3 \frac{2}{3} \mathbf{a}_z \frac{P}{4\pi\epsilon_0} \right] = \epsilon_0 \bar{\alpha}_e \cdot \mathbf{E}_0 - \frac{jk_0^3}{6\pi} \bar{\alpha}_e \cdot \mathbf{P}$$

where the polarizability tensor for the sphere is $\bar{\alpha}_e = 4\pi a^3 \bar{\mathbf{I}}$. We call $-jk_0^3 \mathbf{P} / 6\pi\epsilon_0$ the radiation reaction field \mathbf{E}_r . When we solve the above for the dipole moment \mathbf{P} we obtain a scattered field \mathbf{E}_s with the property that the tangential component of the first term, i.e., $P \sin \theta / 4\pi\epsilon_0 r^3$, plus that of the third-order term, namely, $jP k_0^3 \sin \theta / 6\pi\epsilon_0$, cancels that of the uniform applied field at $r = a$.

A time-harmonic dipole \mathbf{P} is equivalent to a polarization current $j\omega \mathbf{P}$. The rate at which this current radiates energy is given by

$$-\frac{1}{2} \operatorname{Re}(j\omega \mathbf{P})^* \cdot \mathbf{E} = \frac{1}{2} \operatorname{Re}(j\omega \mathbf{P}^* \cdot \mathbf{E}_0 + j\omega \mathbf{P}^* \cdot \mathbf{E}_s).$$

The first term represents power extracted from the incident field and the second term represents the scattered power. For a lossless scatterer these two powers must balance. If we use the static solution for \mathbf{P} then \mathbf{P} and \mathbf{E}_0 are in phase and no power is extracted from the incident wave. The scattered power equals $\omega k_0^3 \mathbf{P} \cdot \mathbf{P}^* / 12\pi\epsilon_0$ so clearly we do not have power conservation.

However, with the corrected expression for \mathbf{P} the power extracted from the incident wave is

$$\frac{1}{2} \operatorname{Re} \frac{j\omega(\epsilon_0\alpha_e \mathbf{E}_0 \cdot \mathbf{E}_0^*)}{(1 - jk_0^3 2a^3/3)} = \frac{-\omega k_0^3}{12\pi\epsilon_0} \mathbf{P} \cdot \mathbf{P}^*$$

which clearly now balances the scattered power.

The induced magnetic dipole moment is also corrected in the same way; thus we use

$$\mathbf{M} = \bar{\alpha}_m \cdot (\mathbf{H}_0 + \mathbf{H}_r)$$

where \mathbf{H}_r is the magnetic radiation reaction field. For the sphere problem this field is given by

$$H_r = -jk_0^3 \frac{M}{6\pi} = -jk_0^3 \frac{\alpha_m \cdot \mathbf{H}_0}{6\pi}.$$

In waveguide-coupling problems the leading imaginary terms in the scattered fields are the propagating modes that are excited. These are the only imaginary terms and are included as part of the polarizing fields in order to obtain corrected expressions for the aperture dipole moments. If we define the generator fields \mathbf{E}_{g1} and \mathbf{H}_{g1} to be the incident field for the input waveguide in the absence of the aperture, and similarly for \mathbf{E}_{g2} and \mathbf{H}_{g2} , then the coupling problem is solved by specifying that the dipole strengths for radiation into guides 1 (input) and 2 (output) are

$$\mathbf{M}_0 = \mp \alpha_m \cdot (\mathbf{H}_{g1} - \mathbf{H}_{g2} + \mathbf{H}_{1r} - \mathbf{H}_{2r}) \quad (73a)$$

$$\mathbf{P}_0 = \mp \epsilon_0 \alpha_e \cdot (\mathbf{E}_{g1} - \mathbf{E}_{g2} + \mathbf{E}_{1r} - \mathbf{E}_{2r}) \quad (73b)$$

where the minus sign applies for radiation into guide 2 and the plus sign is used for guide 1. The radiation reaction fields \mathbf{E}_{1r} , \mathbf{H}_{1r} are the dominant mode fields produced by dipoles \mathbf{P}_0 and \mathbf{M}_0 in guide 1 and evaluated at the center of the aperture. The radiation reaction fields \mathbf{E}_{2r} , \mathbf{H}_{2r} are those produced by dipoles $-\mathbf{P}_0$, $-\mathbf{M}_0$ radiating in guide 2. The examples that follow will illustrate how this modified Bethe small-aperture theory is implemented in practice. The use of (73) also accounts correctly for the two waveguides being dissimilar in shape. The basis for the formulas given by (73) is as follows: The scattered fields on the two sides of the aperture can be expressed in terms of the tangential value of the unknown electric field \mathbf{E}_a in the aperture by means of the formulas [Eq. (202a), Chapter 2]

$$\mathbf{E}_{s1} = \iint_{S_a} \mathbf{n} \times \mathbf{E}_a \cdot \nabla \times \bar{\mathbf{G}}_{e1} dS$$

$$\mathbf{E}_{s2} = \iint_{S_a} \mathbf{n}_0 \times \mathbf{E}_a \cdot \nabla \times \bar{\mathbf{G}}_{e2} dS$$

where the dyadic Green's functions satisfy the radiation conditions and the boundary conditions

$$\mathbf{n} \times \bar{\mathbf{G}}_{e1} = \mathbf{n} \times \bar{\mathbf{G}}_{e2} = 0$$

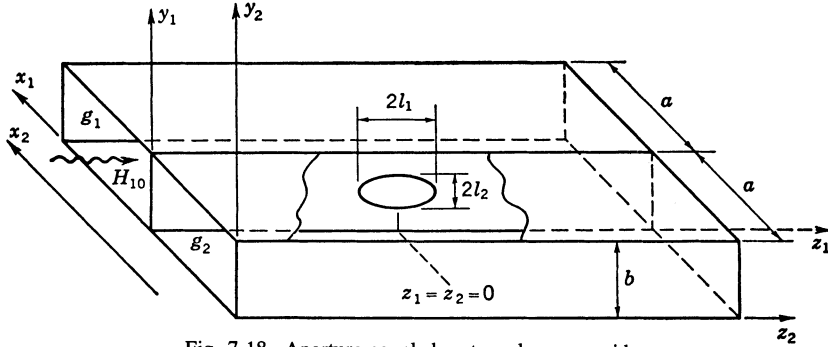


Fig. 7.18. Aperture-coupled rectangular waveguides.

on the waveguide walls and the aperture surface S_a . The boundary-value source $\mathbf{n} \times \mathbf{E}_a$ can be viewed as an equivalent magnetic current $-\mathbf{J}_m$ in the aperture. We can carry out a multipole expansion of the expressions for the scattered field, in the manner done for (56), and we then readily see that scattering into either guide is due to dipoles of equal strength but opposite sign. When we include the radiation reaction fields we are led to the symmetrical forms for the dipole strengths as given by (73). The polarizability tensors in (73) are equal to one-quarter of those for the complete two-sided aperture disk.

Aperture Coupling in Rectangular Guides

Consider an elliptic aperture in the common sidewall of two rectangular guides as in Fig. 7.18. The coordinates x_1, y_1, z_1 pertain to guide g_1 , and x_2, y_2, z_2 to guide g_2 . The center of the aperture is at $y_1 = b/2, z_1 = 0$. The major and minor semiaxes are l_1 and l_2 . An H_{10} mode is incident from the left in guide g_1 . We will assume that only the H_{10} mode propagates, and hence we will evaluate only the amplitudes of the scattered H_{10} modes. The normalized mode functions for the H_{10} mode are

$$\mathbf{E}_{10}^+ = \mathbf{e}_{10} e^{-\Gamma_{10} z}$$

$$\mathbf{E}_{10}^- = \mathbf{e}_{10} e^{\Gamma_{10} z}$$

$$\mathbf{H}_{10}^+ = (\mathbf{h}_{10} + \mathbf{h}_{z10}) e^{-\Gamma_{10} z}$$

$$\mathbf{H}_{10}^- = (-\mathbf{h}_{10} + \mathbf{h}_{z10}) e^{\Gamma_{10} z}$$

$$\mathbf{e}_{10} = -jk_0 Z_0 \left(\frac{2}{jabk_0 Z_0 \Gamma_{10}} \right)^{1/2} \sin \frac{\pi x}{a} \mathbf{a}_y$$

$$\mathbf{h}_{10} = \Gamma_{10} \left(\frac{2}{jabk_0 Z_0 \Gamma_{10}} \right)^{1/2} \sin \frac{\pi x}{a} \mathbf{a}_x$$

$$\mathbf{h}_{z10} = \left(\frac{2}{jabk_0 Z_0 \Gamma_{10}} \right)^{1/2} \frac{\pi}{a} \cos \frac{\pi x}{a} \mathbf{a}_z.$$

Let the incident mode be $A_1 \mathbf{E}_{10}^+$, $A_1 \mathbf{H}_{10}^+$, where A_1 is the amplitude constant. The incident mode does not have a component of electric field normal to the aperture, and so there will not be an induced electric dipole \mathbf{P}_0 . The incident magnetic field has a tangential component along the major axis of the ellipse only, and so the induced magnetic dipole moment is in the z direction. In guide g_1 a dipole $M_0 \mathbf{a}_z$ will produce a scattered field with amplitudes determined by (61). Thus in g_1

$$\mathbf{H}_{s1} = \frac{j\omega\mu_0}{2} \begin{cases} \mathbf{H}_{10}^- \cdot M_0 \mathbf{a}_z \mathbf{H}_{10}^+, & z > 0 \\ \mathbf{H}_{10}^+ \cdot M_0 \mathbf{a}_z \mathbf{H}_{10}^-, & z < 0. \end{cases}$$

This field has the following z component at the center of the aperture:

$$H_{s1,z} = \frac{\pi^2 M_0}{\Gamma_{10} a^3 b} = H_{r1}.$$

A dipole $-M_0 \mathbf{a}_z$ radiating into guide g_2 produces a scattered field \mathbf{H}_{s2} given by a similar expression. At the center of the aperture it has the value

$$H_{s2,z} = -\frac{\pi^2 M_0}{\Gamma_{10} a^3 b} = H_{r2}.$$

By using (73a) the dipole strength M_0 is found to be given by

$$M_0 = \frac{\pi l_1^3 e^2}{3[K(e) - E(e)]} \left[A_1 \frac{\pi}{a} \left(\frac{2}{jabk_0 Z_0 \Gamma_{10}} \right)^{1/2} + \frac{2\pi^2 M_0}{\Gamma_{10} a^3 b} \right]$$

or

$$M_0 = \frac{\alpha_m A_1 \frac{\pi}{a} \left(\frac{2}{jabk_0 Z_0 \Gamma_{10}} \right)^{1/2}}{1 - \alpha_m \frac{2\pi^2}{\Gamma_{10} a^3 b}}. \quad (74)$$

Let the scattered field in g_1 be

$$a_1 \mathbf{E}_{10}^+, a_1 \mathbf{H}_{10}^+, \quad z_1 > 0$$

$$b_1 \mathbf{E}_{10}^-, b_1 \mathbf{H}_{10}^-, \quad z_1 < 0.$$

Equations (61) are applicable in the present case, and hence

$$2b_1 = j\omega\mu_0 \mathbf{H}_{10}^+ \cdot \mathbf{M}_0 = j\omega\mu_0 \mathbf{h}_{z10} \cdot \mathbf{M}_0 \quad (75a)$$

$$2a_1 = j\omega\mu_0 \mathbf{H}_{10}^- \cdot \mathbf{M}_0 = j\omega\mu_0 \mathbf{h}_{z10} \cdot \mathbf{M}_0 = 2b_1. \quad (75b)$$

The total field in g_1 is the sum of the incident field plus the scattered field. If a reflection coefficient Γ is defined by the relation $b_1 = \Gamma A_1$, we find that

$$\Gamma = \frac{-j\alpha_m \pi^2 / (\beta_{10} a^3 b)}{1 + 2j\alpha_m \pi^2 / (\beta_{10} a^3 b)} \quad (76)$$

where $\Gamma_{10} = j\beta_{10}$ has been used and α_m is given by the first term in (70b).

In guide g_2 let the scattered field be

$$c_1 \mathbf{E}_{10}^+, c_1 \mathbf{H}_{10}^+, \quad z_2 > 0$$

$$d_1 \mathbf{E}_{10}^-, d_1 \mathbf{H}_{10}^-, \quad z_2 < 0.$$

If we had a current element \mathbf{J} in g_2 , an application of the Lorentz reciprocity theorem would give

$$2c_1 = - \iiint \mathbf{E}_{10}^- \cdot \mathbf{J} dV.$$

If \mathbf{J} consists of a small linear element \mathbf{J}_1 and a circulating element $J_2 \boldsymbol{\tau}$, where $\boldsymbol{\tau}$ is a unit vector tangent to the contour around which J_2 flows, we have

$$2c_1 = - \int \mathbf{E}_{10}^- \cdot \mathbf{J}_1 dl - \oint J_2 \mathbf{E}_{10}^- \cdot \boldsymbol{\tau} dl.$$

The second integral is equal to

$$- J_2 \iint \nabla \times \mathbf{E}_{10}^- \cdot d\mathbf{S} = j\omega\mu_0 J_2 \iint \mathbf{H}_{10}^- \cdot d\mathbf{S}$$

or, for a very small loop,

$$j\omega\mu_0 \mathbf{H}_{10}^- \cdot \iint J_2 d\mathbf{S}.$$

This latter integral defines a magnetic dipole \mathbf{M} , and, since $\int \mathbf{J}_1 dl$ is equivalent to an electric dipole $j\omega\mathbf{P}$, we get

$$2c_1 = -j\omega \mathbf{E}_{10}^- \cdot \mathbf{P} + j\omega\mu_0 \mathbf{H}_{10}^- \cdot \mathbf{M}.$$

For radiation into g_2 the effective aperture dipoles are $-\mathbf{P}_0$, $-\mathbf{M}_0$ in general. In the present case $\mathbf{P}_0 = 0$, and so we have

$$2c_1 = -j\omega\mu_0 \mathbf{H}_{10}^- \cdot \mathbf{M}_0 = -j\omega\mu_0 \mathbf{h}_{z10} \cdot \mathbf{M}_0$$

$$2d_1 = -j\omega\mu_0 \mathbf{H}_{10}^+ \cdot \mathbf{M}_0 = 2c_1.$$

In the coordinate system used for g_2 , we have, at $z_2 = 0$, $x_2 = a$,

$$\mathbf{h}_{z10} = - \left(\frac{2}{jabk_0 Z_0 \Gamma_{10}} \right)^{1/2} \frac{\pi}{a} \mathbf{a}_z$$

and hence $c_1 = d_1 = a_1 = b_1$. Note that the tangential magnetic fields in the scattered waves are of opposite sign at the aperture. This must be the case since their difference must give the nonzero value equal to the tangential component of the incident magnetic field.

The transmission coefficient into guide 2 for the dominant modes equals Γ . The transmission

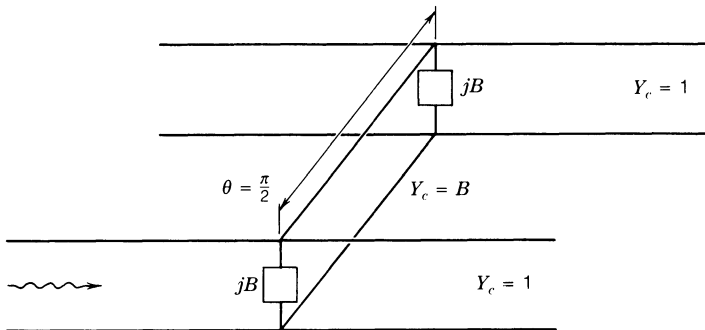


Fig. 7.19. Equivalent circuit for the two-coupled waveguides shown in Fig. 7.18.

coefficient into the output end of guide 1 equals $1 + \Gamma$. An equivalent circuit having these properties and the required fourfold symmetry is shown in Fig. 7.19. For this circuit the input admittance presented to guide 1 is

$$Y_{\text{in}} = 1 + jB + \frac{B^2}{2 + jB} = \frac{2 + 3jB}{2 + jB}.$$

The reflection coefficient is given by

$$\Gamma = \frac{1 - Y_{\text{in}}}{1 + Y_{\text{in}}} = \frac{-2jB}{4 + 4jB} = \frac{-j(B/2)}{1 + jB}.$$

When we compare this with (76) we find that the normalized susceptance B is given by

$$B = \frac{2\alpha_m \pi^2}{\beta_{10} a^3 b} = \frac{2\pi^3 l_1^3 e^2}{3\beta_{10} a^3 b [K(e) - E(e)]} \quad (77)$$

where $e = (1 - l_2^2/l_1^2)^{1/2}$. Since the equivalent circuit is a physically meaningful one it follows that power is conserved in the circuit. If the reaction fields had not been included then the reflection coefficient would have been given by the numerator in (76). A physical circuit having this form for the reflection coefficient and the transmission coefficients into guide g_2 does not exist. The equivalent circuit shows that there is a 90° phase angle associated with coupling from guide 1 to guide 2 when the aperture susceptance B is very small (strictly speaking, in the limit as B vanishes) because the coupling line has an electrical length θ equal to $\pi/2$.

A second straightforward example is the coupling of two rectangular waveguides by means of a small circular aperture in a common transverse wall as shown in Fig. 7.20. The input waveguide has dimensions $a \times b$ and the output waveguide $a' \times b'$. The incident generator fields in the input guide are

$$\mathbf{E}_{1g} = A(\mathbf{E}_{10}^+ - \mathbf{E}_{10}^-)$$

$$\mathbf{H}_{1g} = A(\mathbf{H}_{10}^+ - \mathbf{H}_{10}^-)$$

where the waveguide mode functions are those given earlier. The incident field has a nonzero x component of magnetic field so a magnetic dipole in the x direction is induced in the aperture. We can find the field radiated in the input guide by a dipole $M_0 \mathbf{a}_x$ by using image theory.

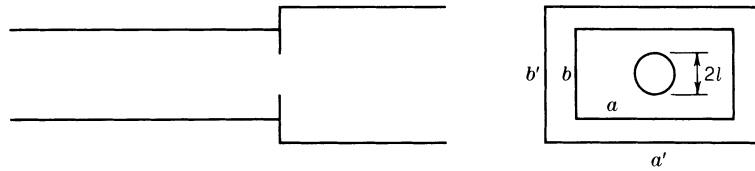


Fig. 7.20. Coupling of two rectangular waveguides by a circular aperture in a common transverse wall.

This gives a field which is the same as that radiated by a dipole $2M_0\mathbf{a}_x$ in the unbounded waveguide. The radiation reaction field for the input waveguide is

$$H_{1r} = j\omega\mu_0 \mathbf{H}_{10}^+ \cdot \mathbf{M}_0 \mathbf{H}_{10}^- \cdot \mathbf{a}_x = -\frac{2j\beta_{10}}{ab} M_0.$$

For the output waveguide the radiation reaction field produced by a dipole $-M_0\mathbf{a}_x$ is

$$H_{2r} = j\omega\mu_0 \mathbf{H}_{10}^- \cdot (-M_0\mathbf{a}_x) \mathbf{H}_{10}^+ \cdot \mathbf{a}_x = \frac{2j\beta'_{10}}{a'b'} M_0$$

where β'_{10} is the dominant mode propagation constant for the output waveguide. Upon using (73a) we obtain

$$M_0 = \alpha_m \left[2A\Gamma_{10} \left(\frac{2}{jabk_0 Z_0 \Gamma_{10}} \right)^{1/2} - \frac{2j\beta_{10}}{ab} M_0 - \frac{2j\beta'_{10}}{a'b'} M_0 \right]$$

which gives

$$M_0 = \frac{2A\alpha_m \Gamma_{10} \left(\frac{2}{jabk_0 Z_0 \Gamma_{10}} \right)^{1/2}}{1 + j\alpha_m \left(\frac{2\beta_{10}}{ab} + \frac{2\beta'_{10}}{a'b'} \right)}$$

where $\alpha_m = 4l^3/3$ and l is the radius of the aperture. The reflected wave in the input guide has an amplitude given by

$$-A + b_1 = j\omega\mu_0 \mathbf{M}_0 \cdot \mathbf{H}_{10}^+ - A.$$

The reflection coefficient Γ equals $(b_1 - A)/A$ and is

$$\Gamma = \frac{4 \frac{j\alpha_m \beta_{10}}{ab}}{1 + 2j\alpha_m \left(\frac{\beta_{10}}{ab} + \frac{\beta'_{10}}{a'b'} \right)} - 1.$$

The aperture admittance presented to the input waveguide is

$$Y_{\text{in}} = \frac{1 - \Gamma}{1 + \Gamma} = \frac{\beta'_{10} ab}{\beta_{10} a'b'} - j \frac{ab}{2\beta_{10}\alpha_m}. \quad (78)$$

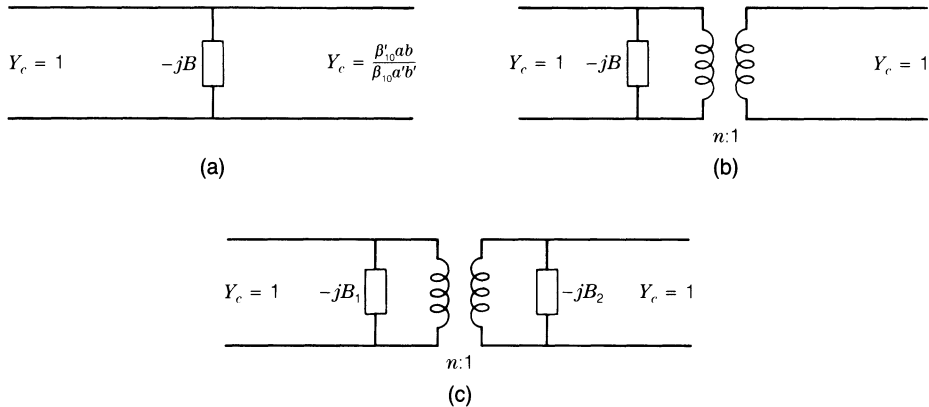


Fig. 7.21. (a) Equivalent circuit for the coupled waveguides shown in Fig. 7.20. (b) Susceptance B located on input side. (c) Susceptance B split into two components.

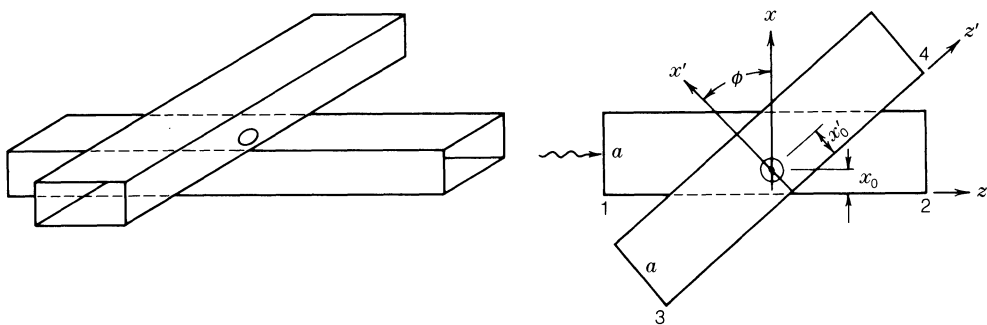


Fig. 7.22. Two waveguides coupled by an offset aperture in the broadwall.

The equivalent circuit consists of an output transmission line with normalized characteristic admittance equal to $(\beta'_{10}ab)/(\beta_{10}a'b')$ with an inductive susceptance of normalized value $ab/2\beta_{10}\alpha_m = 3ab/8\beta_{10}l^3$ in shunt with the junction. The shunt susceptance can be placed on one side of the ideal transformer as shown in Fig. 7.21(b) or split into two parts, one on each side, as shown in Fig. 7.21(c). In the latter circuit $B_1 = B/2$ and $B_2 = B/2n^2$ where $n^2 = \beta_{10}a'b'/\beta'_{10}ab$.

A coupling problem that is considerably more complex is that between two crossed rectangular waveguides coupled by means of an offset circular aperture in the common broadwall as shown in Fig. 7.22. In the input waveguide the center of the aperture is at $x = x_0$, $z = 0$, while in the output waveguide the center is at $x' = x'_0$, $z' = 0$. The axes of the two waveguides are inclined at an angle ϕ . The incident generator fields will be chosen as

$$\mathbf{E}_{g1} = A_1 \mathbf{E}_{10}^+ + A_2 \mathbf{E}_{10}^-, \quad \mathbf{H}_{g1} = A_1 \mathbf{H}_{10}^+ + A_2 \mathbf{H}_{10}^-$$

$$\mathbf{E}_{g2} = A_3 \mathbf{E}_{10}^+ + A_4 \mathbf{E}_{10}^-, \quad \mathbf{H}_{g2} = A_3 \mathbf{H}_{10}^+ + A_4 \mathbf{H}_{10}^-.$$

A full complement of dipoles P_{0y} , M_{0x} , M_{0y} is induced in the aperture. In order to evaluate the radiation reaction fields at the center of the aperture we note that M_{0x} produces a field for which E_y and H_z have odd symmetry about $z = 0$ and hence are zero at the center of the

aperture. The dipoles P_{0y} , M_{0z} produce a field H_x that is odd about $z = 0$ and hence is zero at the center of the aperture. The nonvanishing contributions to the radiation reaction field in the input waveguide are

$$\mathbf{E}_{1r} = \frac{j\omega\mu_0}{2} M_{0z} \mathbf{a}_z \cdot \mathbf{H}_{10}^- \mathbf{E}_{10}^+ - \frac{j\omega}{2} \mathbf{P}_0 \cdot \mathbf{E}_{10}^- \mathbf{E}_{10}^+$$

$$\mathbf{H}_{1r} = \frac{j\omega\mu_0}{2} [M_{0x} \mathbf{a}_x \cdot \mathbf{H}_{10}^- H_{10x}^+ \mathbf{a}_x + M_{0z} \mathbf{a}_z \cdot \mathbf{H}_{10}^- H_{10z}^+ \mathbf{a}_z] - \frac{j\omega}{2} \mathbf{P}_0 \cdot \mathbf{E}_{10}^- H_{10z}^+ \mathbf{a}_z$$

or in component form

$$E_{1ry} = -\frac{P_{0y}}{\epsilon_0} \left[\frac{jk_0^2}{\beta_{10}ab} \sin^2 \frac{\pi x_0}{a} \right] - M_{0z} \left[\frac{\pi k_0 Z_0}{\beta_{10}a^2 b} \sin \frac{\pi x_0}{a} \cos \frac{\pi x_0}{a} \right] \quad (79a)$$

$$H_{1rx} = -M_{0x} \frac{j\beta_{10}}{ab} \sin^2 \frac{\pi x_0}{a} \quad (79b)$$

$$H_{1rz} = \frac{P_{0y}}{\epsilon_0} \left[\frac{\pi k_0 Y_0}{\beta_{10}a^2 b} \sin \frac{\pi x_0}{a} \cos \frac{\pi x_0}{a} \right] - M_{0z} \left[\frac{j\pi^2}{\beta_{10}a^3 b} \cos^2 \frac{\pi x_0}{a} \right]. \quad (79c)$$

In the output waveguide the radiation reaction fields are given by similar expressions apart from a change in sign and replacement of x_0 by x'_0 ; thus

$$E_{2ry} = \frac{P_{0y}}{\epsilon_0} \left[\frac{jk_0^2}{\beta_{10}ab} \sin^2 \frac{\pi x'_0}{a} \right] + M_{0z'} \left[\frac{\pi k_0 Z_0}{\beta_{10}a^2 b} \sin \frac{\pi x'_0}{a} \cos \frac{\pi x'_0}{a} \right] \quad (80a)$$

$$H_{2rx'} = M_{0x'} \frac{j\beta_{10}}{ab} \sin^2 \frac{\pi x'_0}{a} \quad (80b)$$

$$H_{2rz'} = -\frac{P_{0y}}{\epsilon_0} \left[\frac{\pi k_0 Y_0}{\beta_{10}a^2 b} \sin \frac{\pi x'_0}{a} \cos \frac{\pi x'_0}{a} \right] + M_{0z'} \left[\frac{j\pi^2}{\beta_{10}a^3 b} \cos^2 \frac{\pi x'_0}{a} \right]. \quad (80c)$$

In order to evaluate the dipole strengths using (73) we make use of the following relationships:

$$\mathbf{H}_{2r} = (H_{2rx'} \cos \phi + H_{2rz'} \sin \phi) \mathbf{a}_x + (H_{2rz'} \cos \phi - H_{2rx'} \sin \phi) \mathbf{a}_z$$

$$\mathbf{M}_0 = (M_{0x} \cos \phi - M_{0z} \sin \phi) \mathbf{a}_{x'} + (M_{0z} \cos \phi + M_{0x} \sin \phi) \mathbf{a}_{z'} = M_{0x'} \mathbf{a}_{x'} + M_{0z'} \mathbf{a}_{z'}.$$

The equations for the dipole strengths are

$$\begin{aligned} P_{0y} = \epsilon_0 \alpha_e & \left\{ -jk_0 Z_0 N(A_1 + A_2) \sin \frac{\pi x_0}{a} + jk_0 Z_0 N(A_3 + A_4) \sin \frac{\pi x'_0}{a} \right. \\ & - \frac{P_{0y}}{\epsilon_0} \frac{jk_0^2}{\beta_{10}ab} \left(\sin^2 \frac{\pi x_0}{a} + \sin^2 \frac{\pi x'_0}{a} \right) - \frac{\pi k_0 Z_0}{\beta_{10}a^2 b} \\ & \left. \cdot \left[M_{0z} \sin \frac{\pi x_0}{a} \cos \frac{\pi x_0}{a} + (M_{0z} \cos \phi + M_{0x} \sin \phi) \sin \frac{\pi x'_0}{a} \cos \frac{\pi x'_0}{a} \right] \right\} \quad (81a) \end{aligned}$$

$$\begin{aligned}
M_{0x} = \alpha_m & \left\{ j\beta_{10}N(A_1 - A_2) \sin \frac{\pi x_0}{a} - j\beta_{10}N(A_3 - A_4) \sin \frac{\pi x'_0}{a} \cos \phi \right. \\
& - \frac{\pi}{a} N(A_3 + A_4) \cos \frac{\pi x'_0}{a} \sin \phi - \frac{j\beta_{10}}{ab} M_{0x} \sin^2 \frac{\pi x_0}{a} \\
& + \frac{P_{0y}}{\epsilon_0} \frac{\pi k_0 Y_0}{\beta_{10} a^2 b} \sin \phi \sin \frac{\pi x'_0}{a} \cos \frac{\pi x'_0}{a} - M_{0x} \\
& \cdot \left(\frac{j\beta_{10}}{ab} \cos^2 \phi \sin^2 \frac{\pi x'_0}{a} + \frac{j\pi^2}{\beta_{10} a^3 b} \sin^2 \phi \cos^2 \frac{\pi x'_0}{a} \right) \\
& \left. + M_{0z} \sin \phi \cos \phi \left(\frac{j\beta_{10}}{ab} \sin^2 \frac{\pi x'_0}{a} - \frac{j\pi^2}{\beta_{10} a^3 b} \cos^2 \frac{\pi x'_0}{a} \right) \right\} \quad (81b)
\end{aligned}$$

$$\begin{aligned}
M_{0z} = \alpha_m & \left\{ \frac{\pi N}{a} (A_1 + A_2) \cos \frac{\pi x_0}{a} - \frac{\pi N}{a} (A_3 + A_4) \cos \phi \cos \frac{\pi x'_0}{a} \right. \\
& + j\beta_{10}N(A_3 - A_4) \sin \phi \sin \frac{\pi x'_0}{a} + \frac{P_{0y}}{\epsilon_0} \frac{\pi k_0 Y_0}{\beta_{10} a^2 b} \\
& \cdot \left(\sin \frac{\pi x_0}{a} \cos \frac{\pi x_0}{a} + \cos \phi \sin \frac{\pi x'_0}{a} \cos \frac{\pi x'_0}{a} \right) \\
& - M_{0x} \cos \phi \sin \phi \left(\frac{j\pi^2}{\beta_{10} a^3 b} \cos^2 \frac{\pi x'_0}{a} - \frac{j\beta_{10}}{ab} \sin^2 \frac{\pi x'_0}{a} \right) \\
& - \frac{j\pi^2}{\beta_{10} a^3 b} M_{0z} \left(\cos^2 \frac{\pi x_0}{a} + \cos^2 \phi \cos^2 \frac{\pi x'_0}{a} \right) \\
& \left. - \frac{j\beta_{10}}{ab} M_{0z} \sin^2 \phi \sin^2 \frac{\pi x'_0}{a} \right\} \quad (81c)
\end{aligned}$$

where the normalization constant $N = (2/jabk_0Z_0\Gamma_{10})^{1/2}$. Note that there is significant interaction between the dipoles.

If we call the amplitudes of the dominant mode scattered fields a_1 , a_2 , a_3 , and a_4 , then these are given by

$$a_1 = \frac{j\omega\mu_0}{2} \mathbf{M}_0 \cdot \mathbf{H}_{10}^+ - \frac{j\omega}{2} \mathbf{P}_0 \cdot \mathbf{E}_{10}^+ \quad (82a)$$

$$a_2 = \frac{j\omega\mu_0}{2} \mathbf{M}_0 \cdot \mathbf{H}_{10}^- - \frac{j\omega}{2} \mathbf{P}_0 \cdot \mathbf{E}_{10}^- \quad (82b)$$

$$a_3 = -\frac{j\omega\mu_0}{2} \mathbf{M}'_0 \cdot \mathbf{H}_{10}^+ + \frac{j\omega}{2} \mathbf{P}_0 \cdot \mathbf{E}_{10}^+ \quad (82c)$$

$$a_4 = -\frac{j\omega\mu_0}{2} \mathbf{M}'_0 \cdot \mathbf{H}_{10}^- + \frac{j\omega}{2} \mathbf{P}_0 \cdot \mathbf{E}_{10}^- \quad (82d)$$

In the output waveguide $\mathbf{M}'_0 = M_{0x'} \mathbf{a}_{x'} + M_{0z'} \mathbf{a}_{z'} = (M_{0x} \cos \phi - M_{0z} \sin \phi) \mathbf{a}_{x'} +$

$(M_{0z} \cos \phi + M_{0x} \sin \phi) \mathbf{a}_{z'}$. Also, the mode functions $\mathbf{E}_{10}^\pm, \mathbf{H}_{10}^\pm$ for the output waveguide are different but of the same form as those for the input waveguide.

We can identify the following equivalent incident and total scattered wave voltages at each of the four ports of the junction being analyzed:

$$V_1^+ = A_1, \quad V_1^- = A_2 + a_1$$

$$V_2^+ = A_2, \quad V_2^- = A_1 + a_2$$

$$V_3^+ = A_3, \quad V_3^- = A_4 + a_3$$

$$V_4^+ = A_4, \quad V_4^- = A_3 + a_4.$$

The system of equations (81) can be solved for the dipole strengths. We can solve (82) for the amplitudes $a_i, i = 1, \dots, 4$ of the scattered waves. With this information the scattering-matrix elements S_{ij} for the four-port junction can be evaluated using the defined equivalent voltages and setting up the linear system

$$\begin{bmatrix} V_1^- \\ \vdots \\ V_4^- \end{bmatrix} = [S] \begin{bmatrix} V_1^+ \\ \vdots \\ V_4^+ \end{bmatrix}.$$

There is a considerable amount of algebra involved so we will limit the specific solutions to the special case $\phi = \pi/2$ and with the aperture centered for both waveguides so that $x_0 = x'_0 = a/2$ and the case $\phi = 0$. In this instance the junction has fourfold symmetry and can be described by a relatively simple network.

We will assume that $A_3 = A_4 = 0$. The equations for the dipole strengths, with the assumption of a centered aperture, give

$$P_{0y} = \frac{-jk_0Z_0N\epsilon_0\alpha_e(A_1 + A_2)}{1 + 2\frac{jk_0^2\alpha_e}{\beta_{10}ab}} \quad (83a)$$

$$M_{0x} = \frac{j\beta_{10}N\alpha_m(A_1 - A_2)}{1 + \frac{j\beta_{10}}{ab}\alpha_m}. \quad (83b)$$

The scattered wave in the input guide has the amplitude a_1 where

$$a_1 = \frac{j\omega\mu_0}{2} \Gamma_{10}NM_{0x} - \frac{\omega k_0 Z_0}{2} NP_{0y} = \frac{\frac{j\beta_{10}\alpha_m}{ab}(A_1 - A_2)}{1 + \frac{j\beta_{10}\alpha_m}{ab}} - \frac{\frac{jk_0^2\alpha_e}{\beta_{10}ab}(A_1 + A_2)}{1 + \frac{2jk_0^2\alpha_e}{\beta_{10}ab}}.$$

For even excitation $A_2 = A_1 = A$ and the reflection coefficient is

$$\Gamma_e = 1 + \frac{a_1}{A} = \frac{1}{1 + \frac{2jk_0^2\alpha_e}{\beta_{10}ab}}. \quad (84)$$

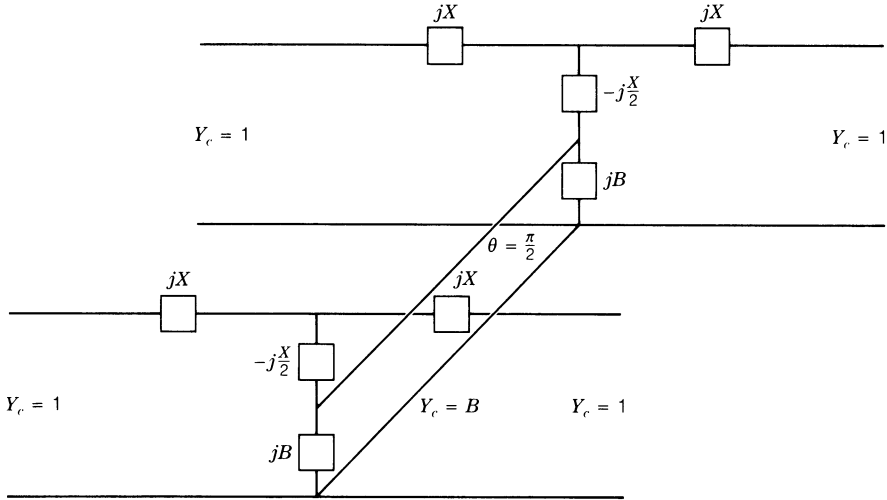


Fig. 7.23. Equivalent circuit for coupling between two orthogonal waveguides by a centered circular aperture in the broadwall.

For odd excitation $A_2 = -A_1 = -A$ and the reflection coefficient is

$$\Gamma_o = -1 + \frac{a_1}{A} = \frac{\frac{j\beta_{10}\alpha_m}{ab} - 1}{\frac{j\beta_{10}\alpha_m}{ab} + 1}. \quad (85)$$

The equivalent circuit that has the required properties is shown in Fig. 7.23. In this circuit the series reactance $X = \beta_{10}\alpha_m/ab$ and the shunt susceptance $B = 2k_0^2\alpha_e/\beta_{10}ab$. The reader can readily verify that with an open circuit at the midplane the circuit shown in Fig. 7.23 has an input admittance given by

$$Y_{in,e} = \frac{1 - \Gamma_e}{1 + \Gamma_e} = \frac{\frac{jk_0^2\alpha_e}{\beta_{10}ab}}{1 + \frac{jk_0^2\alpha_e}{\beta_{10}ab}} \quad (86a)$$

and with a short circuit at the midplane

$$Y_{in,o} = \frac{1 - \Gamma_o}{1 + \Gamma_o} = \frac{1}{j\beta_{10}\alpha_m/ab}. \quad (86b)$$

The amplitudes of the dominant modes coupled into the output waveguide are given by

$$a_3 = a_4 = \frac{\omega k_0 Z_0}{2} N P_{0y} = \frac{\frac{jk_0^2\alpha_e}{\beta_{10}ab} (A_1 + A_2)}{1 + 2j \frac{k_0^2\alpha_e}{\beta_{10}ab}}.$$

When the two waveguides are aligned ($\phi = 0$) but the aperture is not centered there is

interaction between P_{0y} and M_{0z} . The reader can verify that for this case the solutions for the dipole strengths are ($A_3 = A_4 = 0$ is assumed)

$$\frac{P_{0y}}{\epsilon_0} = \frac{-jk_0Z_0NS\alpha_e}{\Delta}(A_1 + A_2) \quad (87a)$$

$$M_{0z} = \frac{\pi NC\alpha_m}{a\Delta}(A_1 + A_2) \quad (87b)$$

$$M_{0x} = \frac{j\alpha_m\beta_{10}NS(A_1 - A_2)}{1 + 2j\frac{\alpha_m\beta_{10}}{ab}S^2} \quad (87c)$$

where

$$S = \sin \frac{\pi x_0}{a}, \quad C = \cos \frac{\pi x_0}{a}$$

and

$$\Delta = 1 + 2j\frac{\alpha_e k_0^2 S^2}{\beta_{10} ab} + 2j\frac{\alpha_m \pi^2 C^2}{\beta_{10} a^3 b}.$$

By considering the two special cases of even excitation with $A_1 = A_2 = A$ and odd excitation with $A_2 = -A_1 = -A$ the even and odd reflection coefficients are found to be

$$\Gamma_e = \frac{1}{1 + jB} \quad (88a)$$

$$\Gamma_o = \frac{-1}{1 + jX} \quad (88b)$$

where

$$B = \frac{2k_0^2 \alpha_e S^2}{\beta_{10} ab} + \frac{2\pi^2 \alpha_m C^2}{\beta_{10} a^3 b} \quad (89a)$$

$$X = \frac{2\beta_{10} \alpha_m S^2}{ab}. \quad (89b)$$

The equivalent circuits for even and odd excitation are shown in Fig. 7.24. For a wave incident at port 1 only, i.e., $A_2 = A_3 = A_4 = 0$, the amplitudes of the waves coupled into ports 3 and 4 are

$$a_3 = \left(\frac{-jX/2}{1 + jX} + \frac{jB/2}{1 + jB} \right) A_1 \quad (90a)$$

$$a_4 = \left(\frac{jX/2}{1 + jX} + \frac{jB/2}{1 + jB} \right) A_1. \quad (90b)$$

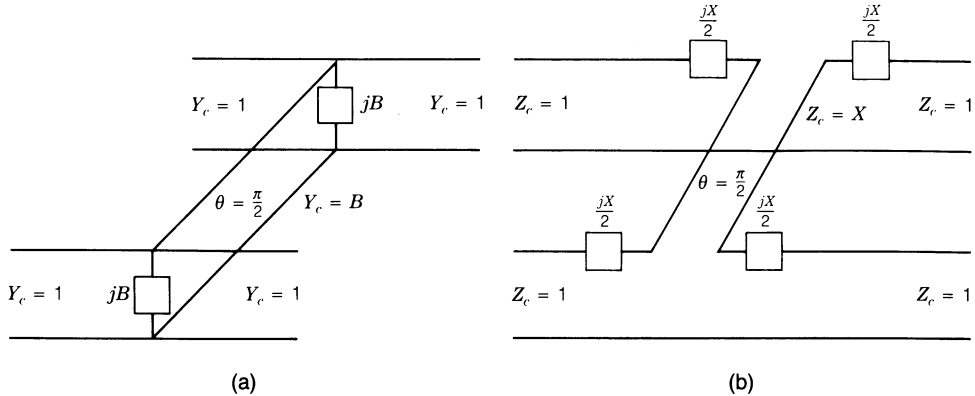


Fig. 7.24. (a) Equivalent circuit for two parallel waveguides coupled by an offset circular aperture in the common broadwall for even excitation. (b) Equivalent circuit for odd excitation.

The dipoles P_{0y} and M_{0z} radiate symmetrically into the upper waveguide, while the dipole M_{0x} radiates an antisymmetrical field. If we choose the aperture position such that $X = B$ then there will be zero transmission into port 3. The junction now has the properties of a directional coupler (Bethe hole coupler). The required position of the circular aperture is given by

$$\sin \frac{\pi X_0}{a} = \frac{\lambda_0}{\sqrt{6}a}. \quad (91)$$

The field at port 4 could be canceled by choosing

$$\sin \frac{\pi X_0}{a} = \frac{\lambda_0}{\sqrt{2(\lambda_0^2 - a^2)}} \quad (92)$$

if the radiation reaction field could be neglected. This equation has a solution only when $\lambda_0 \geq \sqrt{2}a$.

When the radiation reaction field is included and we make $X = -B$, i.e., impose the condition given by (92), then

$$a_3 = \frac{jB}{1+B^2} A_1$$

$$a_4 = \frac{B^2}{1+B^2} A_1.$$

The coupling coefficient C is thus given by

$$C = 20 \log \left| \frac{A_1}{a_3} \right| = 20 \log \frac{1+B^2}{B} \approx 20 \log \frac{1}{B} dB.$$

The directivity is given by

$$D = 20 \log \left| \frac{a_3}{a_4} \right| = 20 \log \frac{1}{B} \approx C dB.$$

It has generally been thought that α_4 could be made equal to zero, but the more general aperture coupling theory that includes the reaction fields shows that this is not possible. The more complete theory shows that only a finite directivity can be obtained.

A directional coupler can also be obtained by using a centered circular aperture and non-aligned waveguides (see Problem 7.10). For this type of coupler the theoretical directivity is also somewhat less than the coupling. Experimentally it is found that the attenuation caused by the finite thickness of the waveguide wall in which the aperture is located reduces the directivity below the theoretical value [7.36].

7.4. CAVITY COUPLING BY SMALL APERTURES

It is common practice to couple cavities to waveguides by means of small apertures. The small-aperture coupling theory presented in the previous section applies equally well to cavity coupling when the reaction fields coming from the cavity are identified to be the resonant mode fields in the cavity. We will illustrate the theory by considering two examples.

End Excited Cavity

A rectangular cavity is formed by placing a transverse wall with a small centered circular aperture into a rectangular waveguide, a distance d from the short-circuited end as shown in Fig. 7.25. The cavity is assumed to be resonant for the TE_{101} mode. The normalized TE_{101} cavity mode fields are

$$\mathbf{E}_{101} = \left(\frac{4}{abd} \right)^{1/2} \sin \frac{\pi x}{a} \sin \frac{\pi z}{d} \mathbf{a}_y$$

$$\mathbf{H}_{101} = \frac{1}{k_{101}} \nabla \times \mathbf{E}_{101} = \left(\frac{4}{abd} \right)^{1/2} k_{101}^{-1} \left[-\frac{\pi}{d} \sin \frac{\pi x}{a} \cos \frac{\pi z}{d} \mathbf{a}_x + \frac{\pi}{a} \cos \frac{\pi x}{a} \sin \frac{\pi z}{d} \mathbf{a}_z \right].$$

A magnetic dipole $-M_0 \mathbf{a}_x$ will excite this mode with an amplitude given by (173) in Chapter

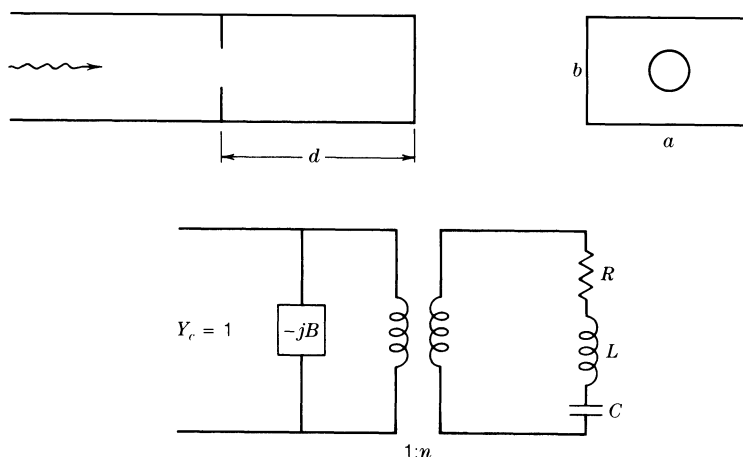


Fig. 7.25. End excited rectangular cavity and its equivalent circuit.

5; thus

$$h_{101} = -\frac{k_0^2 M_0 \mathbf{a}_x \cdot \mathbf{H}_{101}}{k_{101}^2 - k_0^2 \left(1 + \frac{1-j}{Q}\right)} = \frac{\left(\frac{4}{abd}\right)^{1/2} k_0^2 M_0 (\pi/k_{101}d)}{k_{101}^2 - k_0^2 \left(1 + \frac{1-j}{Q}\right)}$$

where $k_{101}^2 = (\pi/a)^2 + (\pi/d)^2$ and Q is the quality factor for the mode. The x component of the magnetic field at the center of the aperture is

$$-h_{101} \left(\frac{4}{abd}\right)^{1/2} \frac{\pi}{k_{101}d}.$$

This field is taken as the reaction field because it is large when the cavity is tuned to resonate for the TE₁₀₁ mode. In the rectangular waveguide the radiation reaction field is the same as it is for the aperture in a transverse wall, which was analyzed in the previous section. Thus the equation for M_0 is

$$M_0 = \alpha_m \left\{ 2A j \beta_{10} N - \frac{2j\beta_{10}}{ab} M_0 + \frac{4k_0^2 \pi^2 M_0}{k_{101}^2 ab d^3 \left[k_{101}^2 - k_0^2 \left(1 + \frac{1-j}{Q}\right) \right]} \right\}$$

which gives

$$M_0 = \frac{2\alpha_m j \beta_{10} N A}{1 + jX + W}$$

where $X = 2\alpha_m \beta_{10}/ab$,

$$W = -\frac{4\alpha_m k_0^2 \pi^2}{k_{101}^2 ab d^3 \left[k_{101}^2 - k_0^2 \left(1 + \frac{1-j}{Q}\right) \right]}$$

and A is the amplitude of the incident TE₁₀ mode.

The total reflected TE₁₀ mode amplitude is

$$-A + j\omega\mu_0 M_0 \mathbf{a}_x \cdot \mathbf{H}_{10}^+ = -A + \frac{4j\alpha_m \beta_{10} A / ab}{1 + jX + W}.$$

The reflection coefficient is obtained by dividing by A . The input admittance is

$$Y_{in} = \frac{1 - \Gamma}{1 + \Gamma} = \frac{1 + W}{jX} = -jB + Y \quad (93a)$$

where

$$B = \frac{ab}{2\alpha_m \beta_{10}} \quad (93b)$$

$$Y = \frac{j2k_0^2\pi^2}{\beta_{10}k_{101}^2d^3 \left[k_{101}^2 - k_0^2 \left(1 + \frac{1-j}{Q} \right) \right]}. \quad (93c)$$

In the equivalent circuit shown in Fig. 7.25 the inductance L is the sum of that for the cavity, L_c , plus L_s arising from the surface impedance of the cavity walls. The input admittance is

$$Y_{\text{in}} = \frac{n^2}{j\omega L_c + j\omega L_s + R - j/\omega C} - jB.$$

We can express the denominator in the form

$$\frac{j}{\omega\omega_0^2 C} (\omega^2 + \omega^2\omega_0^2 L_s C - \omega_0^2 - j\omega\omega_0^2 RC)$$

where $\omega_0 = (L_c C)^{-1/2}$ is the loss-free cavity resonant frequency. We now take note of the relations

$$\frac{R}{\omega_0 L_c} = \omega_0 RC = \frac{1}{Q} = \frac{\omega_0 L_s}{\omega_0 L_c} = \omega_0^2 L_s C$$

and use the approximation $\omega\omega_0^2 RC \approx \omega^2/Q$ to obtain

$$Y_{\text{in}} = -jB + \frac{j\omega\omega_0^2 C n^2}{\omega_0^2 - \omega^2 \left(1 + \frac{1-j}{Q} \right)}. \quad (94)$$

In order to determine the parameter n^2 we need to specify the impedance level of the cavity. We will do this by considering the line integral of the electric field across the center of the cavity as the equivalent voltage V_c across the capacitor C in the equivalent circuit. The electric field is given by

$$E_y = \frac{V_c}{b} \sin \frac{\pi x}{a} \sin \frac{\pi z}{d}.$$

The stored electric energy is

$$W_e = \frac{\epsilon_0}{4} \int_0^a \int_0^b \int_0^d E_y^2 dz dy dx = \frac{\epsilon_0 ad}{16b} V_c^2 = \frac{1}{4} C V_c^2$$

and hence $C = \epsilon_0 ad / 4b$. We now obtain

$$Y_{\text{in}} = -jB + \frac{j k_0 Y_0 \omega_0^2 a d n^2}{4b \left[\omega_0^2 - \omega^2 \left(1 + \frac{1-j}{Q} \right) \right]} \quad (95)$$

upon using $\omega\epsilon_0 = k_0 Y_0$. When we compare this expression with Y given by (93c) we find that

$$n^2 = \frac{8\pi^2 b Z_0}{k_0 \beta_{10} k_{101}^2 a d^4}. \quad (96)$$

We will define the resonant frequency of the coupled cavity as the frequency at which Y_{in} is real. From (93) we find that the imaginary part of Y_{in} vanishes when

$$\left(\frac{1+Q}{Q} k_0^2 - k_{101}^2 \right) \left[B\beta_{10} k_{101}^4 d^3 - k_0^2 \left(2\pi^2 + B\beta_{10} k_{101}^2 d^3 \frac{1+Q}{Q} \right) \right] = \frac{\beta_{101} k_{101}^4 d^3 B}{Q^2}. \quad (97)$$

For a high- Q cavity we can set the term on the right equal to zero; thus

$$k_0^2 = \frac{k_{101}^2}{1 + \frac{2\pi^2}{B\beta_{10} k_{101}^2 d^3}} \approx k_{101}^2 - \frac{2\pi^2}{B\beta_{10} k_{101}^2 d^3} = k_{101}^2 - \frac{4\pi^2 \alpha_m}{abd^3}.$$

We now use $k_0^2 - k_{101}^2 \approx 2k_{101}(k_0 - k_{101})$ to obtain

$$k_0 \approx k_{101} - \frac{2\pi^2 \alpha_m}{k_{101} abd^3}. \quad (98)$$

In order to obtain critical coupling we require $Y_{\text{in}} = 1$ at resonance. From (93a) we see that this requires Y to have a unit conductance. This condition gives

$$\frac{2k_0^4 \pi^2}{\beta_{10} k_{101}^2 d^3 Q} = \left(k_{101}^2 - k_0^2 \frac{1+Q}{Q} \right)^2 + \frac{k_0^4}{Q^2} \approx \left(\frac{4\pi^2 \alpha_m}{abd^3} \right)^2 + \frac{k_0^4}{Q^2} \approx \left(\frac{4\pi^2 \alpha_m}{abd^3} \right)^2$$

which can be solved for α_m to yield

$$\alpha_m = \frac{k_0^2 abd}{\pi k_{101} \sqrt{8\beta_{10} Q/d}} = \frac{4}{3} l^3. \quad (99)$$

We can use $k_0 = k_{101}$ to get the first approximation to α_m and then use (98) to calculate a corrected value for k_0 to use in (99).

As a typical example consider a cavity with $d = a = 2.2$ cm, $b = 1$ cm, and having a Q of 6000. For this cavity $k_{101} = 202$. We now use $k_0 \approx k_{101}$, $\beta_{10} = [k_0^2 - (\pi/a)^2]^{1/2} \approx [k_{101}^2 - (\pi/a)^2]^{1/2} = \pi/d$ and from (99) obtain $\alpha_m \approx 17.63 \times 10^{-9}$. The corrected value for k_0 is $202 - 0.735$ which is not a large enough change to warrant calculating a corrected value for α_m . The required aperture radius is $l = 0.236$ cm. The reader can readily verify that the approximations made to obtain (98) and (99) are fully justified since the detuning effect of the aperture susceptance $-jB$ is very small.

Two-Port Cavity

The two-port cavity shown in Fig. 7.26 has the property that maximum power is transmitted through the cavity at resonance. We will assume that the cavity resonates in the TE_{101} mode. In the apertures x -directed magnetic dipoles are induced. At the center of the input aperture the incident TE_{10} mode produces the following x -directed generator field H_{g1} :

$$H_{g1} = 2j\beta_{10}NA$$

where A is the amplitude of the incident mode. The resonant frequency of the cavity is given

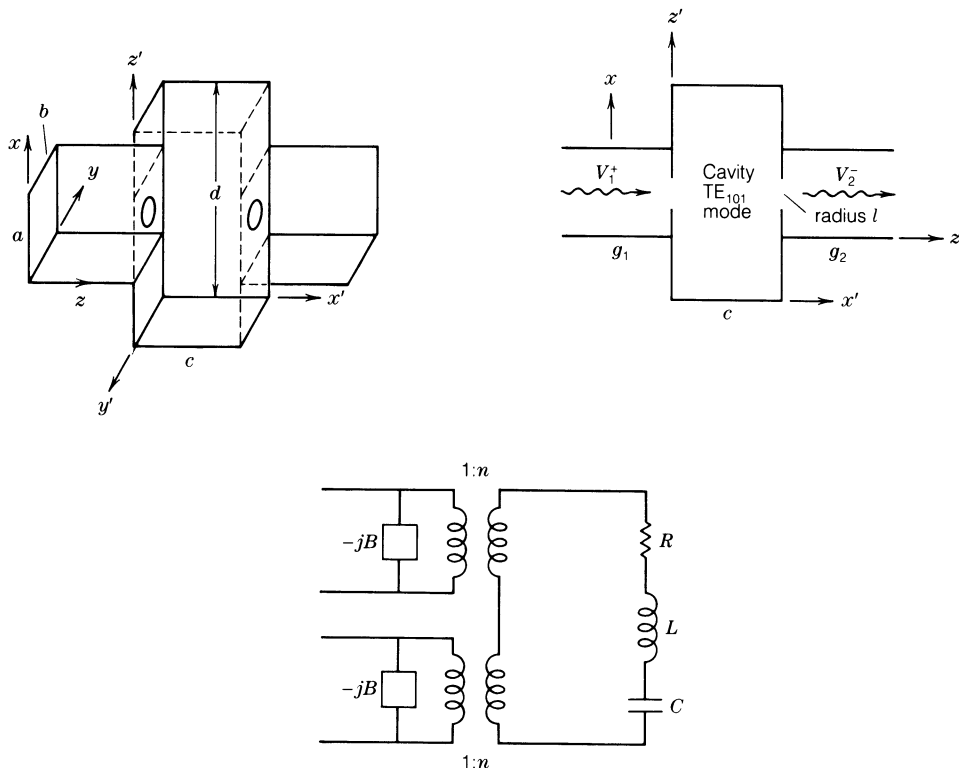


Fig. 7.26. A two-port cavity system and its equivalent circuit.

by

$$\omega_0 = \omega_{101} = k_{101}(\mu_0\epsilon_0)^{-1/2}$$

where

$$k_{101} = [(\pi/c)^2 + (\pi/d)^2]^{1/2}.$$

The cavity field will excite a magnetic dipole in the output aperture which will cause some power to be radiated into the output guide g_2 . In g_1 and g_2 a dipole $M_0 \mathbf{a}_x$ radiates a TE₁₀ mode with H_x at the center of the aperture given by $H_{1rx} = H_{2rx} = -2j\beta_{10}M_0/ab$. In order to find the reaction field from the cavity consider dipoles $M_{z'1}$ and $M_{z'2}$ in the input and output apertures. These produce a TE₁₀₁ mode with amplitude h_{101} for the \mathbf{H}_{101} mode field where

$$\mathbf{H}_{101} = \sqrt{\frac{4}{bcd}} k_{101}^{-1} \left[-\frac{\pi}{d} \sin \frac{\pi x'}{c} \cos \frac{\pi z'}{d} \mathbf{a}_{x'} + \frac{\pi}{c} \cos \frac{\pi x'}{c} \sin \frac{\pi z'}{d} \mathbf{a}_{z'} \right]$$

$$h_{101} = \frac{k_0^2}{k_{101}^2 - k_0^2 \left(1 + \frac{1-j}{Q} \right)} \sqrt{\frac{4}{bcd}} \frac{\pi}{k_{101} c} (M_{z'1} - M_{z'2}).$$

Note that $k_{101}^2 = \omega_0^2 k_0^2 / \omega^2$, $\omega_0 = \omega_{101}$. The field $H_{z'}$ is given by

$$H_{z'} = H_{z'r} = \frac{\omega^2}{\omega_0^2 - \omega^2 \left(1 + \frac{1-j}{Q}\right)} \frac{4}{bcd} \left(\frac{\pi}{k_{101}c}\right)^2 (M_{z'1} - M_{z'2})$$

at the center of the input aperture and the negative of this at the center of the output aperture. Let the factor W be

$$W = \frac{\omega^2}{\omega_0^2 - \omega^2 \left(1 + \frac{1-j}{Q}\right)} \frac{4\pi^2}{bcd(k_{101}c)^2}. \quad (100)$$

We can also write $M_{z'1} = M_{x1}$, $M_{z'2} = M_{x2}$. For the input aperture we now have

$$M_0 = M_{x1} = \alpha_m \left(H_{g1} - \frac{2j\beta_{10}}{ab} M_{x1} + WM_{x1} - WM_{x2} \right) \quad (101a)$$

while for the output aperture we have

$$M_{x2} = \alpha_m \left(-\frac{2j\beta_{10}}{ab} M_{x2} + WM_{x2} - WM_{x1} \right) \quad (101b)$$

since H_{g2} is zero. We can solve the second equation for M_{x2} and the first equation then gives

$$M_{x1} \left[1 + \alpha_m \left(\frac{2j\beta_{10}}{ab} - W \right) - \frac{\alpha_m^2 W^2}{1 + \alpha_m \left(\frac{2j\beta_{10}}{ab} - W \right)} \right] = \alpha_m H_{g1}. \quad (102)$$

The total reflected field in g_1 is $-A + a_1 = -A - k_0 Z_0 \beta_{10} N M_{x1}$, and $\Gamma = -1 + a_1/A$ is given by

$$\Gamma = -1 + \frac{2jX(1 + \alpha_m U)}{(1 + \alpha_m U)^2 - \alpha_m^2 W^2}$$

where

$$X = \frac{2\alpha_m \beta_{10}}{ab}, \quad U = \frac{2j\beta_{10}}{ab} W.$$

We now find that

$$Y_{\text{in}} = \frac{1 - \Gamma}{1 + \Gamma} = \frac{1}{jX} - \frac{\alpha_m W}{jX \left(1 - \frac{\alpha_m W}{1 + jX} \right)}. \quad (103)$$

Let $K = (4\alpha_m/bcd)(\pi/k_{101}c)^2$; then we get

$$Y_{\text{in}} = \frac{1}{jX} - \frac{\frac{K\omega^2}{bcd} \left[\omega_0^2 - \omega^2 \left(1 + \frac{1-j}{Q} \right) \right]}{jX \left[\omega_0^2 - \omega^2 \left(1 + \frac{1-j}{Q} \right) \right] - \frac{\omega^2 K}{1 + (1/jX)}}. \quad (104)$$

The equivalent circuit for the two-port cavity is shown in Fig. 7.26. For this circuit

$$\begin{aligned} Y_{\text{in}} &= -jB + \frac{n^2}{j\omega L + \frac{1}{j\omega C} + R + \frac{n^2}{1-jB}} \\ &= -jB + \frac{n^2\omega^2}{j\omega L \left(\omega^2 - \omega_0^2 - j\frac{R}{\omega L}\omega^2 \right) + \frac{n^2\omega^2}{1-jB}} \end{aligned} \quad (105)$$

where $\omega_0^2 = 1/LC$. Now $\omega L/R = Q$ so we have

$$Y_{\text{in}} = -jB - \frac{n^2\omega^2}{j\omega L \left(\omega_0^2 - \omega^2 + \omega^2 \frac{j}{Q} \right) - \frac{n^2\omega^2}{1-jB}}. \quad (106)$$

Hence we must choose

$$\frac{1}{jX} = -jB$$

so $B = ab/2\beta_{10}\alpha_m$. In addition,

$$\frac{n^2}{\omega L} = \frac{K}{X} = \frac{2ab}{\beta_{10}bcd} \left(\frac{\pi}{k_{101}c} \right)^2.$$

The input admittance Y_{in} for the cavity has the factor $\omega_0^2 - \omega^2((1-j)/Q) - \omega^2/Q$. The last term comes from the additional inductance due to the surface impedance $(1+j)/\sigma\delta_s$. This can be included in the equivalent circuit as a series inductance $j\omega L_s = R$. Then $(R + j\omega L_s)/j\omega L$ becomes $(1+j)/Q$ and Y_{in} becomes

$$Y_{\text{in}} = -jB - \frac{n^2\omega^2}{j\omega L \left(\omega_0^2 - \omega^2 + \frac{\omega^2 j}{Q} - \frac{\omega^2}{Q} \right) - \frac{n^2\omega^2}{1-jB}} \quad (107)$$

which is the same function of ω as occurs in (104). We need to add L_s in series with L and then the new resonant frequency is

$$\omega'_0 = \frac{1}{\sqrt{C(L+L_s)}} = \sqrt{\frac{Q}{1+Q}}\omega_0.$$

For convenience, we assume that L_s is included in L .

The field radiated into g_2 is given by

$$a_2 = \beta_{10}k_0Z_0NM_{x2}.$$

Now $M_{x2} = -\alpha_mWM_{x1}/[1 + \alpha_m(2j\beta_{10}/ab - W)]$ and since M_{x1} radiates a wave with

amplitude $-\beta_{10}k_0Z_0NM_{x1} = (1 + \Gamma)A$ we see that

$$a_2 = \frac{\alpha_m W}{1 + \alpha_m \left(\frac{2j\beta_{10}}{ab} - W \right)} (1 + \Gamma)A.$$

The factor $A(1 + \Gamma)$ is the input voltage in the equivalent circuit. This appears as a series voltage $A(1 + \Gamma)n$ in the resonator circuit. The total loop impedance is

$$j\omega(L + L_s) + \frac{1}{j\omega C} + R + \frac{n^2}{1 - jB} = Z_L.$$

A fraction

$$\left(\frac{-n^2}{1 - jB} \right) \frac{1}{Z_L}$$

appears across the output transformer and produces an output voltage $1/n$ smaller. Thus

$$a_2 = \frac{-n(1 + \Gamma)An}{(1 - jB)Z_L} = \frac{-n^2 A(1 + \Gamma)}{(1 - jB)Z_L}.$$

This is the same result obtained by the small-aperture coupling theory.

The parameter $n^2/\omega L$ occurs as a single parameter. n^2 is arbitrary which corresponds to the arbitrary choice of the impedance level $\sqrt{L/C}$ of the equivalent resonant circuit representing the cavity. A useful choice in practice is to make the voltage V_c across the capacitor C correspond to the line integral of the electric field across the cavity at the center. We then find from energy considerations that

$$C = \frac{\epsilon_0 cd}{4b}.$$

The equivalent inductance is given by the resonance condition

$$L = \frac{1}{\omega_0^2 C}$$

when the surface impedance term L_s is excluded. The parameter n^2 is given by

$$n^2 = \frac{2a}{\beta_{10}cd} \left(\frac{\pi}{k_{101}c} \right)^2 \omega_0 L = \frac{8ab}{\beta_{10}k_0 c^2 d^2} \left(\frac{\pi}{k_{101}c} \right)^2 Z_0 \quad (108)$$

which is of the same form as (96).

The two-port cavity represents a lossy network that couples the input and output waveguides together. Consequently, it is not possible to obtain complete power transmission through the cavity. The output waveguide presents a resistive loading of the cavity. This loading should be large relative to the cavity losses so that most of the power will be transmitted to the output

waveguide. We note that (105) can be expressed as

$$Y_{\text{in}} = -jB + \frac{n^2}{j\omega L + \frac{1}{j\omega C} + \frac{jn^2B}{1+B^2} + R + \frac{n^2}{1+B^2}}.$$

Since normally B is very large the effective series loading resistance R_e equals n^2/B^2 . If we make $n^2/B^2 \gg R$ then only a small fraction of the input power is dissipated in the cavity. The loading resistance is given by

$$R_e = \frac{n^2}{B^2} = \frac{8\alpha_m^2\beta_{10}Z_0}{k_0ab(cd)^2} \left(\frac{\pi}{k_{101}c} \right)^2. \quad (109)$$

The external Q_e associated with this resistance is

$$Q_e = \frac{B^2}{n^2\omega C} = \frac{acdb^2}{8\alpha_m^2\beta_{10}} \left(\frac{k_{101}c}{\pi} \right)^2. \quad (110)$$

In order to illustrate typical values that can be obtained consider a waveguide with $a = 2.3$ cm, $b = 1$ cm, $c = 2.5$ cm, $d = 3$ cm, and an aperture radius $l = 0.25$ cm. For this case $Q_e = 9353$. It is quite clear that it will be difficult to achieve a high degree of loading unless a large aperture is used. If we increase l to 0.35 cm then $Q_e = 1242$ which would normally be significantly smaller than the unloaded Q of the cavity. However, an aperture radius of this size is large enough to raise questions as to the validity of the small-aperture theory.

7.5. GENERAL REMARKS ON APERTURE COUPLING

If the medium in g_1 has electrical constitutive parameters ϵ_1 and μ_1 and that in guide g_2 has ϵ_2 , μ_2 then the dipole strengths for radiation into g_1 are \mathbf{P}_1 , \mathbf{M}_1 , where [7.30]

$$(\epsilon_1 + \epsilon_2)\mathbf{P}_1 = 2\epsilon_1\bar{\alpha}_e \cdot [\epsilon_1\mathbf{E}_{g1} - \epsilon_2\mathbf{E}_{g2} + \epsilon_1(\bar{\mathbf{A}}_1 \cdot \mathbf{P}_1 + \bar{\mathbf{B}}_1 \cdot \mathbf{M}_1) - \epsilon_2(\bar{\mathbf{A}}_2 \cdot \mathbf{P}_2 + \bar{\mathbf{B}}_2 \cdot \mathbf{M}_2)] \quad (111a)$$

$$(\mu_1 + \mu_2)\mathbf{M}_1 = 2\mu_2\bar{\alpha}_m \cdot \left[\mathbf{H}_{g1} - \mathbf{H}_{g2} + \left(\bar{\mathbf{C}}_1 + \frac{\epsilon_2}{\epsilon_1}\bar{\mathbf{C}}_2 \right) \cdot \mathbf{P}_1 - \left(\bar{\mathbf{D}}_1 + \frac{\mu_1}{\mu_2}\bar{\mathbf{D}}_2 \right) \cdot \mathbf{M}_1 \right]. \quad (111b)$$

For radiation into guide g_2 the dipole strengths are $-\mathbf{P}_2$ and $-\mathbf{M}_2$ where

$$\epsilon_1\mathbf{P}_2 = \epsilon_2\mathbf{P}_1 \quad (111c)$$

$$\mu_2\mathbf{M}_2 = \mu_1\mathbf{M}_1. \quad (111d)$$

The tensors $\bar{\mathbf{A}}_1$, $\bar{\mathbf{B}}_1$, $\bar{\mathbf{C}}_1$, and $\bar{\mathbf{D}}_1$ are defined by expressing the radiation reaction fields in g_1 due to \mathbf{P}_1 and \mathbf{M}_1 in the form

$$\mathbf{E}_{1r} = \bar{\mathbf{A}}_1 \cdot \mathbf{P}_1 + \bar{\mathbf{B}}_1 \cdot \mathbf{M}_1 \quad (112a)$$

$$\mathbf{H}_{1r} = \bar{\mathbf{C}}_1 \cdot \mathbf{P}_1 + \bar{\mathbf{D}}_1 \cdot \mathbf{M}_1. \quad (112b)$$

The tensors $\bar{\mathbf{A}}_2$, $\bar{\mathbf{B}}_2$, $\bar{\mathbf{C}}_2$, and $\bar{\mathbf{D}}_2$ are defined so that the radiation reaction fields in g_2 due to $-\mathbf{P}_2$ and $-\mathbf{M}_2$ are given by

$$\mathbf{E}_{2r} = -\bar{\mathbf{A}}_2 \cdot \mathbf{P}_2 - \bar{\mathbf{B}}_2 \cdot \mathbf{M}_2 \quad (112c)$$

$$\mathbf{H}_{2r} = -\bar{\mathbf{C}}_2 \cdot \mathbf{P}_2 - \bar{\mathbf{D}}_2 \cdot \mathbf{M}_2. \quad (112d)$$

The small-aperture theory does not take into account the reduction of the coupling due to the finite thickness of the wall that the aperture is located in. This reduction in coupling can be as large as 1 or 2 dB in typical waveguide walls. Some theoretical results for the effects of finite wall thickness may be found in the papers by McDonald [7.33] and Leviatan *et al.* [7.32].

The problem of coupling through an aperture in a thick wall may be formulated in an exact way. With reference to Fig. 7.27 consider an aperture in a wall of thickness t . Let $\bar{\mathbf{G}}_{e1}$ and $\bar{\mathbf{G}}_{e2}$ be electric-type dyadic Green's functions for the input and output guides. These satisfy the radiation conditions and the boundary conditions $\mathbf{n} \times \bar{\mathbf{G}}_{e1} = \mathbf{n} \times \bar{\mathbf{G}}_{e2} = 0$ on the waveguide walls and the aperture surfaces S_1 and S_2 . Let the unknown tangential electric fields on S_1 and S_2 be \mathbf{E}_1 and \mathbf{E}_2 . The equivalent magnetic currents are

$$\mathbf{J}_{m1} = -\mathbf{n}_1 \times \mathbf{E}_1, \quad \mathbf{J}_{m2} = -\mathbf{n}_2 \times \mathbf{E}_2.$$

The scattered fields in g_1 and g_2 are given by [Eq. (202a), Chapter 2]

$$\mathbf{E}_{s1} = - \iint_{S_1} \mathbf{J}_{m1} \cdot \nabla \times \bar{\mathbf{G}}_{e1} dS \quad (113a)$$

$$\mathbf{E}_{s2} = - \iint_{S_2} \mathbf{J}_{m2} \cdot \nabla \times \bar{\mathbf{G}}_{e2} dS. \quad (113b)$$

We also need an equation that connects \mathbf{J}_{m1} and \mathbf{J}_{m2} . For this purpose we introduce a dyadic Green's function $\bar{\mathbf{G}}_e$ for the cavity formed by the two surfaces S_1 , S_2 and the sidewalls of the aperture opening. Inside the cavity the scattered field is given by

$$\mathbf{E}_s = \iint_{S_1} \mathbf{J}_{m1} \cdot \nabla \times \bar{\mathbf{G}}_e dS + \iint_{S_2} \mathbf{J}_{m2} \cdot \nabla \times \bar{\mathbf{G}}_e dS. \quad (114)$$

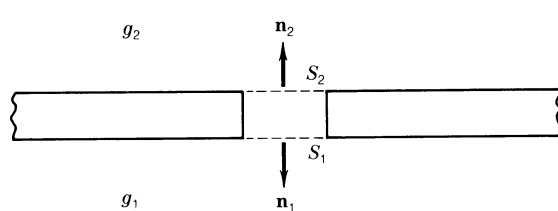


Fig. 7.27. Aperture in a thick wall.

Equations (113) and (114) will ensure the continuity of the tangential electric field through the aperture opening. The equivalent magnetic currents must be determined so that the tangential magnetic field is also continuous through the aperture. This requirement can be stated in the form

$$\mathbf{n} \times (\mathbf{H}_{g1} + \mathbf{H}_{s1}) = \mathbf{n} \times \mathbf{H}_s \quad \text{on } S_1 \quad (115a)$$

$$\mathbf{n} \times (\mathbf{H}_{g2} + \mathbf{H}_{s2}) = \mathbf{n} \times \mathbf{H}_s \quad \text{on } S_2 \quad (115b)$$

where \mathbf{H}_{g1} and \mathbf{H}_{g2} are the incident generator fields and the scattered magnetic fields are obtained from the corresponding electric fields by using Maxwell's equations. For the aperture cavity the dyadic Green's function \mathbf{G}_e can be approximated by its quasi-static value. For a circular aperture it can be constructed from the waveguide modes in a circular waveguide below cutoff. The two most important and least attenuated modes are the TE₁₁ and TM₀₁ modes which are the ones needed to describe coupling from the magnetic and electric dipoles, respectively. For small apertures a multipole expansion of the integrals given by (113) and (114) can be carried out in the same way that (56) was expanded. In general, the available theoretical results for coupling by apertures in thick walls is very limited. The edge conditions are different for an aperture in a thick wall as compared to an aperture in an infinitely thin wall. Consequently, some difference in the polarizability of the aperture would be expected. A detailed analysis of this problem is not available at this time.

7.6. TRANSIENTS IN WAVEGUIDES

In any waveguide, the phase velocity v_p is a function of frequency. As a consequence, all signals having a finite frequency spectrum will undergo dispersion when transmitted through a length of guide. The phase relationship between the frequency components of the original signal at the feeding point continually changes as the signal progresses along the guide. The analysis of this phenomenon belongs in the domain of transient analysis, and may be handled by the conventional techniques utilizing Laplace and Fourier transforms. Any realistic analysis should take into account the frequency characteristics of the antenna or aperture that couples the signal into the guide as well as the characteristics of the circuit elements used to extract the signal at the receiving end. In this section we shall consider only the properties of the guide itself. The effect of losses and their variation will also be neglected. In practice, this does not lead to significant errors, because in most cases the frequency bandwidth of the signal is relatively narrow, and the mid-band frequency of operation is usually chosen far enough above the cutoff frequency so that the attenuation curve is approximately constant throughout the band.

Before some time, which we choose as the time origin $t = 0$, the disturbance in the guide is zero. When a current element is introduced into the guide, a disturbance or signal is generated. This signal is a solution of the time-dependent field equations. Let $\mathbf{E}(\mathbf{r}, t)$, $\mathbf{J}\mathbf{C}(\mathbf{r}, t)$ be the time-dependent field vectors. For a unit impulse current element $\delta(t - t')$ applied at time $t = t'$ and located at the point (x', y', z') , the field vectors are a solution of

$$\nabla \times \mathbf{E} = -\mu_0 \frac{\partial \mathbf{J}\mathbf{C}}{\partial t} \quad (116a)$$

$$\nabla \times \mathbf{J}\mathbf{C} = \epsilon_0 \frac{\partial \mathbf{E}}{\partial t} + \tau \delta(t - t') \delta(\mathbf{r} - \mathbf{r}') \quad (116b)$$

where τ is a unit vector giving the direction of the current element, and \mathbf{r} designates the field point (x, y, z) , while \mathbf{r}' designates the source point or location. If the Laplace transform of these equations is taken, we get

$$\nabla \times \mathbf{E}(\mathbf{r}, p) = -\mu_0 p \mathbf{H}(\mathbf{r}, p) \quad (117a)$$

$$\nabla \times \mathbf{H}(\mathbf{r}, p) = \epsilon_0 p \mathbf{E}(\mathbf{r}, p) + \tau e^{-pt'} \delta(\mathbf{r} - \mathbf{r}') \quad (117b)$$

where

$$\mathbf{E}(\mathbf{r}, p) = \int_0^\infty \mathbf{E}(\mathbf{r}, t) e^{-pt} dt$$

with a similar definition for $\mathbf{H}(\mathbf{r}, p)$. These equations are formally the same as those obtained by assuming a time dependence $e^{j\omega t}$, and the solution may be obtained by the methods we have previously discussed. All our previous solutions may be converted into solutions of (117) by replacing $j\omega$ by p and $e^{j\omega t}$ by $e^{-pt'}$. The Laplace transform has the effect of suppressing the time variable. The solution to (117) constitutes the Laplace transform of the time-dependent Green's function. Inverting the transform yields the time-dependent Green's function. For an arbitrary spatial and time variation, the solution may be obtained by a superposition integral.

If we restrict ourselves to a line current extending across the narrow dimension of a rectangular guide, the appropriate Green's function is obtained from Chapter 5, Eq. (74). We have

$$E_y(\mathbf{r}, p) = G(\mathbf{r}|\mathbf{r}', p) = \frac{-\mu_0}{a} \sum_{n=1}^{\infty} \Phi_n(x) \Phi_n(x') \cdot \frac{p \exp\{-pt' - [(n\pi/a)^2 + \mu_0\epsilon_0 p^2]^{1/2}|z - z'|\}}{[(n\pi/a)^2 + \mu_0\epsilon_0 p^2]^{1/2}} \quad (118)$$

where $\Phi_n(x) = \sin(n\pi x/a)$. The inversion of this expression gives us the time-dependent Green's function corresponding to the disturbance set up in the waveguide by an impulse line current located at x', z' . The Laplace transform of the time derivative of a function $f(t)$ is

$$\mathcal{L} \frac{df}{dt} = \int_0^\infty e^{-pt} \frac{df}{dt} dt = f e^{-pt} \Big|_0^\infty + p \int_0^\infty e^{-pt} f dt.$$

If f vanishes at $t = 0$, we have $\mathcal{L} df/dt = p \mathcal{L} f$, where \mathcal{L} indicates the operation of taking the Laplace transform of the function. Using this result, we may invert each term in (118) disregarding the factor p in the numerator, and then differentiate the result with respect to t . A typical term from (118) gives

$$\begin{aligned} & \frac{1}{2\pi j} \int_C \frac{\exp\{p(t - t') - [(n\pi/a)^2 + \mu_0\epsilon_0 p^2]^{1/2}|z - z'|\}}{[(n\pi/a)^2 + \mu_0\epsilon_0 p^2]^{1/2}} dp \\ &= \begin{cases} v_c J_0 \left\{ \frac{n\pi}{a} [v_c^2(t - t')^2 - (z - z')^2]^{1/2} \right\}, & 0 < \frac{|z - z'|}{v_c} < t - t' \\ 0, & \text{otherwise} \end{cases} \end{aligned}$$

where J_0 is the Bessel function of the first kind, and $v_c = (\mu_0 \epsilon_0)^{-1/2}$ is the velocity of light in a vacuum.³ At any given distance $|z - z'|$ from the source, the disturbance is zero until a time $t = t' + |z - z'|/v_c$ is reached when the presence of the signal first becomes known to the observer at this position. No information reaches the observer in a time interval less than the time required to propagate a disturbance with the velocity of light. The velocity of light is, therefore, the wavefront velocity.

The time derivative of the above function is

$$\frac{-v_c^3(n\pi/a)(t-t')}{[v_c^2(t-t')^2-(z-z')^2]^{1/2}}J_1\left\{\frac{n\pi}{a}[v_c^2(t-t')^2-(z-z')^2]^{1/2}\right\}+v_c\delta\left(t-t'-\frac{|z-z'|}{v_c}\right)$$

where J_1 is the Bessel function of the first kind and order 1. The solution for the time-dependent Green's function which is equal to $\mathcal{E}_y(\mathbf{r}, t)$ becomes

$$\begin{aligned}\mathcal{G}(\mathbf{r}|\mathbf{r}', t-t') &= \frac{Z_0}{a} \sum_{n=1}^{\infty} \Phi_n(x)\Phi_n(x') \\ &\cdot \left[v_c^2 \frac{n\pi}{a} (t-t') \frac{J_1\{(n\pi/a)[v_c^2(t-t')^2-(z-z')^2]^{1/2}\}}{[v_c^2(t-t')^2-(z-z')^2]^{1/2}} - \delta\left(t-t'-\frac{|z-z'|}{v_c}\right) \right] \quad (119)\end{aligned}$$

for $t' < t' + |z - z'|/v_c \leq t$. Outside this range for t the Green's function is zero. In the interpretation of (119) it should be noted that

$$\lim_{u \rightarrow 0} \frac{J_1(ku)}{u} = \lim_{u \rightarrow 0} \frac{dJ_1}{du} = \lim_{u \rightarrow 0} \frac{k}{2} [J_0(ku) - J_2(ku)] = \frac{k}{2}.$$

Alternatively, the recurrence relation $J_1(ku) = (ku/2)[J_2(ku) + J_0(ku)]$ may be used to eliminate the factor $[v_c^2(t-t')^2-(z-z')^2]^{1/2}$ in the denominator. The field contributed by each mode first makes its appearance as an impulse plus a step change, and thereafter oscillates similar to a damped sinusoidal wave. Thus what was originally a pulse localized in both time and space has become a disturbance distributed throughout both space and time.

For an impressed current $\mathbf{J}(\mathbf{r}, t)$ which varies arbitrarily with time for $t > 0$, the response is obtained by a superposition integral, i.e.,

$$\iiint_0^t \mathcal{G}(\mathbf{r}|\mathbf{r}', t-t')J(\mathbf{r}', t') dt' dS' \quad (120)$$

when $J(t) = 0$ for $t < 0$. For a step input, the solution is readily found since the Laplace transform of a unit step applied at $t = t'$ is $p^{-1}e^{-pt'}$. This corresponds to (118) with the factor p deleted from the numerator. The terms that arise are those obtained in arriving at (119) before the derivative with respect to time was taken.

Impulse and step inputs are not typical of the signal we wish to transmit along a waveguide. More realistic signals are those consisting of a narrow spectrum of frequencies, centered around some high frequency ω_0 , such as is encountered in amplitude-modulated sinusoids. For an analysis of these we turn to an application of Fourier transforms.

³This transform is listed by Churchill in [7.9].

Let the input current at $x = a/2$, $z = 0$ be of the form of an amplitude-modulated signal

$$I = I_0[1 + f(t)] \cos \omega_0 t \quad (121)$$

where $f(t)$ is an arbitrary function of time subject to the restriction that it contains frequencies in the range $0 \leq \omega \leq \omega_1$ with $\omega_1 \ll \omega_0$. Thus the resultant signal has frequency components in the range $\omega_0 - \omega_1 \leq \omega \leq \omega_0 + \omega_1$, and ω_0 corresponds to the carrier frequency. Furthermore, let ω_1 be chosen so that $(\pi/a)v_c < \omega < (2\pi/a)v_c$. This latter restriction ensures us that only the H_{10} mode in a rectangular guide of width a will propagate.

The current input is the real part of $(1+f)e^{j\omega_0 t}$. The function $f(t)$ has a frequency spectrum given by the Fourier transform of $f(t)$:

$$g(\omega) = \int_{-\infty}^{\infty} e^{-j\omega t} f(t) dt. \quad (122)$$

The function $f(t)$ may be recovered by the inverse transform relation

$$f(t) = \frac{1}{2\pi} \int_{-\infty}^{\infty} e^{j\omega t} g(\omega) d\omega = \frac{1}{2\pi} \int_{-\omega_1}^{\omega_1} e^{j\omega t} g(\omega) d\omega. \quad (123)$$

The transform of $e^{j\omega_0 t}$ is $2\pi\delta(\omega - \omega_0)$, and, hence, for the function $(1+f)e^{j\omega_0 t}$ the frequency spectrum is given by $2\pi\delta(\omega - \omega_0) + g(\omega - \omega_0)$. Each frequency component propagates along the guide in a manner described by the steady-state solution corresponding to an impressed current varying with time according to $e^{j\omega t}$. For the H_{10} mode, the y component of electric field, at a distance z from the origin, arising from a single frequency component is

$$-\frac{j\omega\mu_0}{a} \Phi_1(x) \frac{\exp\{j\omega t - j|z|[(\omega/v_c)^2 - (\pi/a)^2]^{1/2}\}}{[(\omega/v_c)^2 - (\pi/a)^2]^{1/2}} = -\frac{j\omega\mu_0}{a} \Phi_1(x) \frac{e^{j\omega t - j\beta(\omega)|z|}}{\beta(\omega)}$$

where $\beta(\omega) = [(\omega/v_c)^2 - (\pi/a)^2]^{1/2}$. This expression without the factor $e^{j\omega t}$ may be considered as the transfer function, in the frequency domain, relating the response at $|z|$ to the input at $z = 0$. With the specified input current, the total response is

$$\begin{aligned} \mathcal{E}_y &= -\text{Re} \frac{\mu_0 I_0}{a 2\pi} \Phi_1 \int_{-\infty}^{\infty} \frac{j\omega e^{-j\beta(\omega)|z|}}{\beta(\omega)} [2\pi\delta(\omega - \omega_0) + g(\omega - \omega_0)] e^{j\omega t} d\omega \\ &= -\frac{\mu_0 I_0}{2\pi a} \Phi_1 \text{Re} \left[\frac{j2\pi\omega_0 e^{j\omega_0 t - j\beta_0|z|}}{\beta_0} + \int_{-\infty}^{\infty} \frac{j\omega e^{j\omega t - j\beta(\omega)|z|}}{\beta(\omega)} g(\omega - \omega_0) d\omega \right] \end{aligned} \quad (124)$$

where $\beta_0 = \beta(\omega_0)$. The first term in (124) corresponds to the unmodulated carrier and does not contain any information. The second term is the signal containing the original modulation-frequency components. In this term, the integration need be extended only over the range $\omega_0 - \omega_1$ to $\omega_0 + \omega_1$, since $g(\omega - \omega_0)$ is zero outside this range.

To evaluate the integral, we expand $\beta(\omega)$ in a Taylor series about the point ω_0 to get

$$\beta(\omega) = \beta_0 + \beta'_0(\omega - \omega_0) + \frac{1}{2!} \beta''_0(\omega - \omega_0)^2 + \dots \quad (125)$$

where $\beta'_0 = d\beta/d\omega|_{\omega=\omega_0}$, etc. For a signal containing only a narrow band of frequencies, we

retain only the first two terms in (125) and approximate the factor ω/β by ω_0/β_0 . For this case we then get

$$\begin{aligned} \frac{1}{2\pi} \int_{-\infty}^{\infty} \frac{j\omega e^{j\omega t - j\beta|z|}}{\beta} g(\omega - \omega_0) d\omega &\approx \frac{j\omega_0}{2\pi\beta_0} e^{j\omega_0 t - j\beta_0|z|} \int_{\omega_0 - \omega_1}^{\omega_0 + \omega_1} e^{j(\omega - \omega_0)(t - \beta'_0|z|)} g(\omega - \omega_0) d\omega \\ &= \frac{j\omega_0}{\beta_0} e^{j\omega_0 t - j\beta_0|z|} f(t - \beta'_0|z|). \end{aligned} \quad (126)$$

The latter result follows by making the change of variables $\omega - \omega_0 = \omega'$ and comparing with (123). Combining the two terms and taking the real part, we obtain the total response at $|z|$:

$$\mathcal{E}_y = \frac{\mu_0 I_0}{a} \Phi_1(x) \frac{\omega_0}{\beta_1} [1 + f(t - \beta'_0|z|)] \sin \omega_0 \left(t - \frac{\beta_0}{\omega_0} |z| \right). \quad (127)$$

To this order of approximation the original modulation is reproduced without distortion but delayed in time by an amount $\beta'_0|z|$. The velocity with which the signal propagates is equal to the distance $|z|$ divided by the time delay, and hence is given by

$$v_g = \frac{1}{\beta'_0} = \left[\frac{d\beta(\omega)}{d\omega} \Big|_{\omega_0} \right]^{-1} = \frac{v_c^2 \beta_0}{\omega_0} = \frac{v_c^2}{v_p} \quad (128)$$

where the carrier phase velocity v_p is equal to $\omega_0/\beta_0 = (k_0/\beta_0)v_c$. This particular definition of signal velocity is called the group velocity, since it corresponds to the velocity with which a narrow band or group of frequency components is propagated. It is also equal to the velocity of energy propagation introduced in Chapter 3 and is always less than the velocity of light for a uniform hollow waveguide.

If the band of frequencies involved is too large for only two terms of the Taylor series expansion of $\beta(\omega)$ to give a good representation of $\beta(\omega)$ throughout the band, then additional terms must be included. These higher order terms always lead to distortion of the signal. In general, these terms are difficult to evaluate unless $f(t)$ happens to be of such a form that the inverse transforms can be found. Forrer has presented an analysis for the propagation of a pulse of the form $e^{-(t+t_0)^2}$. In this case terms up to and including $\frac{1}{2}\beta''_0(\omega - \omega_0)^2$ in the expansion of β may be evaluated, since the transforms involved are of the type that may be readily inverted [7.10]. Several other papers that treat various types of transients in waveguides have also been published. Several of these papers are listed in the general references below.

REFERENCES AND BIBLIOGRAPHY

- [7.1] R. W. P. King, *The Theory of Linear Antennas*. Cambridge, MA: Harvard University Press, 1956, sect. II.39.
- [7.2] E. Jahnke and F. Emde, *Tables of Functions*, 4th ed. New York, NY: Dover Publications, 1945.
- [7.3] E. P. Augustin, U.S. Patent 4,528,528, July 9, 1985.
- [7.4] H. T. Howard, U.S. Patent 4,414,516, Nov. 8, 1983.
- [7.5] H. A. Bethe, "Theory of diffraction by small holes," *Phys. Rev.*, vol. 66, pp. 163–182, 1944.
- [7.6] S. B. Cohn, "Determination of aperture parameters by electrolytic tank measurements," *Proc. IRE*, vol. 39, pp. 1416–1421, Nov. 1951.
- [7.7] J. A. Stratton, *Electromagnetic Theory*. New York, NY: McGraw-Hill Book Company, Inc., 1941, sect. 3.27.
- [7.8] R. E. Collin, "Rayleigh scattering and power conservation," *IEEE Trans. Antennas Propagat.*, vol. AP-29, pp. 795–798, 1981.

- [7.9] R. V. Churchill, *Operational Mathematics*, 2nd ed. New York, NY: McGraw-Hill Book Company, Inc., 1958, p. 329.
- [7.10] M. P. Forrer, "Analysis of millimicrosecond RF pulse transmission," *Proc. IRE*, vol. 46, pp. 1830–1835, Nov. 1958.

Waveguide Antennas

- [7.11] L. Infeld, A. F. Stevenson, and J. L. Synge, "Contributions to the theory of waveguides," *Can. J. Res.*, vol. 27, pp. 68–129, July 1949.
- [7.12] H. Motz, *Electromagnetic Problems of Microwave Theory*, Methuen Monograph. London: Methuen & Co., Ltd., 1951.
- [7.13] L. Lewin, "A contribution to the theory of probes in waveguides," *Proc. IEE (London)*, vol. 105, part C, pp. 109–116, Mar. 1958.
- [7.14] M. J. Al-Hakkak, "Experimental investigation of the input impedance characteristics of an antenna in a rectangular waveguide," *Electron. Lett.*, vol. 5, pp. 513–514, 1969.
- [7.15] A. G. Williamson and D. V. Otto, "Coaxially fed hollow cylindrical monopole in a rectangular waveguide," *Electron. Lett.*, vol. 9, pp. 218–220, 1973.
- [7.16] A. G. Williamson, "Coaxially fed hollow probe in a rectangular waveguide," *Proc. IEE*, vol. 132, part H, pp. 273–285, 1985.
- [7.17] J. M. Jarem, "A multifilament method-of-moments solution for the input impedance of a probe-excited semi-infinite waveguide," *IEEE Trans. Microwave Theory Tech.*, vol. MTT-35, pp. 14–19, 1987.
- [7.18] M. D. Deshpande and B. N. Das, "Input impedance of coaxial line to circular waveguide feed," *IEEE Trans. Microwave Theory Tech.*, vol. MTT-25, pp. 954–957, 1977.
- [7.19] M. D. Deshpande and B. N. Das, "Analysis of an end launcher for a circular cylindrical waveguide," *IEEE Trans. Microwave Theory Tech.*, vol. MTT-26, pp. 672–675, 1978.
- [7.20] G. L. Ragan, *Microwave Transmission Circuits*, vol. 9 of Rad. Lab. Series. New York, NY: McGraw-Hill Book Company, Inc., 1948.

Aperture Coupling

- [7.21] L. B. Felson and N. Marcuvitz, "Slot coupling of rectangular and spherical waveguides," *J. Appl. Phys.*, vol. 24, pp. 755–770, June 1953.
- [7.22] S. B. Cohn, "The electric polarizability of apertures of arbitrary shape," *Proc. IRE*, vol. 40, pp. 1069–1071, Sept. 1952.
- [7.23] S. B. Cohn, "Microwave coupling by large apertures," *Proc. IRE*, vol. 40, pp. 696–699, 1952.
- [7.24] E. Arvas and R. F. Harrington, "Computation of the magnetic polarizability of conducting disks and the electric polarizabilities of apertures," *IEEE Trans. Antennas Propagat.*, vol. AP-31, pp. 719–725, 1983.
- [7.25] N. A. McDonald, "Polynomial approximations for the electric polarizabilities of some small apertures," *IEEE Trans. Microwave Theory Tech.*, vol. MTT-33, pp. 1146–1149, 1985.
- [7.26] J. Van Bladel, "Small hole coupling of resonant cavities and waveguides," *Proc. IEE*, vol. 117, pp. 1098–1104, 1970.
- [7.27] J. Van Bladel, "Small holes in a waveguide wall," *Proc. IEE*, vol. 118, pp. 43–50, 1971.
- [7.28] R. F. Harrington and J. R. Mautz, "A generalized network formulation for aperture problems," *IEEE Trans. Antennas Propagat.*, vol. AP-24, pp. 870–873, 1976.
- [7.29] Y. Rahmat-Samii and R. Mittra, "Electromagnetic coupling through small apertures in a conducting screen," *IEEE Trans. Antennas Propagat.*, vol. AP-25, pp. 180–187, 1977.
- [7.30] R. E. Collin, "Small aperture coupling between dissimilar regions," *Electromagnetics*, vol. 2, pp. 1–24, 1982. (In this reference the polarizability tensors are twice as large and the radiation reaction fields in the output waveguide are defined with the opposite sign.)
- [7.31] C. H. Liang and D. K. Cheng, "Generalized network representations for small-aperture coupling between dissimilar regions," *IEEE Trans. Antennas Propagat.*, vol. AP-31, pp. 177–182, 1983.
- [7.32] Y. Levitan, R. F. Harrington, and J. R. Mautz, "Electromagnetic transmission through apertures in a cavity in a thick conductor," *IEEE Trans. Antennas Propagat.*, vol. AP-30, pp. 1153–1165, 1982.
- [7.33] N. A. McDonald, "Electric and magnetic coupling through small apertures in shield walls of any thickness," *IEEE Trans. Microwave Theory Tech.*, vol. MTT-20, pp. 689–695, 1972.
- [7.34] R. Levy, "Analysis and synthesis of waveguide multi-aperture directional couplers," *IEEE Trans. Microwave Theory Tech.*, vol. MTT-16, pp. 995–1006, 1968.

- [7.35] R. Levy, "Improved single and multiaperture waveguide coupling theory, including explanation of mutual interactions," *IEEE Trans. Microwave Theory Tech.*, vol. MTT-28, pp. 331–338, 1980.
- [7.36] C. G. Montgomery, *Technique of Microwave Measurements*, vol. 11 of Rad. Lab. Series. New York, NY: McGraw-Hill Book Company, Inc., 1947. Sec. 14.3.

Waveguide Transients

- [7.37] M. Cerillo, "Transient phenomena in waveguides," *Electronics Tech. Rep.* 33, MIT Research Lab., 1948.
- [7.38] G. I. Cohn, "Electromagnetic transients in waveguides," in *Proc. Nat. Electronics Conf.*, vol. 8, pp. 284–295, 1952.
- [7.39] M. Cotte, "Propagation of a pulse in a waveguide," *Onde Elec.*, vol. 34, pp. 143–146, 1954.
- [7.40] R. S. Elliott, "Pulse waveform degradation due to dispersion in waveguides," *IRE Trans. Microwave Theory Tech.*, vol. MTT-5, pp. 245–257, 1957.
- [7.41] A. E. Karbowiak, "Propagation of transients in waveguides," *Proc. IEE (London)*, vol. 104, part C, pp. 339–349, 1957.

PROBLEMS

7.1. A small probe antenna is located in the center of the end wall of a rectangular guide (see Fig. P7.1). The

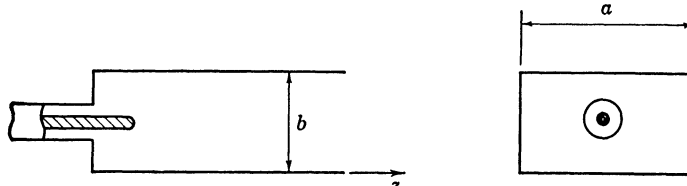


Fig. P7.1.

guide dimensions are such that the only E mode that will propagate is the E_{11} mode. Obtain an expression for the radiation resistance of the antenna.

7.2. Consider a small circular loop antenna of radius d , carrying a uniform current I_0 and located in free space. Expand $e^{-jk_0\rho}$ to get $1 - jk_0\rho - \frac{1}{2}k_0^2\rho^2 + (jk_0^3/6)\rho^3 + \dots$. Evaluate the self-flux linkage through the loop contributed by the terms in phase quadrature with the current, and show that the term with the factor $jk_0\rho$ does not contribute while the term with the factor $(jk_0^3/6)\rho^3$ gives $(-\jmath\mu_0\pi I_0/6k_0)(k_0d)^4$. Evaluate the induced emf around the loop due to this portion of the flux linkage, and show that it leads to an input resistance $Z_0(k_0d)^4\pi/6$. Compute the power radiated by the loop by integrating the complex Poynting vector over the surface of a large sphere. If P is the radiated power, use the relation $\frac{1}{2}RI_0^2 = P$ to define a radiation resistance, and show that this is equal to the input resistance obtained from a consideration of the flux linkages.

7.3. Perform the summations leading to (38).

7.4. Sum the following series directly, and compare with the sum obtained by using the Poisson summation formula:

$$\sum_{n=1}^{\infty} \frac{e^{-(n^2+1)^{1/2}}}{(n^2+1)^{1/2}}.$$

7.5. Use the Poisson summation formula to sum the following series:

$$\sum_{n=1}^{\infty} e^{-\alpha(n^2+\beta^2)^{1/2}} \quad \sum_{n=1}^{\infty} e^{-\pi n^2/1000}.$$

Note the large difference in the rate of convergence of the second series and its transformed equivalent. Consult a table of Fourier transforms for the required transforms.

7.6. Modify the small-aperture theory for waveguides to obtain an approximate theory for the reflected and transmitted fields from a small aperture in an infinite-plane conducting screen. Assume a parallel-polarized TEM wave incident at an angle θ_i with respect to the normal (see Fig. P7.6).

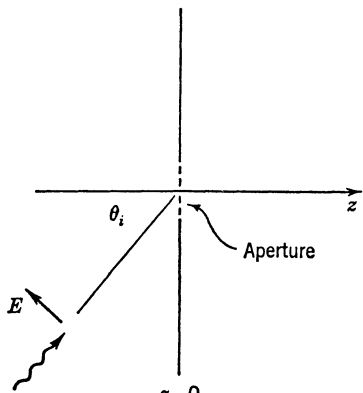


Fig. P7.6.

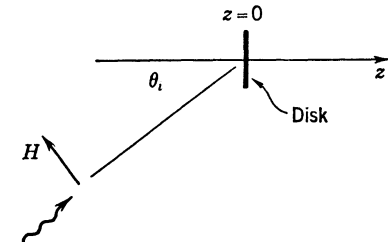


Fig. P7.7.

7.7. Develop a theory, similar to that in Problem 7.6, for the scattered field from a small conducting disk when a perpendicular-polarized TEM wave is incident at an angle θ_i (see Fig. P7.7). (For an expansion of the vector potential which gives the radiation from a small-volume distribution of current as radiation from an electric and magnetic dipole and other higher order multipoles see J. A. Stratton, *Electromagnetic Theory*. New York, NY: McGraw-Hill Book Company, Inc., 1941, sect. 8.4.) Use Babinet's principle to obtain the solution for a small aperture in a conducting screen from the solution of the disk problem. Show that this leads to the solution obtained in Problem 7.6.

7.8. Show that an elliptic aperture in a transverse wall in a rectangular guide as illustrated in Fig. P7.8 is

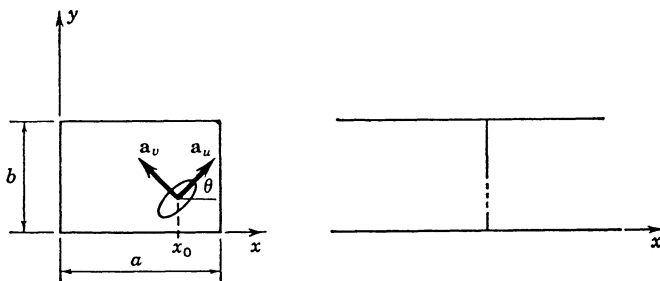


Fig. P7.8.

equivalent to a shunt inductive susceptance

$$B = \left(\frac{-2\beta_{10}}{ab} \sin^2 \frac{\pi x_0}{a} \bar{\alpha}_m : \mathbf{a}_x \mathbf{a}_x \right)^{-1}$$

where $\bar{\alpha}_m : \mathbf{a}_x \mathbf{a}_x$ is the double-dot product of $\bar{\alpha}_m$ with the unit vectors \mathbf{a}_x and x_0 is the coordinate of the center of the aperture.

7.9. A small circular aperture of radius l is located in the center of the transverse wall in a circular guide of radius a (see Fig. P7.9). Show that, for a TE₁₁ mode, the aperture is equivalent to an inductive susceptance

$$B = \frac{-0.955a^2\lambda_g}{4\alpha_m}$$

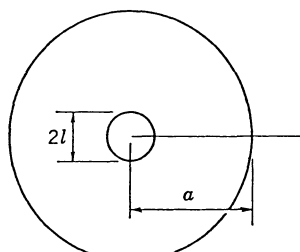


Fig. P7.9.

where λ_g is the guide wavelength, and $\alpha_m = \frac{4}{3}l^3$. For a TM₀₁ mode, show that the aperture is equivalent to a shunt capacitive susceptance

$$B = \frac{0.92a^4}{|\alpha_e|\lambda_g}, \quad |\alpha_e| = \frac{2}{3}l^3.$$

7.10. The Bethe hole directional coupler consists of two rectangular guides with their axes oriented with an angle θ between them and coupled through a small circular aperture in the center of the broadwall (see Fig. P7.10). Find

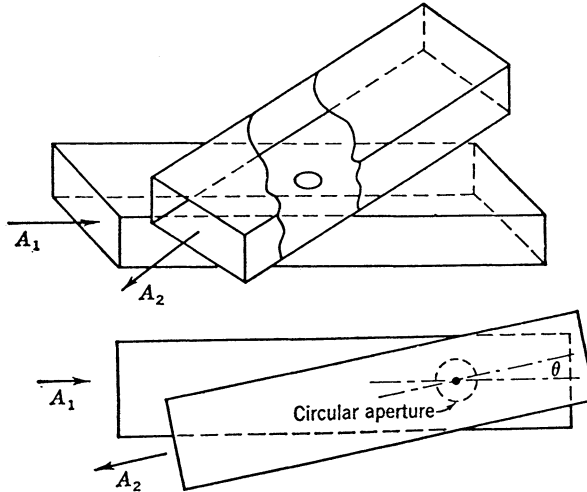


Fig. P7.10.

the required angle θ such that the electric and magnetic dipole coupling results in a wave propagating in the direction of arrow A_2 when a wave is incident along the direction of arrow A_1 . Find approximate expressions for the coupling coefficient and the directivity of this coupler. Note that when the radiation reaction fields are included the wave propagating in the direction opposite to that of arrow A_2 cannot be made to vanish, although its amplitude can be made small.

Answer:

$$a_{3,4} = \left[\frac{\mp 2jX \cos \theta}{4 + 4jX - X^2 \sin^2 \theta} + \frac{jB}{2 + 2jB} \right] A_1$$

where $X = 2\beta_{10}\alpha_m/ab$ and $B = 2k_0^2\alpha_e/\beta_{10}ab$. Let $B = -X \cos \theta$, then $C \approx 20 \log(1/X \cos \theta)$ and $D \approx C + 20 \log[2 \cos \theta/(1 + \cos \theta)]$.

7.11. If it is desirable to maintain the angle θ between the two guide axes equal to zero in Problem 7.10, a similar type of coupler may be built, using a properly oriented elliptical aperture or an offset circular aperture as illustrated in Fig. P7.11. Determine the orientation angle θ of the elliptical aperture and the offset d of the circular aperture in order to obtain a directional coupler.

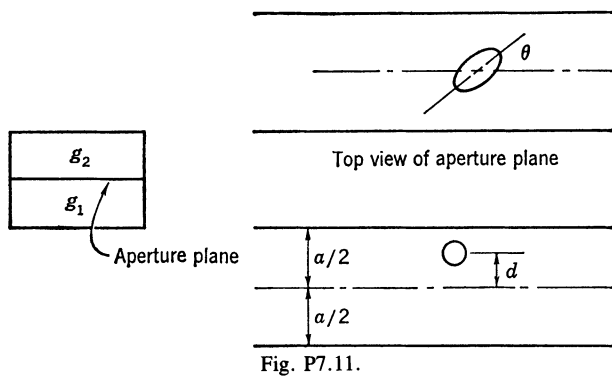


Fig. P7.11.

Answer:

$$\alpha_{mu} \sin^2 \theta + \alpha_{mv} \cos^2 \theta = \frac{k_0^2}{\beta_0^2} |\alpha_e|.$$

7.12. Consider a rectangular guide closed at $z = 0$ by an electric wall in which a small magnetic disk carrying a linear magnetic current of density \mathbf{J}_m is located (see Fig. P7.12). Let the field radiated by the magnetic current in

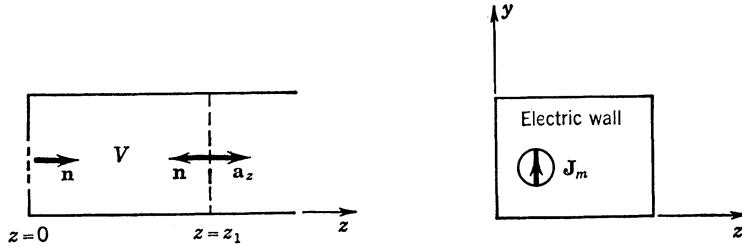


Fig. P7.12.

the region $z > 0$ be

$$\mathbf{E}_s = \sum c_n \mathbf{E}_n e^{-\Gamma_n z}$$

$$\mathbf{H}_s = \sum c_n \mathbf{H}_n e^{-\Gamma_n z}.$$

In the volume bounded by the guide walls and transverse planes at $z = 0$ and $z = z_1$, the field \mathbf{E}_s , \mathbf{H}_s is source-free. On the electric wall at $z = 0$ we have $\mathbf{n} \times \mathbf{E}_s = 0$, while on the surface of the magnetic disk $\mathbf{n} \times \mathbf{E}_s = -\mathbf{J}_m$. Let \mathbf{E} , \mathbf{H} be a normal-mode standing wave:

$$\begin{aligned} \mathbf{E} &= \mathbf{e}_m (e^{-\Gamma_m z} - e^{\Gamma_m z}) + \mathbf{e}_{zm} (e^{-\Gamma_m z} + e^{\Gamma_m z}) \\ \mathbf{H} &= \mathbf{h}_m (e^{-\Gamma_m z} + e^{\Gamma_m z}) + \mathbf{h}_{zm} (e^{-\Gamma_m z} - e^{\Gamma_m z}). \end{aligned}$$

This field is also source-free in V . The Lorentz reciprocity theorem gives

$$\iint_S \mathbf{n} \cdot (\mathbf{E}_s \times \mathbf{H} - \mathbf{E} \times \mathbf{H}_s) dS = 0.$$

Show that, over the plane $z = z_1$, the integral gives $-2c_m \iint \mathbf{e}_m \times \mathbf{h}_m \cdot \mathbf{a}_z dS$, while, over the $z = 0$ plane, the result is $-\iint \mathbf{J}_m \cdot \mathbf{H} dS = -2 \iint \mathbf{J}_m \cdot \mathbf{h}_m dS$. A linear magnetic current element is equivalent to a magnetic dipole, and, if \mathbf{h}_m is assumed constant over the magnetic disk, the coefficient c_m is found to be given by

$$2c_m \iint \mathbf{e}_m \times \mathbf{h}_m \cdot \mathbf{a}_z dS = -j\omega\mu_0 2\mathbf{M}_0 \cdot \mathbf{h}_m$$

where \mathbf{M}_0 is the magnetic dipole moment associated with the current \mathbf{J}_m .

7.13. Consider a z -directed magnetic dipole $M\mathbf{a}_z$ located at the origin between two infinite conducting planes placed parallel with the xz plane at $y = \pm b/2$. Obtain the solution for the magnetic Hertzian potential Π_z by solving the scalar Helmholtz equation

$$\nabla^2 \Pi_z + k_0^2 \Pi_z = -M\delta(x)\delta(y)\delta(z)$$

in cylindrical coordinates. The solution is the same as that given by (38).

HINT: Expand Π_z in a Fourier series of the form

$$\Pi_z = \sum_{m=0}^{\infty} a_m \cos \frac{2m\pi y}{b} K_0(\Gamma_m r) \quad \Gamma_m^2 = \left(\frac{2m\pi}{b} \right)^2 - k_0^2.$$

Next use Fourier analysis to obtain

$$\left(\frac{1}{r} \frac{\partial}{\partial r} r \frac{\partial}{\partial r} - \Gamma_m^2 \right) a_m K_0(\Gamma_m r) = -\frac{M \epsilon_{0m}}{b} \delta(r).$$

Each term must have a logarithmic singularity $-(M \epsilon_{0m}/2b\pi) \ln r$, and hence $a_m = M \epsilon_{0m}/2\pi b$, $\epsilon_{0m} = 1$, $m = 0$; $\epsilon_{0m} = 2$, $m > 0$.

7.14. Figure P7.14 shows a directional coupler consisting of two rectangular waveguides coupled by small circular

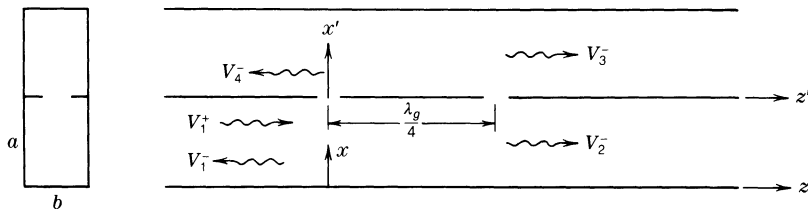


Fig. P7.14.

apertures in the common sidewall. Find the amplitudes V_1^- , V_2^- , V_3^- , V_4^- at the four ports when a TE_{10} mode with amplitude V_1^+ is incident at port 1.

HINT: Assume dipoles of strength M_{z1} and M_{z2} in the two apertures and find the total H_z reaction fields from these.

Answer: Generator fields at the two apertures are $-Nk_c V_1^+$ and $jNk_c V_1^+$. Equations for the dipole strengths are

$$M_{z1} = \alpha_m [-Nk_c V_1^+ + jk_0 Z_0 k_c^2 N^2 (M_{z1} - jM_{z2})]$$

$$M_{z2} = \alpha_m [jNk_c V_1^+ + jk_0 Z_0 k_c^2 N^2 (M_{z2} - jM_{z1})]$$

$$M_{z1} = -\alpha_m k_c N V_1^+ (1 + jB) / (1 + 2jB - 2B^2)$$

$$M_{z2} = j\alpha_m k_c N V_1^+ / (1 + 2jB - 2B^2) = -jM_{z1} / (1 + jB)$$

$$V_1^- = V_4^- = k_0 Z_0 N k_c B M_{z1} / (1 + 2jB)$$

$$V_3^- = -k_0 Z_0 N k_c M_{z1} (1 + jB) / (1 + 2jB) = V_2^- + jV_1^+$$

where $k_c = \pi/a$, $B = 2\alpha_m k_c^2 / \beta_{10} ab$.

7.15. The equivalent circuit for the directional coupler in Problem 7.14 is shown in Fig. P7.15. Show that this circuit gives the same scattered field amplitudes when a wave of amplitude V_1^+ is incident at port 1.

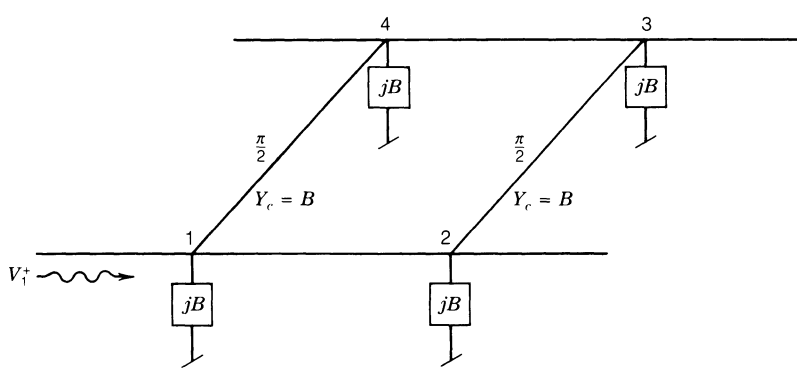


Fig. P7.15.

7.16. Repeat the analysis of the directional coupler in Problem 7.14 but let the apertures be spaced a distance d apart so that $\beta_{10}d = \theta$. Find the value of θ that will make $V_4^+ = 0$.

Answer: $M_{z1} = -M_{z2}e^{-j\theta}$, $\theta = -\tan^{-1} B + \pi/2$.

7.17. A rectangular cavity is coupled to a rectangular waveguide by a small circular aperture in the common sidewall as shown in Fig. P7.17. Find the equivalent circuit for this system. The cavity resonates in the TE_{101} mode.

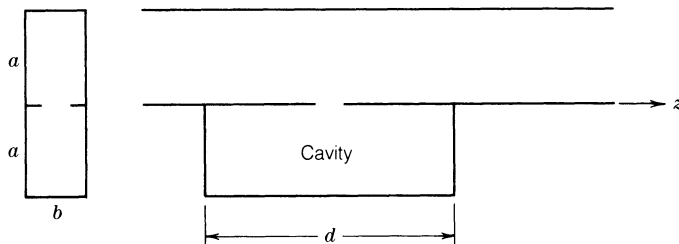
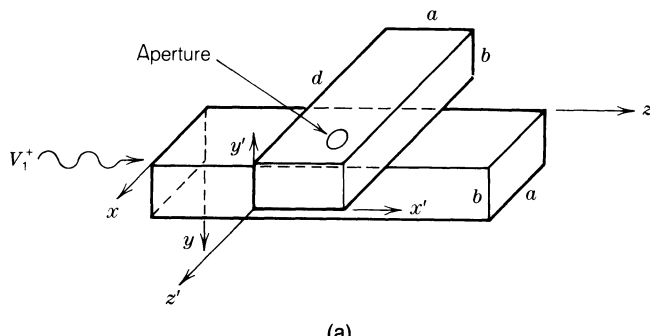
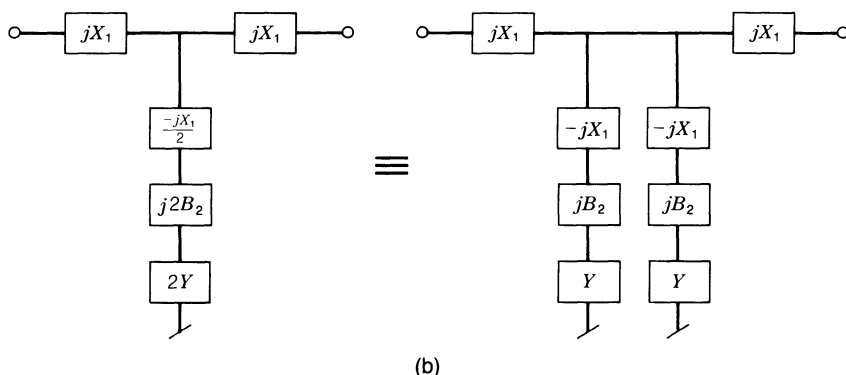


Fig. P7.17.

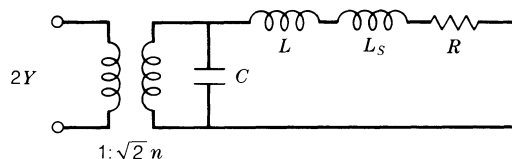
7.18. Figure P7.18(a) shows a cavity coupled to a rectangular guide by a circular aperture with radius r_0 and which is centered in the broad wall of the guide and cavity. The cavity is excited in the TE_{101} mode. The incident



(a)



(b)



(c)

Fig. P7.18.

field has

$$E_y = V_1^+ N \sin \frac{\pi x}{a} e^{-j\beta z}, \quad H_x = -Y_w E_y$$

where $N = (2Z_w/ab)^{1/2}$.

Find the amplitudes of the TE₁₀₁ cavity mode and the reflected and transmitted TE₁₀ modes in the waveguide. Note that dipoles P_y and M_x are excited but only P_y couples to the TE₁₀₁ mode (why?).

Verify that

$$M_x = -\frac{\alpha_m N Y_w V_1^+}{2 + j\alpha_m \beta / ab}, \quad P_y = \frac{\epsilon_0 \alpha_e N V_1^+}{2 + \alpha_e W + j\alpha_e k_0^2 / ab}, \quad W = \frac{4\omega^2}{abd \left[\omega^2 \left(1 + \frac{1-j}{Q} \right) - \omega_0^2 \right]}$$

where ω_0 is the resonant frequency of the cavity mode.

The equivalent circuit for the coupled cavity is also shown in Fig. P7.18(b). Show that for even and odd excitation the input reflection coefficients are

$$\Gamma_e = 1 - \frac{2jB_2}{1 + jB_2 + jB_2/Y}, \quad \Gamma_o = -1 + \frac{2jX_1}{1 + jX_1}.$$

By superimposing the two solutions show that the input reflection coefficient is given by

$$\Gamma = \frac{1}{2}(\Gamma_e + \Gamma_o) = \frac{jX_1}{1 + jX_1} - \frac{jB_2}{1 + jB_2 + jB_2/Y}.$$

By comparing this expression with your analytical solution show that

$$X_1 = \frac{\alpha_m \beta}{2ab}, \quad B_2 = \frac{k_0^2 \alpha_e}{2\beta ab}, \quad Y = \frac{jk_0^2 d}{2\omega^2 \beta} \left[\omega^2 \left(1 + \frac{1-j}{Q} \right) - \omega_0^2 \right].$$

Verify that for the resonant circuit shown in Fig. P7.18(c)

$$Y \approx \frac{j\omega C n^2}{\omega^2} \left[\omega^2 \left(1 + \frac{1-j}{Q} \right) - \omega_0^2 \right]$$

where $\omega_0^2 LC = 1$, $C = \epsilon_0 ad / 4b$, $n^2 = k_0 b Z_0 / \beta a$.